Geophysical and Hydrogeological Studies of Al-Foah Area, North Al Ain, United Arab Emirates (UAE)

Sameh Yahyia Ali Suleiman

United Arab Emirates University
Deanship of Graduate Studies
M. Sc. Water Resources Program

Geophysical and Hydrogeological Studies of Al-Foah Area, North Al Ain, United Arab Emirates (UAE)

By

Sameh Yahyia Ali Suleiman

A Thesis Submitted to

Deanship of Graduate Studies
United Arab Emirates University

In the Partial Fulfillment of the Requirements for the M.Sc. Degree in

Water Resources

Deanship of Graduate Studies
United Arab Emirates University
June, 2007

United Arab Emirates University
Deanship of Graduate Studies
M. Sc. Water Resources Program

Thesis Title

Geophysical and Hydrogeological Studies of Al-Foah Area, North Al Ain, United Arab Emirates (UAE)

Author's Name

Sameh Yahyia Ali Suleiman

Supervisors

No	Name	Position
1	Dr. Ahmed Murad	Head of Geology Department, Assistant Professor of Hydrogeology, Geology Department, College of Science, United Arab Emirates University.
2	Dr. Ahmad El-Sayed El-Mahmoudi	Associate Professor of Geophysics, Geology Department, College of Science, King Faisl University, KSA.
3.	Dr. Haydar A. Baker	Professor of Applied Geophysics, Geology Department, College of Science, United Arab Emirates University.

Thesis of Sameh Suleiman
Submitted in Partial Fulfillment for the Degree of
Master of Science in Water Resources

Chair of Examination Committee
Dr. Ahmed Murad, Assistant Professor of Hydrogeology ....
Geology Department
United Arab Emirates University

External Examiner
Prof. Ole Bernt Lile, Professor of Applied Geophysics
Petroleum Engineering and Applied Geophysics Department ....
Norwegian University of Science and Technology

Internal Examiner
Prof. Abdulrazag Y. Zekri, ...
Chemical & Petroleum Engineering Department
United Arab Emirates University

Dean of Graduate Studies
Dr. James E. Fletcher ....

United Arab Emirates University
2006/2007

ACKNOWLEDGMENT

I am deeply indebted to my advisors, Dr. Ahmed Murad, Dr. Ahmad Al-Mahmoudi and Dr. Haydar Baker, for their constant support. Without their help, this work would not be possible.

My sincere thanks go to Dr. Hassan Garamoon for helping and supporting me and Dr.Osman Abdulghani for providing me his valuable papers and articles.

I would also like to thank Gaber Latif for his invaluable advice on parallel processing and map preparing.

I would like to thank Wendy Straughton for her comments and suggestions for the editing of my thesis. I would like to thank the laboratory staff at UAE University for their tireless efforts with me.

I would like also to extend my deep thanks and appreciation to the NDC Staff especially for Mr. Kamal Al Aidarous (Manager of NDC Al Ain) and Mr. Juanito Tamayo (GIS department) for their efforts and providing me with maps.

My sincere thanks go to Ministry of Presedintional Affairs, Meteorological Department for helping and providing me with meteorological data of my study area.

Words fail me to express my appreciation to my wife Amani whose dedication, love and persistent confidence in me, has taken the load off my shoulder. I owe her for unselfishly letting her intelligence, passions, and ambitions collide with mine.

I am deeply and forever indebted to my parents for their love, support and encouragement throughout my entire life. I am also very grateful to my brothers and to my only sister.

Finally, I would like to thank everybody who was important to the successful realization of this thesis, as well as expressing my apologies that I could not mention everyone personally.

ACKNOWLEDGMENT

I am deeply indebted to my advisors, Dr. Ahmed Murad, Dr. Ahmad Al-Mahmoudi and Dr. Haydar Baker, for their constant support. Without their help, this work would not be possible.

My sincere thanks go to Dr. Hassan Garamoon for helping and supporting me and Dr.Osman Abdulghani for providing me his valuable papers and articles.

I would also like to thank Gaber Latif for his invaluable advice on parallel processing and map preparing.

I would like to thank Wendy Straughton for her comments and suggestions for the editing of my thesis. I would like to thank the laboratory staff at UAE University for their tireless efforts with me.

I would like also to extend my deep thanks and appreciation to the NDC Staff especially for Mr. Kamal Al Aidarous (Manager of NDC Al Ain) and Mr. Juanito Tamayo (GIS department) for their efforts and providing me with maps.

My sincere thanks go to Ministry of Presedintional Affairs, Meteorological Department for helping and providing me with meteorological data of my study area.

Words fail me to express my appreciation to my wife Amani whose dedication, love and persistent confidence in me, has taken the load off my shoulder. I owe her for unselfishly letting her intelligence, passions, and ambitions collide with mine.

I am deeply and forever indebted to my parents for their love, support and encouragement throughout my entire life. I am also very grateful to my brothers and to my only sister.

Finally, I would like to thank everybody who was important to the successful realization of this thesis, as well as expressing my apologies that I could not mention everyone personally.

ABSTRACT

Groundwater constitutes an important water resource in United Arab Emirates. Al Ain area, where the study area is located, has experienced a rapid urbanization of the last few decades. Because of its fertile land, Al Ain area is considered the main focal point for agricultural activities which in turn depend on the groundwater of the Quaternary aquifer and fractured limestone aquifer of Simsima Formation. Despite the severe shortage in the natural water resources, the per capita water consumption in the UAE is among the highest rates of the world.

Al-Foah area (previously Al Oha) located to the north of Al Ain city. This area is regarded as one of the cultivated areas in Abu Dhabi Emirate. Most of the water demand for domestic and agriculture purposes in this area is met by groundwater. Due to the expansion in the development activities and population growth, the groundwater is excessively over pumping. Groundwater levels dropped dramatically and salinity increased. Moreover, using of chemical fertilizers, pesticides and herbicides for agriculture purposes are enhancing the contamination of the existing aquifers via infiltration through the permeable loose sandy soil and fractures.

This study is devoted to the investigation of the water potentiality and quality at Al-Foha area. It defines the hydrogeological parameters of Al-Foah using different techniques. To the end, detailed geophysical, hydrogeological and hydrochemical investigations were conducted. To achieve this aim, previous studies were reviewed. The required information and data about geology, hydrogeology, and climatology hydrochemistry and geoelectric investigations were collected.

In the hydrogeological aspects of this study, the prevailing climatic conditions in Al Ain area including temperature, rainfall, humidity, evaporation, and aridity are outlined. The groundwater bearing formations encompassing the Quaternary aquifer and Jabal Al Oha fractured limestone aquifer are presented. Few cross sections were deduced for Al Oha area.

In the hydrogeochemical aspects, the physical properties including the Hydrogen Ion concentration (pH), Electrical Conductivity (EC), total salinity distribution and total hardness and the chemical properties including the major cations and anions are discussed. The distribution of various physical and chemical elements and the ion dominance in the groundwater are elaborated. The water genesis including analyses by trilinear diagram is discussed. To show the spatial distribution of each

hydrochemical parameters, contour maps of each parameter have been constructed using Surfer mapping system software Ver.8. This hydrogeochemical concluded with an assessment for the suitability of groundwater for irrigation purposes based on SAR, EC, sodium content and residual carbonate.

One of the new developments in recent years is the use of 2-D electrical imaging/tomography surveys to map areas with moderately complex geology. A more accurate mode of the subsurface is a two-dimensional (2-D) model where the resistivity changes in the vertical direction, as well as in the horizontal direction along the survey line. 2-D electrical imaging/tomography surveys is implemented. In this respect, nine 2-D resistivity profiles were conducted and oriented along the strike direction of the limestone exposure north of Al-Ain known as Jabal Al Oha area to intersect the maximum possible number of geologic features. Each profile consisted of 30 electrodes spaced 20m apart which penetrate to about 120m depth. Wenner array was used in this survey and apparent resistivity data was collected and inverted using Res2dinv, ver. 3.54 to create a model of subsurface resistivity that approximated the true subsurface resistivity distribution and displayed this as a cross section. Resistivity data interpretation was constrained by the available borehole lithologies and groundwater salinity data.

The conclusions and main findings of the study are presented. Recommendations for future investigations are also made. Such results will guide planners, decision makers, and researchers for future development plans and better management of this vital resource at Al-Foah area.

TABLE OF CONTENTS

LIST OF FIGURES

LIST OF TABLES

ABBREVIATIONS

mm	Millimeter
cm	Centimeter
km	Kilometer
asl	Above sea level
UTM	Universal Transverse Mercator
MCM	Million Cubic Meters
NDC	National Drilling Company
μmhos	Micromohs
˚C	Degree Centigrade
ppm	Part per million
BH	Borehole
TDS	Total Dissolved Solids
EC	Electrical Conductivity
ha	Hectare=10.000 Square Meters
Ω-m	Ohm meter
RSC	Residual Sodium Carbonate
WED	Water & Electricity Department
epm	Equivalent per milliliter
DC	Direct Current
VES	Vertical Electrical Sounding
TDEM	Time Domain Electromagnetic
S.P	Self Potential
R_w	Resistivity of formation water
R_{mf}	Resistivity of the mud filtrate
R_t	True resistivity
φ	Porosity
F	Tortuosity
Δt's	The travel times (in microsecond)
ρ	Resistivity
GWP	Groundwater project
TH	Total Hardness
SAR	Sodium Adsorption Ratio
pH	Hydrogen Ion Concentration
2-D	Two Dimensional

Chapter I

INTRODUCTION

CHAPTER I

INTRODUCTION

Due to the rapid developments of domestic, industrial, and agricultural water supplies, the conventional water resources have been critically depleted. The scarcity of natural water resources and the growing gap between demand and supply of potable water in most of the UAE forced the government to face the water challenge with wise policies and decisions. The government realizes that the situation goes beyond just a gap in water quantity and quality and needs to be seen in the context of emerging environmental problems.

Moreover, there has been an increasing concern in the UAE about the development of the water sectors and the efficient utilization of the water resources for sustainable water development.

Non-conventional water resources such as water desalination and effluent water reuse have gained increasing profiles in the planning and development of additional water supplies.

1.1 Location

The United Arab Emirates (UAE) is situated along the southeastern tip of the Arabian Peninsula between 22° 50' and 26° north latitudes and between 51° and 56 ° 25' east longitudes (Figure 1.1). Qatar lies to the northwest, Saudi Arabia to the west, south and southwest and Oman to the southeast and northeast. The country occupies a total area of about 83, 600 km^2 (32,400 $mile^2$) and it has 700 km of coastline, 600 km along the Arabian Gulf and 100 km bordering the Gulf of Oman (Bin Braik, 1997).

Al-Ain is the largest city in the Eastern Region of the Emirate of Abu Dhabi. It is located approximately 160 km east of the Abu Dhabi capital. Al-Ain, whose name means 'the spring' in Arabic, derives from its originally plentiful supply of fresh water, which makes its way underground across most of the plain lying before the Omani mountains.

Al-Foah lies in the northern side of Al- UAE and Sultanate of Oman between longitudes of 55° 20' and 55° 50' E and latitudes of 24° 10' and 24° 30' N (Figure 1.2).

Figure (1.1) Map showing the location of the United Arab Emirates in Arabian Peninsula.

Figure (1.2) Location map of Al-Foah area.

1.2 Objectives

The objectives of this study are to identify the geometry of the aquifers in the Al-Foah area and the subsurface limestone units and location of Karst areas within delineated limestone zones as it is considered to be of high hydrologic potential.

The study aims also to determine the quality of the groundwater and evaluate its degree of contamination by agriculture practices. A possible hydraulic connection between the Limestone aquifer and the surfacial Quaternary aquifer will be examined.

1.3 Methodology

In order to implement and achieve the goals of this study, several methods have been used. These methods include the followings:

1) All relevant information about geology of the aquifer, hydrogeological parameters and climatological data has been collected, cross-checked and analyzed.

2) Groundwater samples have been collected from available production wells for routine chemical analyses.

A) Field measurements were conducted for Electrical Conductivity (mg/l), Total Dissolved Solid (mg/l), Salinity (%) and Temperature (°C).

B) Laboratory analyses were conducted for major ions, cations and heavy metals in groundwater samples.

3) Direct Current (DC) resistivity investigations have been implemented to map the hydrostratgraphic units of the main two aquifers at Al-Foah area.

4) Integration of all the geological. hydrogeological and geophysical results.

Chapter II

GEOMORPHOLOGY

AND

GEOLOGY

CHAPTER II

GEOMORPHOLOGY AND GEOLOGY

2.1 Geomorphology

There are many features present in Al-Ain area which include: mountains, gravel plains and sand dunes. Below is a detailed description for each geomorphologic feature (Figure 2.1).

2.1.1 Mountains

The main mountains occupying the study area are Jabal Al-Oha and Jabal Huwayyah (Figure 2.2), which lie 8 km northeast of Al-Ain city. They consist of three NW-SE parallel hogback ridges representing fault repetitions of the western limb of the horseshoe shaped southerly plunging anticline of Jabal Huw

Also, Jabal Malaqet and Jabal Mundassah are considered to be part of Oman Mountains, which are located to the south of Jabal Al-Oha and Jabal Huwayyah. The two mountains form asymmetric anticline structures with their eastern limbs forming the main part of the exposures. The western limbs form disconnected strike ridges and are more subdued. These mountains receive a relative high rainfall and represent the recharge area for the fractured limestone aquifer, Quaternary sand and gravel aquifers. The eastern part of Al-Foah is characterized by good water quality and this is due to the low dissolution of hard ophiolitic rocks forming Jabal Malaqet and Jabal Mundassah (Hamdan and El-Deeb, 1990).

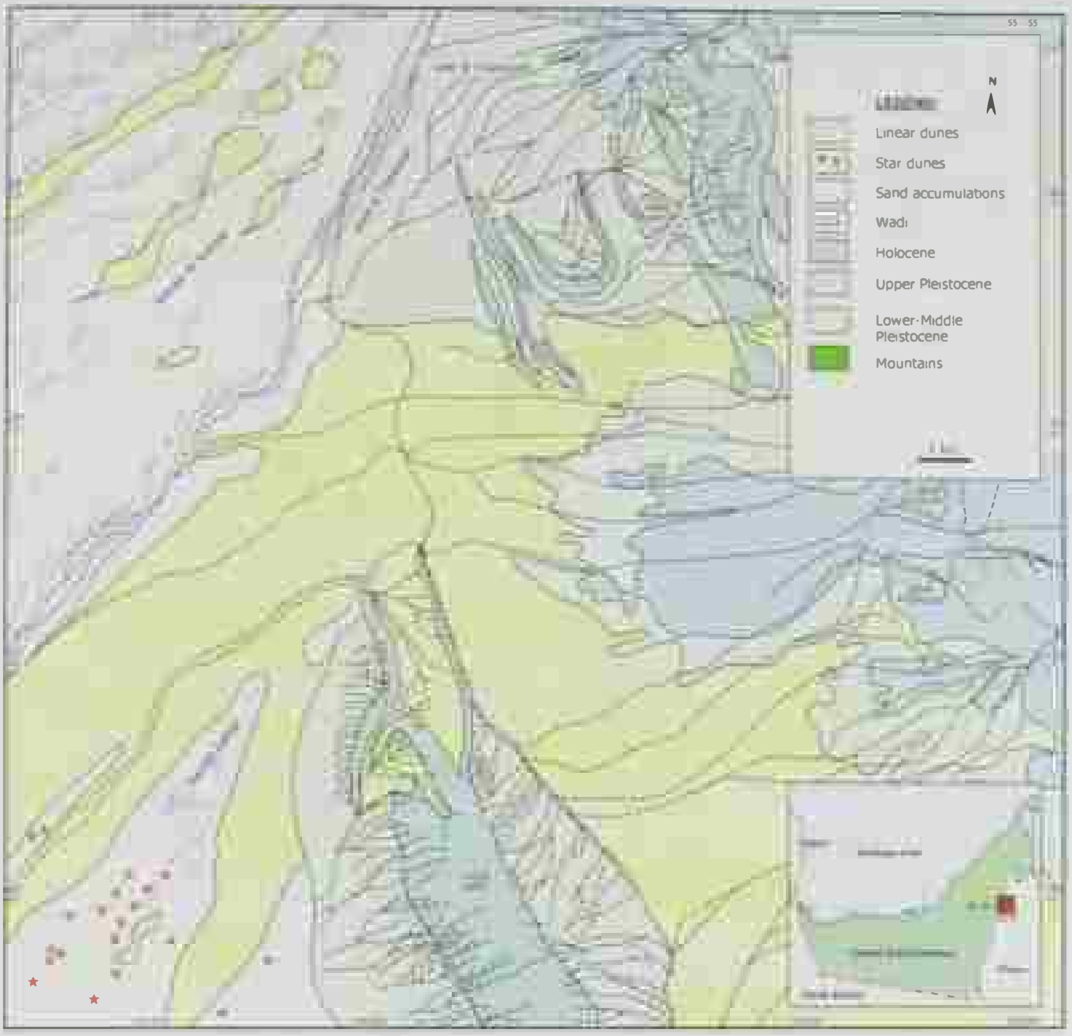

Figure (2.1) Geomorphology of Al Ain region (after the National Atlas of United Arab Emirates, 1993 and Al-Nuaimi, 2003).

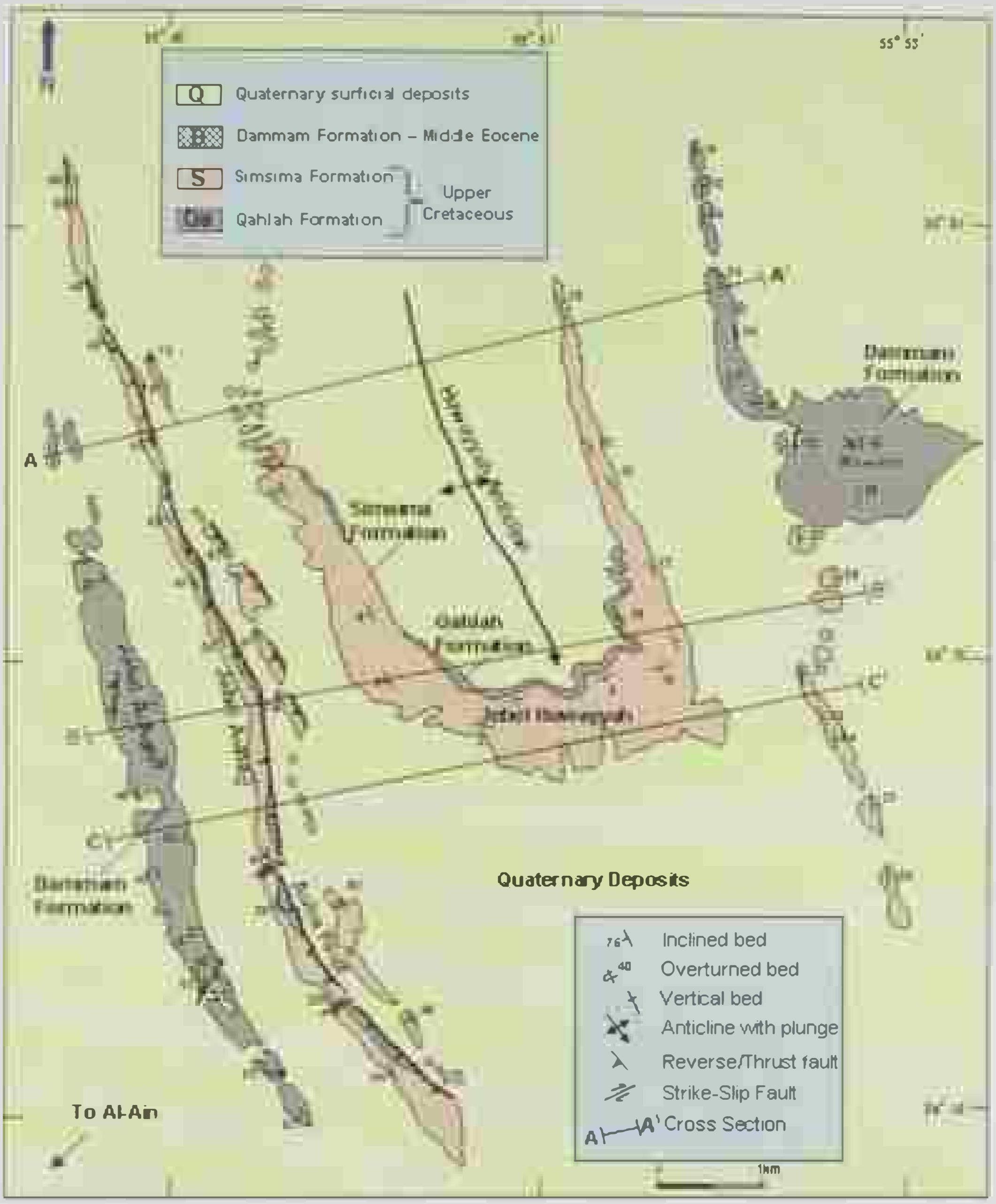

Figure (2.2) Geological map showing the main mountains in the study area (modified from Noweir and Alsharhan, 2000).

2.1.2 Gravel Plains

The gravel plains bound the eastern side of Oman Mountains. These plains occupy the area between the Oman Mountains to the east and sand dunes to the west. The average slope of the plains is 0.001 according to Ghoneim. (1991).

The gravel plains mostly consist of alluvial sand and gravel transported by wadis dissecting the Oman Mountains. The continuity of these plains is locally interrupted by sand dunes. A prominent alluvial fan occurs in the east of Al-Foah.

2.1.3 Sand Dunes

Sand dunes cover about 73% to 76 % of the area of UAE. The dunes of UAE include various types like linear. barchanoid. transverse and star dunes. The major type of dunes within the study area is the linear dunes. which occupy the nort

simple and compound patterns. which are mainly controlled by sand supply. meteorology. topography. lithology and geological structures. Embabi (1991) used satellite images to study dune type. patterns. generations and factors affecting the sand dunes.

2.2 Geology (Stratigraphy)

The age of the major rocks in Al-Foah area is Upper Cretaceous to Holocene (Hamdan and Bahr. 1992). The following subsections present a brief description of the surface stratigraphic column from bottom to top: Semail Ophiolite. Qahlah Formation. Simsima Formation. Dammam Formation and Quaternary deposit (Figures 2.3 and 2.4).

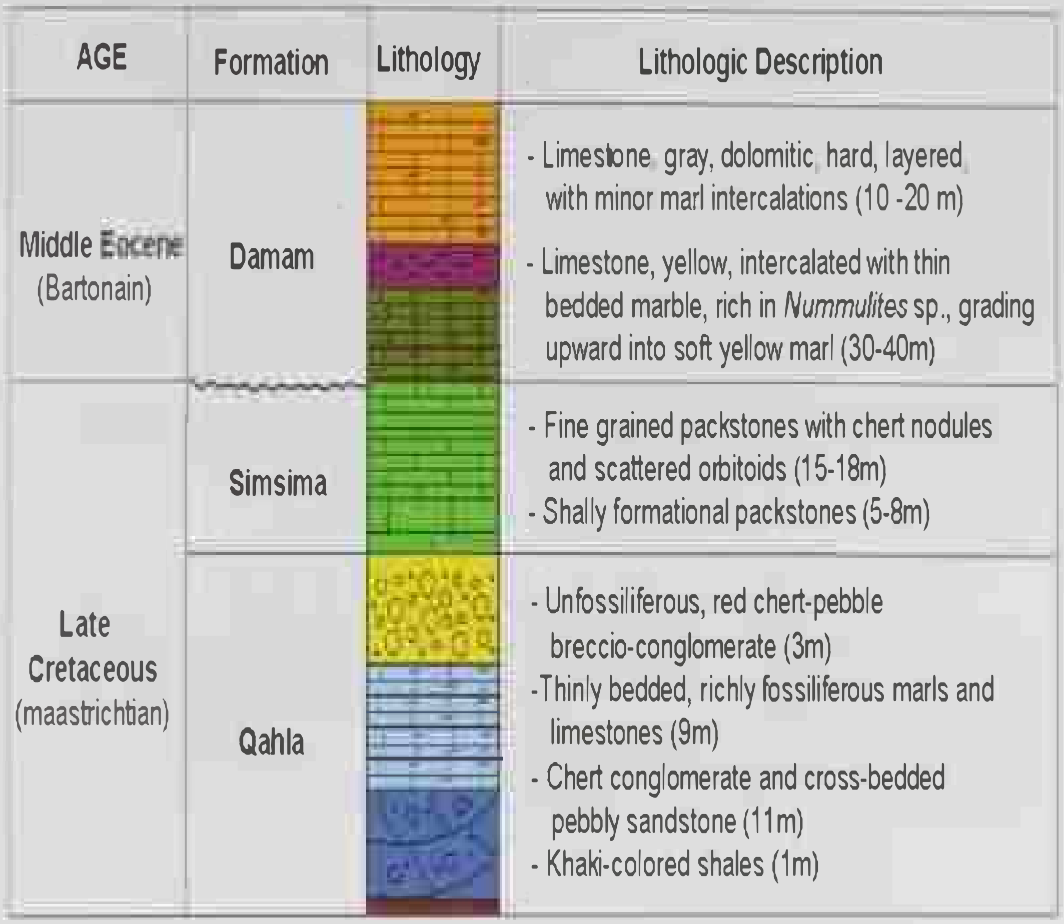

Figure (2.3) Stratigraphic succession in the Jabal Oha and Jabal Huwayyah area (modified from Noweir and Alsharhan, 2000).

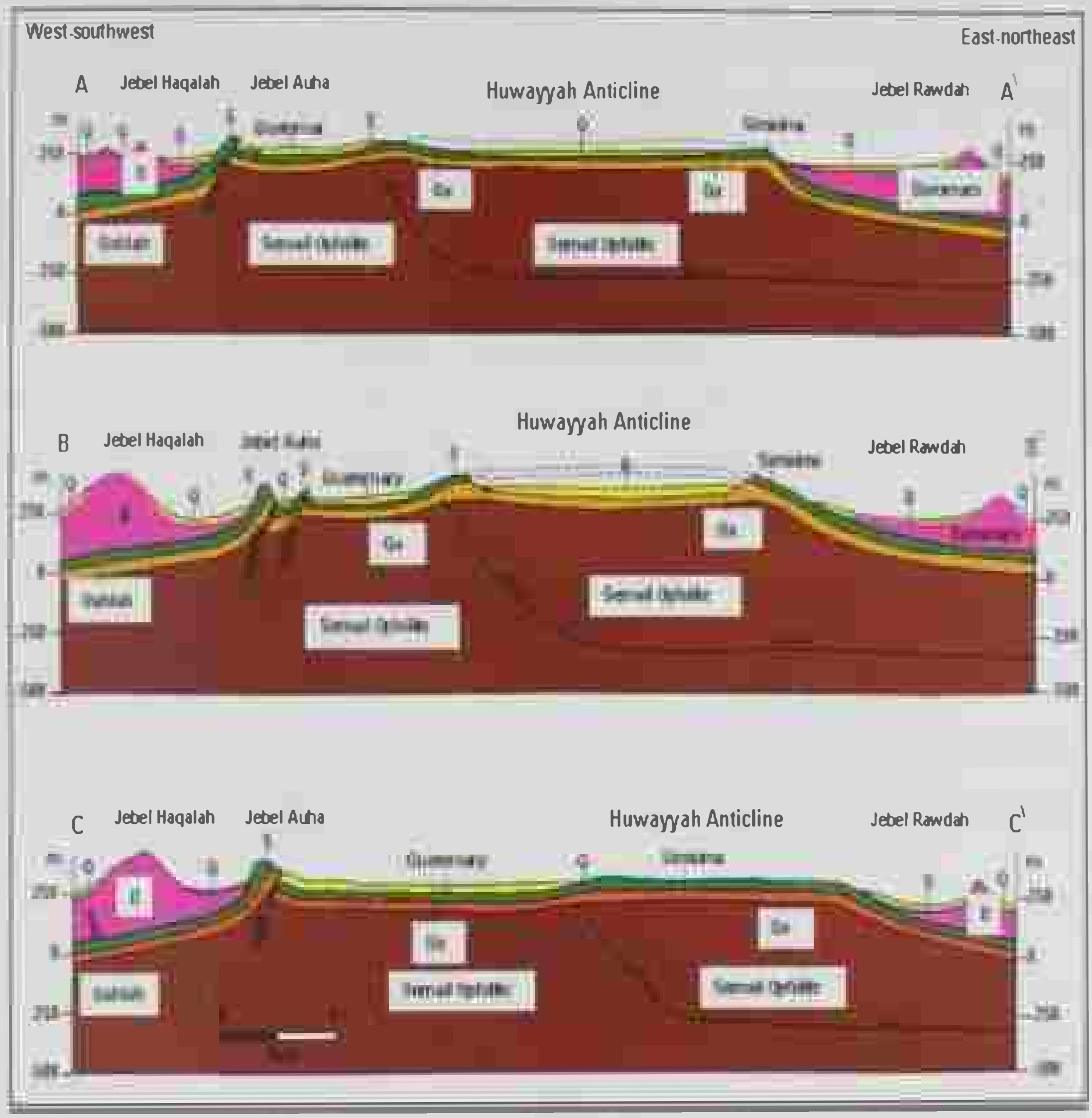

Figure (2.4) Structural cross sections (A-A', B-B' and C-C') through the Oha reverse faults and Huwayyah Anticline (see Figure 2.1 for location and legend of section) (modified from Noweir and Alsharhan, 2000).

2.2.1 Semail Ophiolite

The oldest rock units of Semail Ophiolite are Pre-Maastrichian serpentinite and serpentinized periodotite. These rocks are located at the base of Jabal Oha, Jabal Huwayyah, Jabal Malaqet and Jabal Mundassah (Hamdan and Anan, 1993).

2.2.2 Qahlah Formation

Qahlah Forn s

Jabal Oha and Jabal Huwayyah. The lowest exposure consists of poorly exposed and weathered khaki colored shales, overlain by cross-bedded pebbly brown sandstones and chert conglomerates. The succession passes into thinly bedded, abundantly fossiliferous marl and limestone. The Qahlah Formation is capped by a 3 m thick unit of red chert-pebble conglomerate. The Formation shows a general and gradual decrease in thickness from south to north and it thins out completely toward the extreme north of the study area. This lateral variation in thickness is interpreted to be the result of structural growth (Noweir and Alsharhan, 2000).

2.2.3 Simsima Formation

In the study area as in many parts of the Oman Mountain, the Maastrichtain Simsima Formation conformably overlies the Qahlah Formation. Simsima Formation is 85 m thick according to Sayed and Mersal (1998). However, the thickness of Simsima Formation at Jabal Faiyah is 140 m as measured by Noweir et al. (1998). In the study area, the Simsima Formation is 20 m to 26 m thick and consists of two units (Noweir and Alsharhan, 2000). The lower 5 m to 8 m is composed of shelly, foraminiferal packstone of shallow water origin overlain by 15 m to 18 m thick of fine-grained deep-water packstone. Small outcrops of Maastrichtian limestone belonging to the Simsima Formation are restricted to the northern end of the western flank of

Jabal Zarub and a small ridge on the eastern side of Jabal Malaqet (Hamdan and Anan. 1993).

2.2.4 Dammam Formation

The Simsima Formation in Jabal Oha and Jabal Huwayyah is unconformably overlain by limestone intercalated with thin bedded marl that grades upward into soft yellow marl for a total thickness of 30 m to 40 m. The yellow is overlain with sharp contact by 10 m to 20 m of hard gray dolomitic limestone (Figure 2.3). Most of the recorded carbonate facies of Dammam Formation have a grain supported fabric. Generally grains are fine to coarse. moderately sorted and show a marked orientation that indicates an active shallow marine environment (Noweir and Alsharhan. 2000).

2.2.5 Quaternary Deposits

Most of Al-Foah area is covered by Quaternary deposits. Four sediment types were recognized by Hunting (1979). Three of these units are described in the following subsections from bottom to top.

2.2.5.1 Aeolian Sand

The color of dune forming sand changes from red and pink in the east to lighter color westwards. The dune sediments are well-rounded grains of quartz and carbonate with minor proportions of basic and ultra basic grains. The sorting is generally poor and no pure silica sands were observed (Hunting. 1979).

2.2.5.2 Desert Plain Deposits

These deposits are inter-layered laminated silts and carbonate cemented

w

cemented by gypsum at times of higher water table and have been subsequently re-exposed by ablation. Sections exposed in barrow pits near Jabal Muhayer show inter-layered gravel, calcrete, nodular limestone and calcareous silt (Hunting, 1979).

2.2.5.3 Alluvial Deposits

Alluvial deposits occur beneath the piedmont plains fingering the Oman Mountains and Jabal Hafit. These deposits range from boulder gravel to conglomerate in the east and fine sand to silt further west. A typical section in the alluvial of Al Jaww plain consists of pebbles and cobbles of gabbros, serpentinite, limestone and chert set in fine-grained matrix of carbonate silt. At some localities, pebbles are un-cemented or loosely held together by coarse-grained recry

which make excellent aquifers. Towards Al-Ain city and further west, the gravel and conglomerate are replaced by inter bedded sand, silt and calcrete which tend to be more cemented than conglomerate. The calcrete is typically white, lacks obvious bedding, and contains scattered grains of altered igneous rocks and irregular fractured surfaces coated with iron and manganese oxides (Hunting, 1979).

Chapter III

HYDROGEOLOGY

CHAPTER III

HYDROGEOLOGY

3.1 The Climate

The United Arab Emirates lies within the area of the hot desert climate, which is characterized by two main seasons: a long and dry summer, with high temperatures between May and September with low rainfall; and a short to moderate winter between December and March with slight to moderate rainfall, with low temperatures.

Meteorological data of solar radiation, temperature, rainfall, humidity, wind speed and evaporation were obtained from the Department of Civil Aviation (Abu Dhabi International Airport) for Al-Ain International Airport Meteorological Station and Ministry of Presedintional Affairs, Meteorological Department for the period of 1994 – 2006. The analyses of the climate data of Al-Ain area are given below.

3.1.1 Solar Radiation

June receives the highest solar radiation in UAE of 796 wh/cm^2 and December is the lowest with 425 wh/cm^2, with a general increase from December to June and decrease from July to September (Al Shamsei, 1993). The average annual hours of sunshine in UAE is 10.1 hr/day, with a maximum of 11.9 hr in May and a minimum of 8.8 hr in December (Abu Dhabi Airport Meteorological Station) (see Appendix A).

3.1.2 Temperature

The coolest month in the year is January

month. The mean monthly temperature varies in the study area between 17.1°C in winter and 38.1°C in summer (Figure 3.1). The season of high temperatures extends from April to September. The temperature variation from year to another is relatively small with an annual mean temperature of 28.5°C (Table 3.1).

3.1.3 Rainfall

It is noticeable that the mountainous area receives the highest amount of rainfall, followed by the eastern region, and the gravel plain. The amount of rainfall declines towards the desert and western coast areas. The annual average rainfall is recorded at 91.1 mm, and highest rainfall was recorded in 2006, when it reached 201 mm. Most of the rainfalls in winter, as a result of the atmospheric depression accompanied with northwesterly winds coming from the Mediterranean or by orographic effects. Some of the rain events in the country are accompanied by thunder and lightning, and the fall may continue for up to three days. Summer rain is observed mainly in mountain areas especially in the eastern region of the study area, (see Figure 3.2 and Table 3.2).

Table (3.1) Temperature data in Al-Ain area.

A) Mean maximum Temperature (°C) at Al-Ain (1995-2006).

Year	Jan	Feb	Mar	Apr	May	Jun	Jul	Aug	Sep	Oct	Nov	Dec
1995	25.7	26.7	28.0	35.0	41.4	44.7	41.9	44.3	41.7	38.0	31.7	25.9
1996	24.0	27.7	29.8	37.1	42.2	43.7	46.3	44.2	41.5	36.7	30.6	26.4
1997	23.9	27.1	27.7	33.3	40.8	44.2	44.1	44.6	43.2	37.7	30.2	25.9
1998	23.5	26.8	32.3	37.7	42.8	46.7	45.9	45.0	42.7	38.5	33.1	30.3
1999	26.0	29.7	30.7	38.9	43.1	46.4	45.2	46.0	42.2	38.5	32.9	28.1
2000	26.3	27.4	31.3	40.2	43.1	44.6	46.0	45.0	41.1	37.6	31.0	26.9
2001	24.3	27.3	31.8	37.5	43.4	44.4	44.5	44.8	42.0	38.1	31.6	30.0
2002	25.5	27.1	32.1	36.3	43.2	44.7	45.5	45.1	42.2	38.5	31.2	27.1
2003	24.1	28.0	31.8	35.9	40.7	44.5	42.5	44.0	41.6	36.7	30.1	26.2
2004	24.8	27.9	33.2	36.2	41.2	43.5	44.1	43.2	40.2	37.1	31.1	24.7
2005	22.6	25.2	30.4	36.2	39.4	43.9	43.2	44.3	41.4	36.9	31.3	27.3
2006	23.3	28.0	30.1	35.7	42.0	45.4	44.0	43.1	41.2	37.5	30.8	22.3

B) Mean minimum temperature (°C) at Al-Ain (1995-2006).

Year	Jan	Feb	Mar	Apr	May	Jun	Jul	Aug	Sep	Oct	Nov	Dec
1995	12.7	13.8	15.7	19.8	23.8	25.7	26.5	30.2	26.2	23.3	17.8	16.0
1996	13.9	14.9	18.2	20.5	26.0	28.0	30.9	29.6	26.4	21.7	17.2	13.1
1997	11.8	13.9	16.1	19.1	23.5	27.8	28.7	28.5	27.0	24.0	18.8	14.5
1998	12.9	14.7	18.1	21.2	25.9	29.9	30.9	30.7	28.3	24.7	18.5	16.1
1999	12.9	16.5	16.0	21.4	24.3	28.4	29.7	31.4	27.5	23.1	19.3	14.1
2000	13.3	13.1	15.2	23.0	23.8	26.3	30.5	30.6	27.0	23.3	19.1	14.0
2001	10.8	12.7	16.3	20.1	25.6	27.3	30.3	30.0	26.9	23.4	18.1	17.4
2002	13.2	13.2	18.1	20.6	26.0	27.8	28.8	29.2	27.1	23.5	18.2	14.8
2003	10.4	14.5	17.0	20.2	23.5	26.8	30.0	30.1	27.3	21.2	16.5	13.0
2004	12.7	12.8	16.2	21.0	23.2	26.3	29.3	29.2	26.1	21.3	16.6	13.2
2005	11.4	13.2	16.2	20.3	24.0	26.6	29.4	28.9	26.0	22.0	18.0	13.4
2006	10.4	15.1	15.3	19.6	24.6	27.3	29.5	30.9	26.6	22.9	17.0	12.9

C) Mean monthly temperature (°C) at Al-Ain (1995-2006).

Year	Jan	Feb	Mar	Apr	May	Jun	Jul	Aug	Sep	Oct	Nov	Dec
1995	18.5	19.8	21.0	26.9	32.1	34.7	33.1	36.5	33.4	30.2	24.2	20.2
1996	18.5	20.7	23.4	28.5	34.1	35.3	38.1	36.3	33.4	28.7	23.4	19.3
1997	17.5	19.9	21.5	25.7	32.0	35.7	35.6	35.9	34.7	30.3	24.0	19.7
1998	17.8	20.4	24.7	29.2	34.1	37.9	37.8	37.4	35.2	31.0	25.3	22.6
1999	19.1	22.6	23.1	29.9	33.2	37.2	37.1	38.1	34.3	30.3	25.4	20.5
2000	19.3	19.6	22.6	31.3	32.9	35.2	37.8	37.2	33.4	30.1	24.6	20.1
2001	17.2	19.7	24.0	28.6	34.4	35.7	36.9	37.1	34.0	30.5	24.3	23.1
2002	19.0	19.9	24.8	28.3	34.6	35.8	37.1	36.7	34.2	30.7	24.3	20.7
2003	17.7	21.5	24.9	28.5	32.8	36.1	36.0	37.1	34.5	29.4	23.6	19.6
2004	19.0	20.3	25.2	29.0	32.9	35.5	37.0	36.4	33.0	29.7	24.2	19.3
2005	17.1	19.5	23.5	28.6	32.4	35.6	36.3	36.7	33.8	29.6	24.8	20.5
2006	17.1	21.7	22.9	28.1	33.7	36.0	37.0	37.0	34.0	30.4	24.2	17.6

D) Maximum monthly temperature (^{O}C) at Al-Ain (2003-2006).

Year	Jan	Feb	Mar	Apr	May	Jun	Jul	Aug	Sep	Oct	Nov	Dec
2003	28 9	33 5	38 0	40.5	43.8	47.0	46.1	46.8	44.3	41.2	34 5	30.8
2004	30 5	32.6	38 0	41 5	46 8	45.7	47 4	46 6	43.7	40.7	33.5	29.9
2005	26 8	29 1	35 6	41 0	43.8	47.1	46.5	48.0	43.9	41.1	36.2	32.9
2006	28.8	33.6	35 1	40 2	46 2	47.6	46.7	46.1	43.3	41.6	36.5	29.1

E) Minimum monthly temperature (^{O}C) at Al-Ain (2003-2006).

Year	Jan	Feb	Mar	Apr	May	Jun	Jul	Aug	Sep	Oct	Nov	Dec
2003	5.5	8.3	8.4	14 3	16.7	24.7	25.1	26.6	22.4	17.7	10.4	8.3
2004	7 6	8 5	11.6	16.8	17.5	19.9	24.6	25.5	22.8	18.5	14.6	7.0
2005	9 0	7 6	10.4	11.7	16.3	22.9	25.4	26.1	22.3	18.0	15.2	10.5
2006	5 7	8.8	9 0	12.9	20.2	22.5	25.5	27.6	22.8	20.1	13	9.8

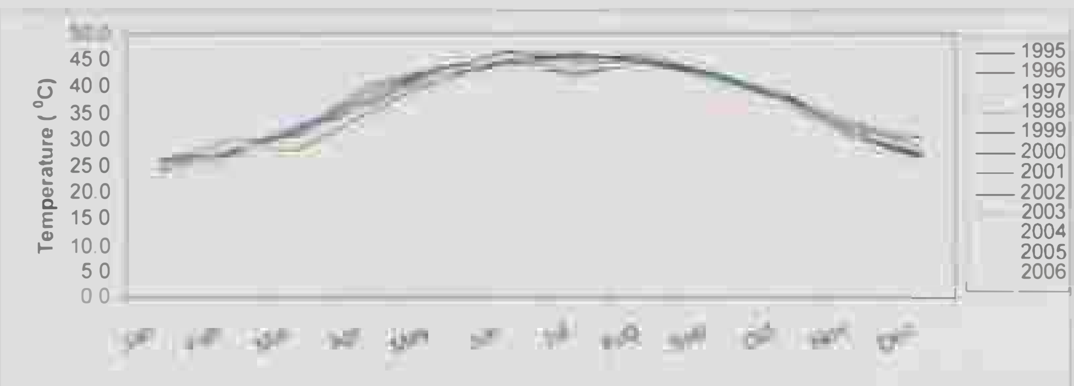

Fig. 3.1(a) Mean maximum temperatures at Al-Ain (1995-2006)

Fig. 3.1(b) Mean minimum tempertature at Al-Ain (1995-2006)

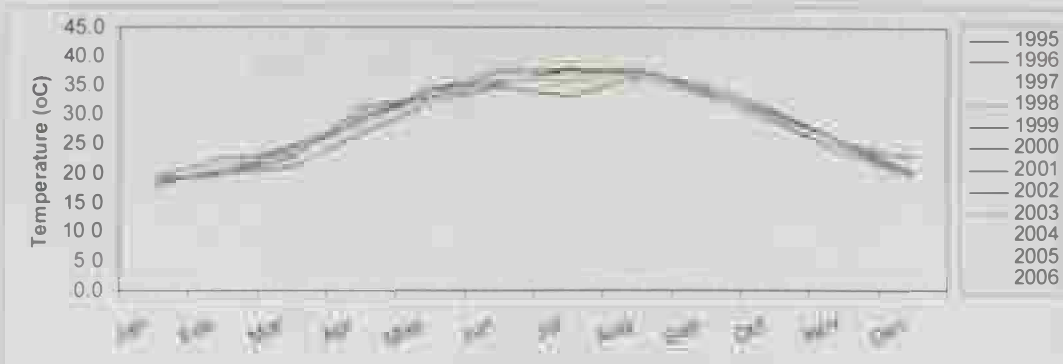

Fig. 3.1(c) Mean tempertature at Al-Ain (1995-2006)

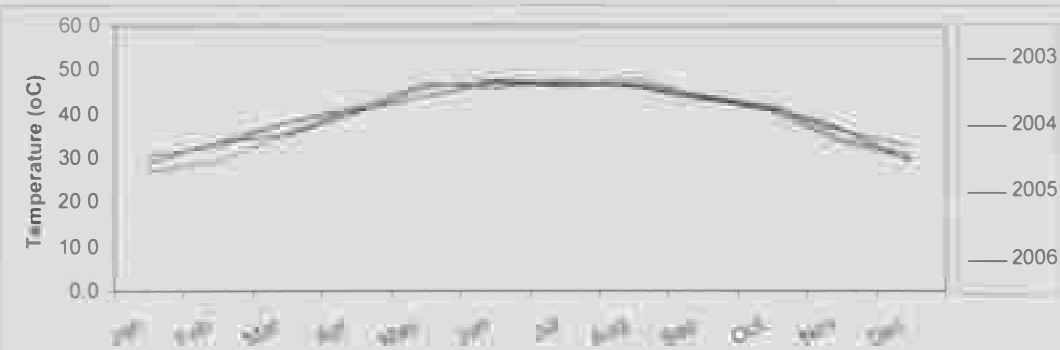

Fig. 3.1(d) Maximum tempertature at Al-Ain (2003-2006)

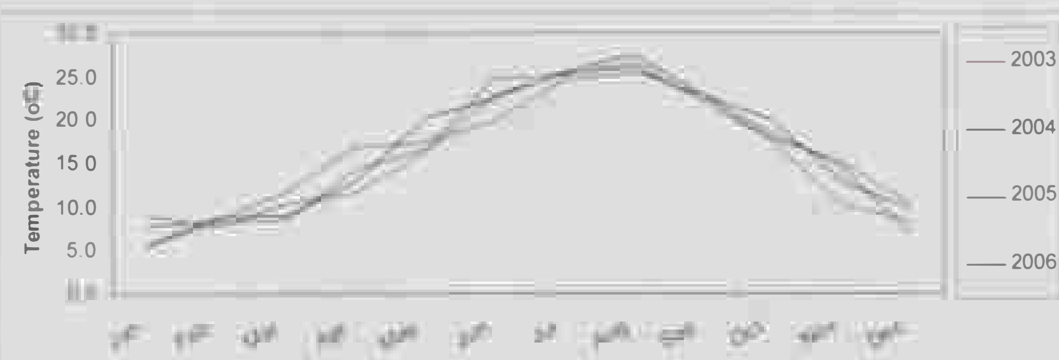

Fig. 3.1(e) Minimum tempertature at Al-Ain (2003-2006)

Table (3.2) Monthly total rainfall amount (mm) at Al-Ain (1995-2006).

Year	Jan	Feb	Mar	Apr	May	Jun	Jul	Aug	Sep	Oct	Nov	Dec
1995	0.0	14.8	40.8	1.0	0.5	0.0	48.8	1.1	0.0	0.0	0.0	12.8
1996	77.3	0.6	63.3	Trace	0.0	10.6	4.2	4.7	0.0	0.0	0.6	1.2
1997	53.5	0.0	55.9	9.0	0.0	0.0	Trace	Trace	0.0	3.4	4.4	8.7
1998	28.2	30.5	7.6	5.3	0.0	0.4	Trace	7.0	Trace	0.0	0.0	0.0
1999	Trace	Trace	16.8	0.0	3.6	0.0	0.0	1.8	Trace	0.0	0.0	0.0
2000	Trace	0.0	Trace	0.0	0.0	0.0	17.3	Trace	0.0	3.4	Trace	10.6
2001	Trace	0.0	Trace	0.0	0.0	0.0	Trace	0.0	Trace	Trace	0.0	0.0
2002	0.0	0.0	24.9	10.8	1.8	0.0	0.0	0.8	Trace	0.0	1.3	0.2
2003	3.0	0.7	17.4	99.8	0.0	0.0	57.2	0.0	0.0	0.0	0.0	0.0
2004	0.2	0.0	0.0	0.0	0.0	0.0	0.2	0.0	14.2	0.0	0.0	61.2
2005	37.0	0.0	0.8	0.0	0.0	0.0	0.0	10.0	0.0	0.0	0.0	0.2
2006	0.0	64.2	2.2	1.4	0.0	14.0	0.0	20.0	0.0	0.0	0.0	99.6

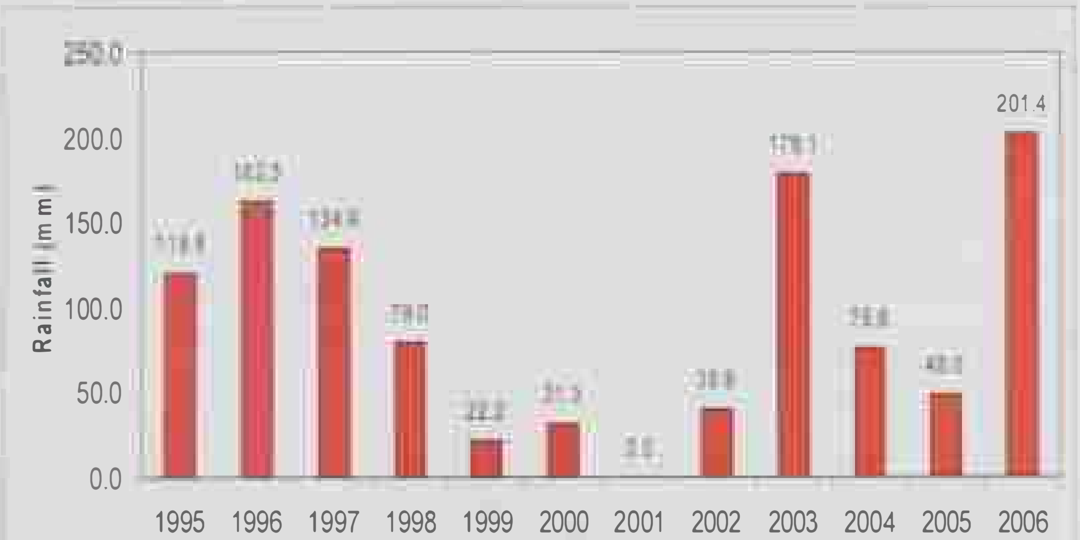

Fig. 3.2 Total yearly rainfull at Al-Ain (1995-2006)

3.1.4 Humidity

Relative humidity is high in the coastal areas, where the average reaches 60%. This rate however declines sharply moving inland from the coastline where its annual average reaches 39%. The relative humidity is lowest in the month of May, and increases during winter months. The mean maximum humidity value recorded in Al-Ain International Airport is 69% in the period of 2003-2006 and was recorded in December 2006. The minimum humidity value is 9% and was recorded in June 2000. The monthly mean maximum humidity is 94% and was recorded in December 2006. The monthly mean minimum humidity is 25% and was recorded in January 2000 (Figure 3.3 and Table 3.3).

3.1.5 Wind speed

Wind speed is generally light to moderate and its annual mean is 2.9 m/s (Table 3.4). There is a tendency for winds to be stronger between March and August. The predominant wind directions are from the northwest and south and southeast. The strongest winds are felt along the Gulf of Oman followed by mountain region, the Arabian Gulf coast and desert foreland. The lighter winds affect the internal parts of UAE (Figure 3.4).

Table (3.3) Humidity values at Al-Ain area.

A) Mean relative humidity (%) at Al-Ain (2003-2006).

Year	Jan	Feb	Mar	Apr	May	Jun	Jul	Aug	Sep	Oct	Nov	Dec
2003	55.0	45.4	35.4	34.1	23.3	27.1	40.0	40.0	30.0	38.6	51.3	55.3
2004	57.8	46.2	30.4	29.6	24.0	20.7	27.6	35.8	37.0	37.3	46.0	59.3
2005	59.1	54.9	44.2	28.0	25.6	30.2	33.9	31.4	35.3	33.3	50.0	57.8
2006	51.4	43.0	39.7	33.4	27.5	27.3	30.6	29.4	31.9	38.4	49.7	69.3

B) Mean maximum relative humidity (%) at Al-Ain (2003-2006).

Year	Jan	Feb	Mar	Apr	May	Jun	Jul	Aug	Sep	Oct	Nov	Dec
1995	88	81	87	57	49	63	81	57.0	66.0	67	78	88
1996	88	84	83	62	44	68	49	58	76	71	77	82
1997	90	83	85	75	52	61	73	78	70	74	84	88
1998	92	86	77	66	50	50	57	54	63	67	85	85
1999	87	84	79	58	59	48	63	48	65	77	81	83
2000	89	85	79	53	62	60	40	43	64	70	73	85
2001	86	82	74	54	76	57	53	44	63	71	76	78
2002	76	75	67	65	47	56	52	61	66	68	73	75
2003	88	87	64	64	48	58	63	55.5	63.6	73	77	86
2004	85	80	64	53	51	44	48	64	65	73	74	87
2005	90	86	76	51	49	67	55	61	70	64	80	92
2006	79	74	80	65	53	53	55	46	63	70	82	95

Fig. 3.3(a) Mean relative humidity at Al-Ain (2003-2006)

Fig. 3.3(b) Mean maximum relative humidity at Al-Ain (1995-2006)

Table (3.4) wind speed values at Al-Ain area.

A) Mean wind speed (m/s) at Al-Ain (2003-2006).

Year	Jan	Feb	Mar	Apr	May	Jun	Jul	Aug	Sep	Oct	Nov	Dec
2003	2.7	3.1	3.6	3.3	3.1	3.1	3.4	3.1	3.3	2.8	2.6	2.3
2004	2.4	2.5	3.2	3.2	3.0	3.2	3.0	2.9	2.3	1.9	1.2	1.1
2005	2.1	3.1	2.9	3.1	3.3	2.8	3.3	3.2	3.1	3	2.6	2.3
2006	2.5	3.0	3.0	3.1	3.2	3.3	3.2	3.5	3.2	2.9	2.6	2.6

B) Maximum wind speed (m/s) at Al-Ain (2003-2006).

Year	Jan	Feb	Mar	Apr	May	Jun	Jul	Aug	Sep	Oct	Nov	Dec
2003	12.7	11.2	14.2	14.2	10.4	9.4	17.1	9.2	13.7	8.5	7.9	11.0
2004	9.8	9.3	13.7	9.9	10.6	12.4	10.6	13.3	15.9	8.3	5.8	10.7
2005	9.8	11.7	8.7	9.9	10.4	12.9	14.8	20.7	9.3	12	10.3	7.7
2006	12.3	11.7	10.6	11.2	9.6	12.5	11.5	14.9	16.2	8.8	12.8	10.4

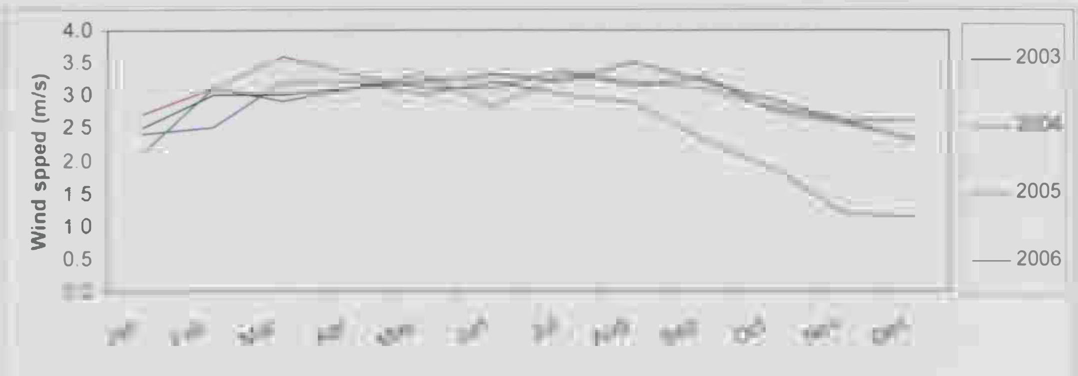

Fig. 3.4(a) Mean wind speed at Al-Ain (2003-2006)

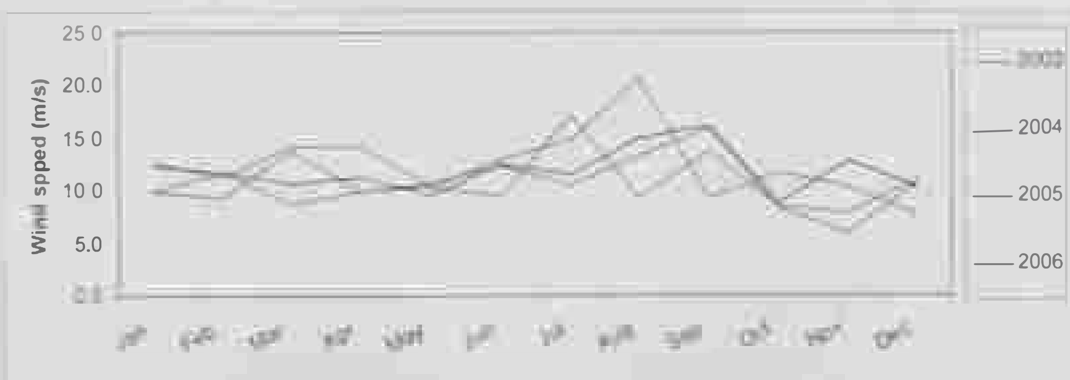

Fig. 3.4(b) Maximum wind speed at Al-Ain (2003-2006)

3.1.6 Evaporation

Air temperature, relative humidity and wind speed are the main factors controlling the evaporation. The western coast has the lowest annual average 7.5 to 8.0 mm/day and the eastern coast has much higher evaporation rate of 9.0 to 9.5 mm/day (Rizk, 1999). The maximum values are recorded in June to August, while the minimum values are recorded in December and January. The maximum mean evaporation in Al-Ain area is 22 mm/day during 1994-2000 and the minimum mean evaporation is 5.1 mm/day during the same period (Figure 3.5 and Table 3.5).

Table (3.5) Mean total evaporation (mm) At Al-Ain area.

Year	Jan	Feb	Mar	Apr	May	Jun	Jul	Aug	Sep	Oct	Nov	Dec
1995	5.7	7.5	8.5	14.5	19.9	19.8	15.4	18.5	16.2	13.7	8.5	5.3
1996	5.1	7.6	10.3	15.7	20.1	18.9	21.5	18.3	16.3	13.1	8.9	6.3
1997	5.5	8.8	8.5	12.9	20.4	21.3	18.0	18.1	17.2	13.6	7.6	5.9
1998	5.3	7.8	12.8	17.0	20.4	21.0	21.9	20.4	17.7	14.0	8.7	7.1
1999	6.4	8.8	11.8	17.1	19.4	22.0	19.7	21.1	16.9	13.0	8.9	6.9
2000	6.7	8.1	12.0	17.0	19.1	19.6	20.4	19.3	15.0	12.9	9.0	6.5
2001	6.3	8.0	11.4	15.8	19.3	19.1	19.4	20.1	16.5	13.0	9.1	7.0
2002	7.1	9.0	11.7	15.8	19.9	20.4	20.3	18.1	17.1	13.6	8.7	7.1

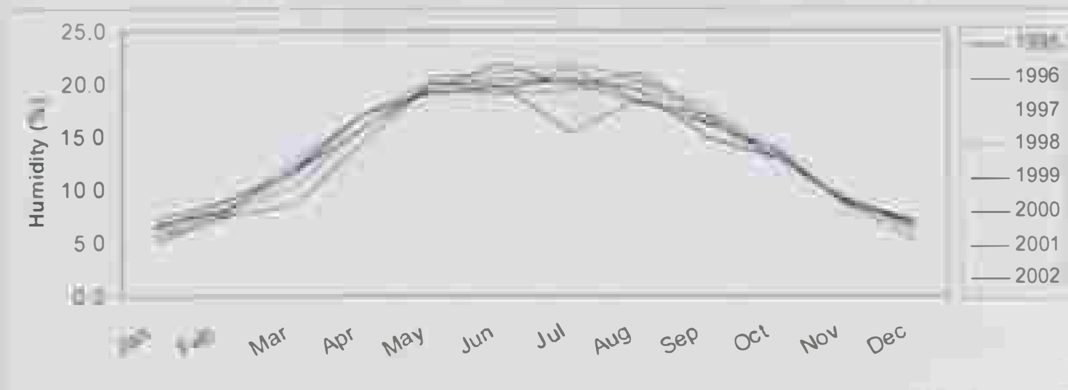

Fig. 3.5 Mean total evaporation at Al-Ain (1995-2002)

3.2 Hydraulic Head

The groundwater depth in Al-Foah area is about 30 m below the ground surface increasing to the north and south (Figure 3.6). The continuous increasing of depth to groundwater in Suweyhan to 50 m and Al Ain to 90 m is a result of excessive groundwater pumping for different purposes (Garamoon, 1996).

3.3 Groundwater Recharge

For estimating groundwater recharge for existing aquifers in study area (Figure 3.7), Al-Ain area should be subdivided into three regions: the piedmont plain, northern basin and southern basin. The northern basin includes Al Jaww plain, Al Ain city and the southern desert area.

Recharge to both basins originates primarily as runoff from the northern Oman Mountains. In the northern basin, which includes Al-Foah area, surface flow through the wadis occasionally reaches the area and recharge occurs by direct infiltration. More often, however, the surface flow ceases before it reaches the northern basin, and recharge occurs through alluvial deposits, principally in buried wadi channels. Small amounts of recharge occur by direct infiltration, although it requires a high intensity rainfall in order to overcome soil moisture requirements. It has also been suggested that recharge occurs as flow through fractures in surrounding limestone ridges or as upward leakage from underlying aquifers (Garamoon, 1996).

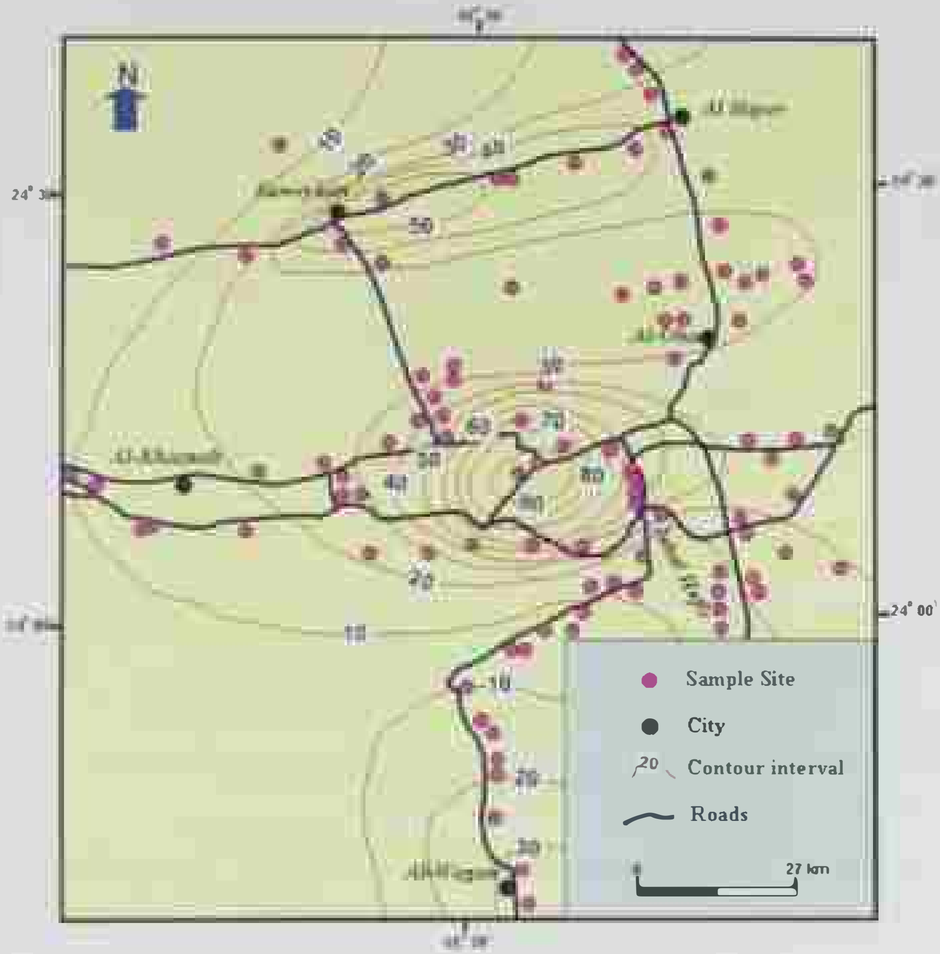

Figure (3.6) Map showing the depth to groundwater (m) of the Quaternary aquifer in Al-Ain area (modified after Garamoon, 1996)

Figure (3.7) The main water bearing units (aquifers) in the United Arab Emirates (after Rizk et al, 1997 and Al-Nuaimi, 2003)

Hyde (1992) also estimated the recharge to the southern Al-Ain basin based on groundwater gradient, transmissivity and length of boundary to be about 14 million m^3/yr.

3.4 Hydraulic Properties of the Al-Ain Aquifers

The Quaternary sediments in Al Ain area is represented by eolian sand in the north, northwest, west and southwest and alluvial gravel in the east (Al Jaww plain) and within the city. The Cretaceous limestone especially at Jabal Muhayer north Al-Ain (Al-Foah) represents a good aquifer with high specific capacity wells. Since there is no known deep fresh water aquifer in the area, water in these fractured limestone rocks is apparently derived from the overlying sands and gravel.

3.5 Surface water – Groundwater Relationship

Because the prevailing climate within Al-Foah area is arid and the mean annual potential evapotranspiration (PET) is much greater than the mean annual rainfall, monthly and daily water surpluses associated with occasional heavy rain acquire a great importance in groundwater recharge.

According to method described by Boonstra and de Ridder (1981), groundwater recharge of Quaternary aquifer in Al-Ain area was calculated by Garamoon in 1996. He concluded that a mean annual rainfall greater than 140 mm can cause groundwater recharge in Al-Ain area. In contrast, no groundwater recharge is expected if the mean annual rainfall is less than 140 mm. Inspection of the rainfall data of Al-Foah meteorological station for the period 1995 – 2006 shows that the annual rainfall that can contribute to groundwater recharge occurs once every four to five years. This recharge is more likely to occur during cycles with the same time intervals of above average rainfall.

Chapter IV

HYDROGEOCHEMISTRY

CHAPTER IV

HYDROGEOCHEMISTRY

Fifty samples were collected for this study from private and government production wells in November and December of 2005 to characterize the Quaternary aquifer of Al-Foah area hydrogeochemically (Figure 4.1). The direct measurements in the field were conducted for electrical conductivity (EC) (μS/cm), total dissolved solid (TDS) (mg/l), hydrogen ion concentration (pH), salinity (%), and temperature (°C). Two bottles of groundwater samples were collected for each well. The samples for anions analyses were stored at 4°C whereas the samples for cations analyses were preserved with a few drops of acid (HNO_3). Then the samples were analyzed for major cations (K^+, Na^+, Mg^+ and Ca^{2+}), major anions (CO_3^{2-}, HCO_3^{2-}, SO_4^{2-}, Cl^-, $PO_4^{4-}$and NO_3^-) and trace metals (Mn, Cu, Fe, F, Pb, B, Ba, Sr, Cr and Zn). The entire chemical analyses for major cations, anions and trace metals were analyzed in the Central Laboratories Unit (CLU) in the United Arab Emirates University. All chemical data is listed in Appendix.

4.1 Electrical Conductivity (EC)

Electrical Conductivity of a solution is a measure of the ability of a solution to conduct an electrical current (George and Edward 1987). Because the electrical current is transported by the ions in solution, the conductivity increases as the concentration of ions increases. The electrical conductivity of water samples collected from the Quaternary aquifer in the Al-Foah area varied between 1 and 12.6 mS/cm. The distribution of electrical conductivity of the groundwater is shown in Figure 4.2. The areas located in the north and south are characterized by high values and the rest of the areas are lower than 12 mS/cm. The high values of

EC are an indication of increasing groundwater salinity, which might be attributed to agricultural activities, and evaporation as discussed in coming sections.

4.2 Total Dissolved Solid (TDS)

The total dissolved solids in groundwater samples include all solid materials in solution whether ionized or not. It does not include suspended sediment, colloids or dissolved gases. The TDS content in groundwater is an indication of its salinity. A simple classification of groundwater salinity depending on the total concentration of dissolved constituents, as proposed by Todd (1980), is given in table 4.1. The average TDS in the study area is 2305 mg/l, with high concentrations observed in the north and south near the agricultural areas (see Figure 4.3). According to Todd's (1980) classification, about 18% of groundwater samples are considered as fresh water and about 82% are considered as brackish water. It is clear that the groundwater progressively becomes saline and the continued increase of salinity in groundwater might be ascribed to the effect of intensive agriculture activities as will be discussed in coming sections.

Table 4.1 Classification of groundwater in the study area according to its TDS content in (mg/l) (Todd, 1980).

Water type	Total Dissolved Solid (TDS) (mg/l)	Well No.	%
Fresh water	0 – 1000	14,17,18,19,20,35,46,47,49	18
Brackish water	1000 – 10000	1,2,3,4,5,6,7,8,9,10,11,12,13 15,16, 21,22,23,24,25,26,27, 28,29,30,31,32,33,34,36,37, 38,39,40,41,42,43,44,45,48, 50.	82
Saline water	10000 – 100000	-	0
Brine	> 100000	-	0

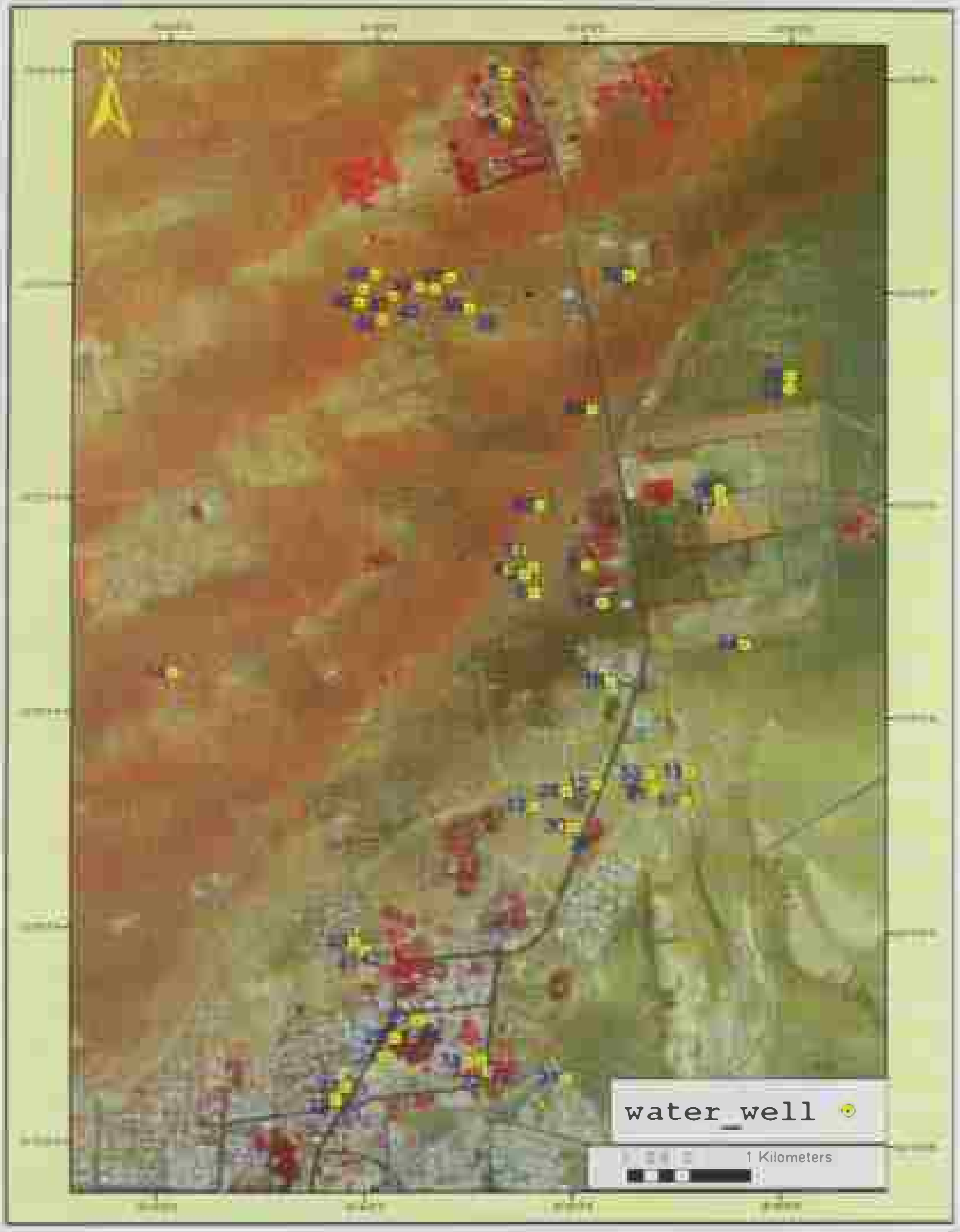

Figure (4.1) A base map showing the location of the wells in Al-Foah area.

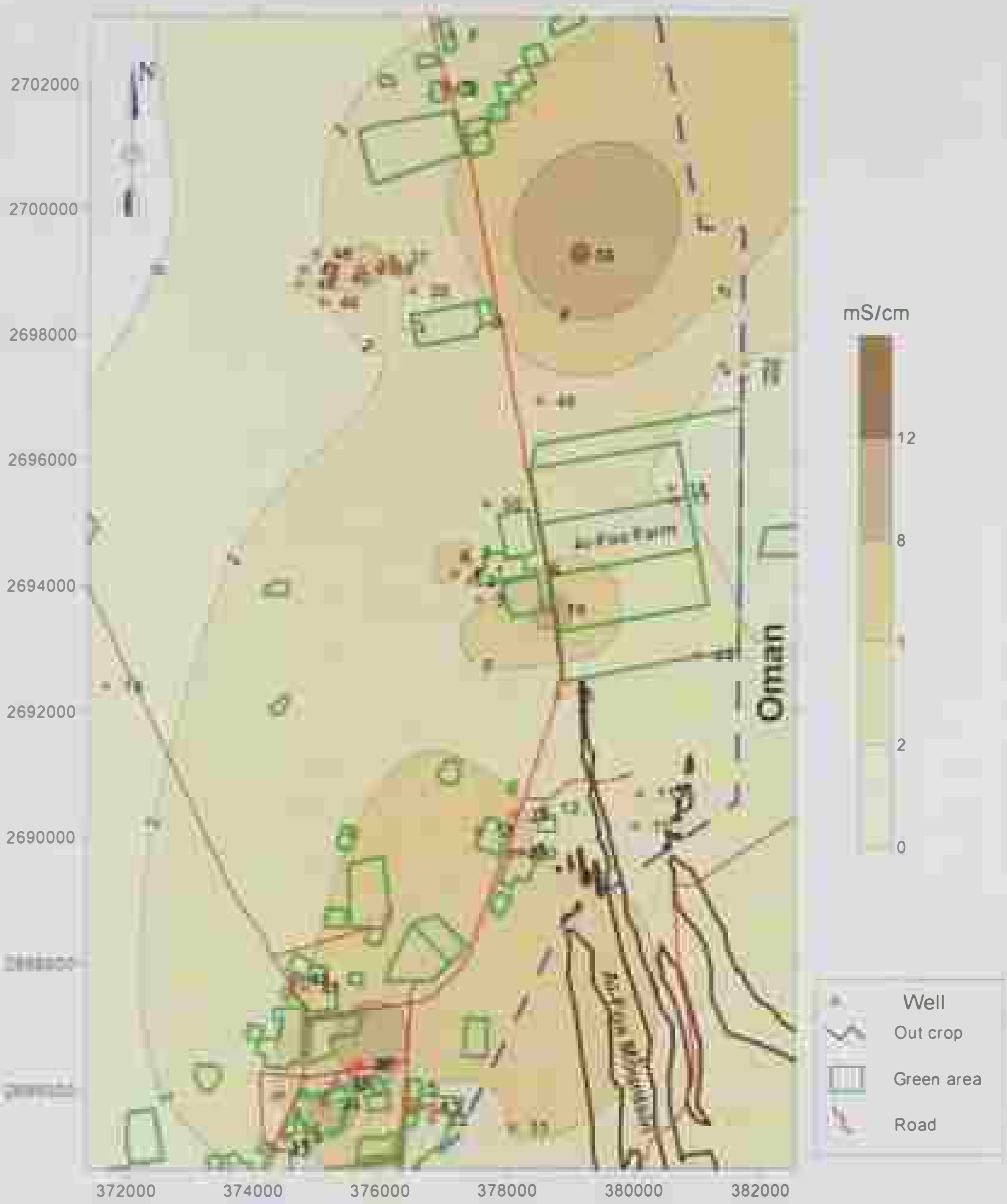

Figure (4.2) Map showing the distribution of the Electrical Conductivity (mS/cm) in Al Foah area.

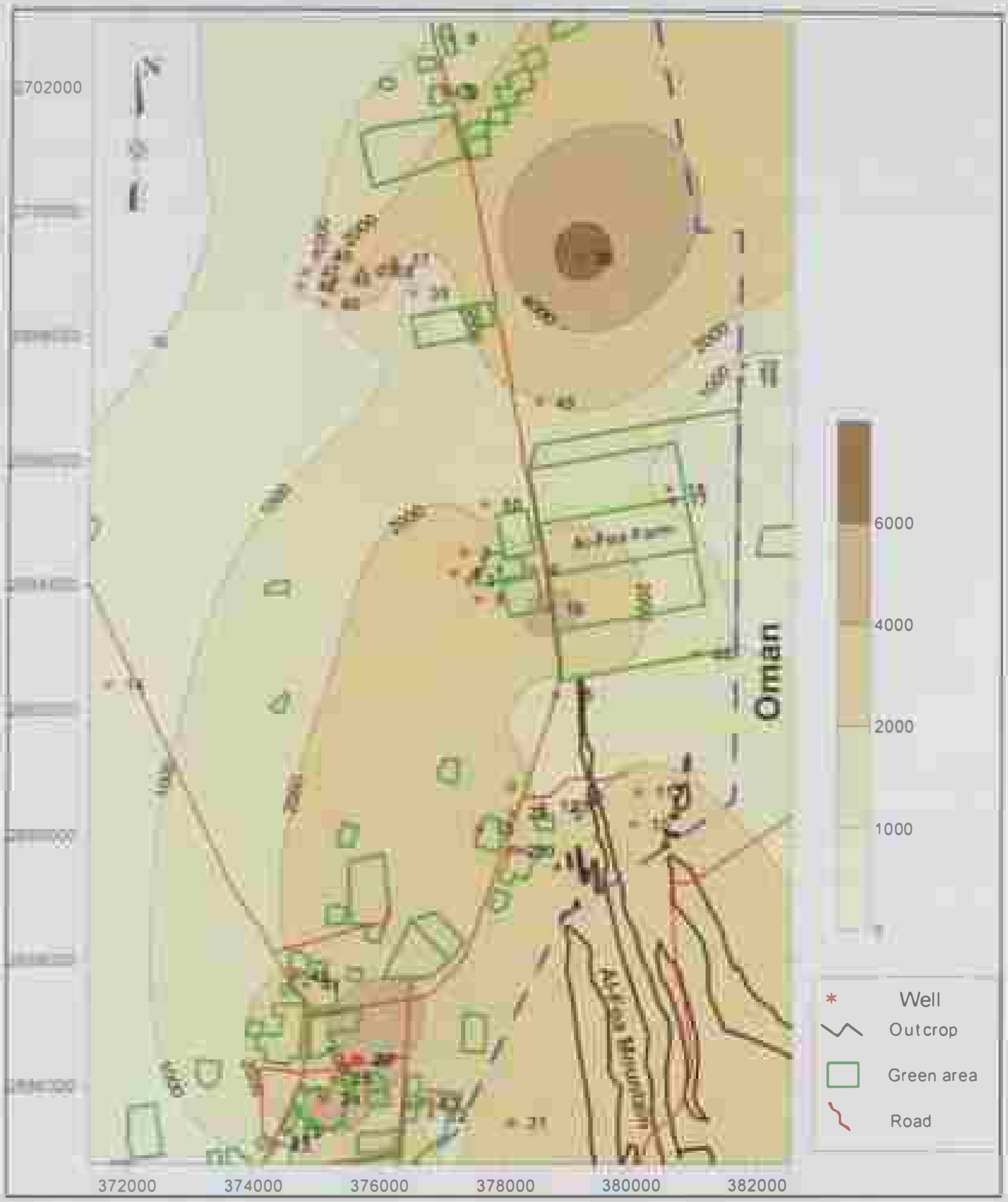

Figure (4.3) Map showing the distribution of Total Dissolved solid (TDS) in Al-Foah area.

4.3 Concentration of Hydrogen Ion (pH)

The pH is a measure of the acidity and alkalinity of the groundwater, or hydrogen ion concentration on a logarithmically calculated scale (Gymer, 1973). The pH of water is controlled by the amount of dissolved carbon dioxide (CO_2), carbonate (CO_3^{2-}) and bicarbonate (HCO_3^-) (Domenico and Schwartz, 1990).

The pH scale ranges from 0 to 14. A pH of 7 indicates neutral water, greater than 7, the water is basic, and less than 7 it is acidic. According to U.S. Environmental Protection Agency criteria, water for domestic use should have a pH between 5.5 and 9. The pH of the groundwater in the study area varied between 6.1 to 7.9 with an average of 7.0. The groundwater samples are consistently neutral water. The distribution of pH of the groundwater is shown in Figure 4.4.

4.4 Temperature

The temperature of groundwater samples in the Al-Foah area varied between 22.7°C and 38.4°C with an average of 31.7°C (Figure 4.5). This is high possibly due to the less recharge (less rainfall) for the aquifers presented in the Al-Foah area as discussed in chapter 3.

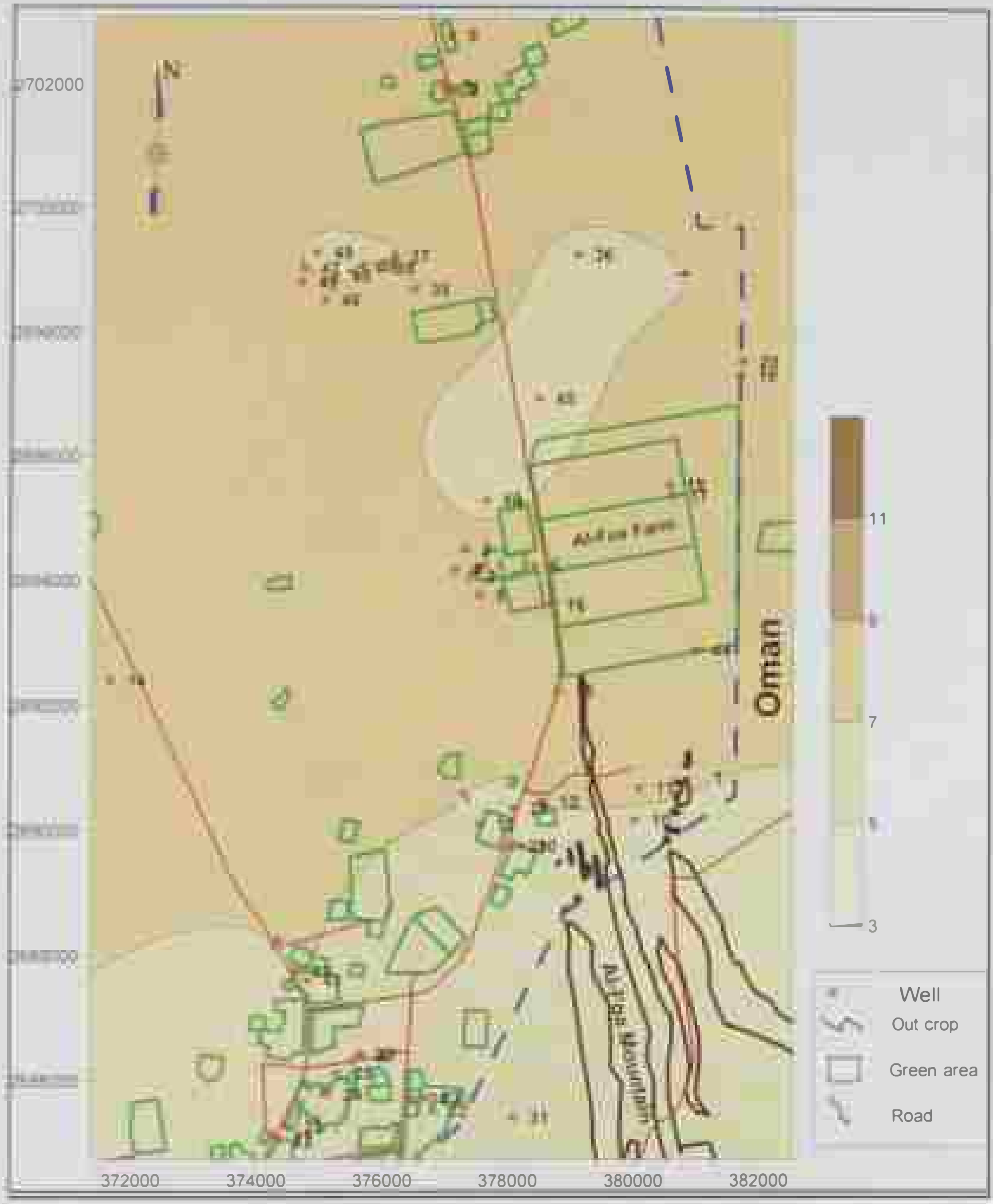

Figure (4.4) Map showing the distribution of pH in Al-Foah area.

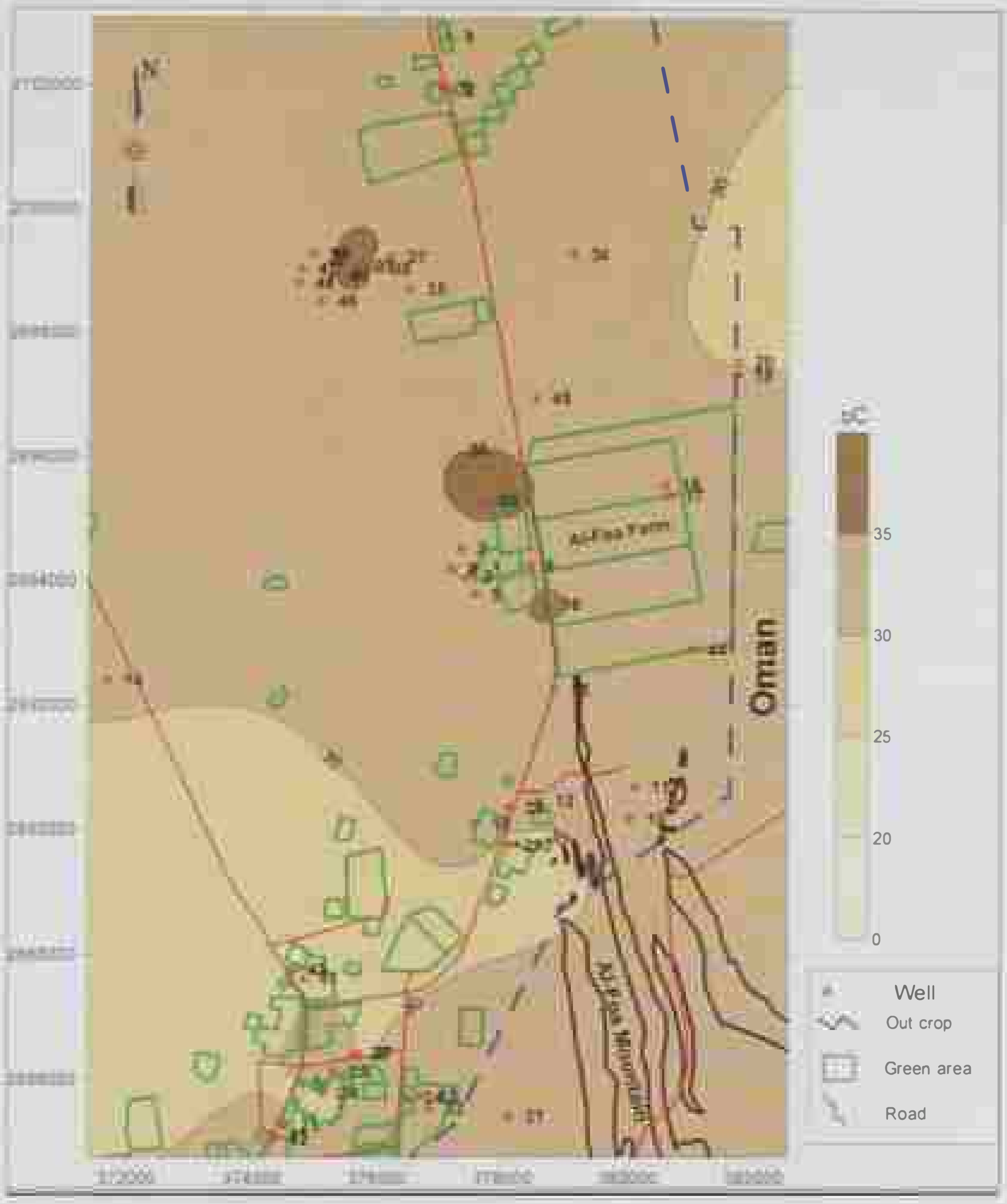

Figure (4.5) Map showing the distribution of groundwater temperature in Al-Foah area.

4.5 Major anions

The sequence of anions dominance in groundwater of the Quaternary aquifer in the Al-Foah area is in the order of: $Cl^- > SO_4^{2-} > HCO_3^{2-} > CO_3^{2-}$. The following is brief discussions of these anions.

4.5.1 Chloride (Cl^-)

Chloride ion concentrations in groundwater of the study area ranged from 96.7 to 3320 mg/l with an average of 911 mg/l, except well no. 36 which has a concentration of 6550 mg/l. Figure 4.6 shows a steady increase of Cl^- concentration in the north of Al-Foah which might be related to intense groundwater pumping, agricultural activities and evaporation of return flow. The majority of samples are located above the line of seawater as seen from the relationship of Cl/Br vs. Cl (Figure 4.7), which clearly indicated that the excess of chloride could come from different sources. In addition, the positive correlation (r^2 = 0.8) between Cl vs. Br (Figure 4.8) supported the fact that both Cl and Br might come from the same sources. One of the sources that releases Br to the system might be the agriculture practices as observed from the positive relationship between K and Br (Figure 4.9).

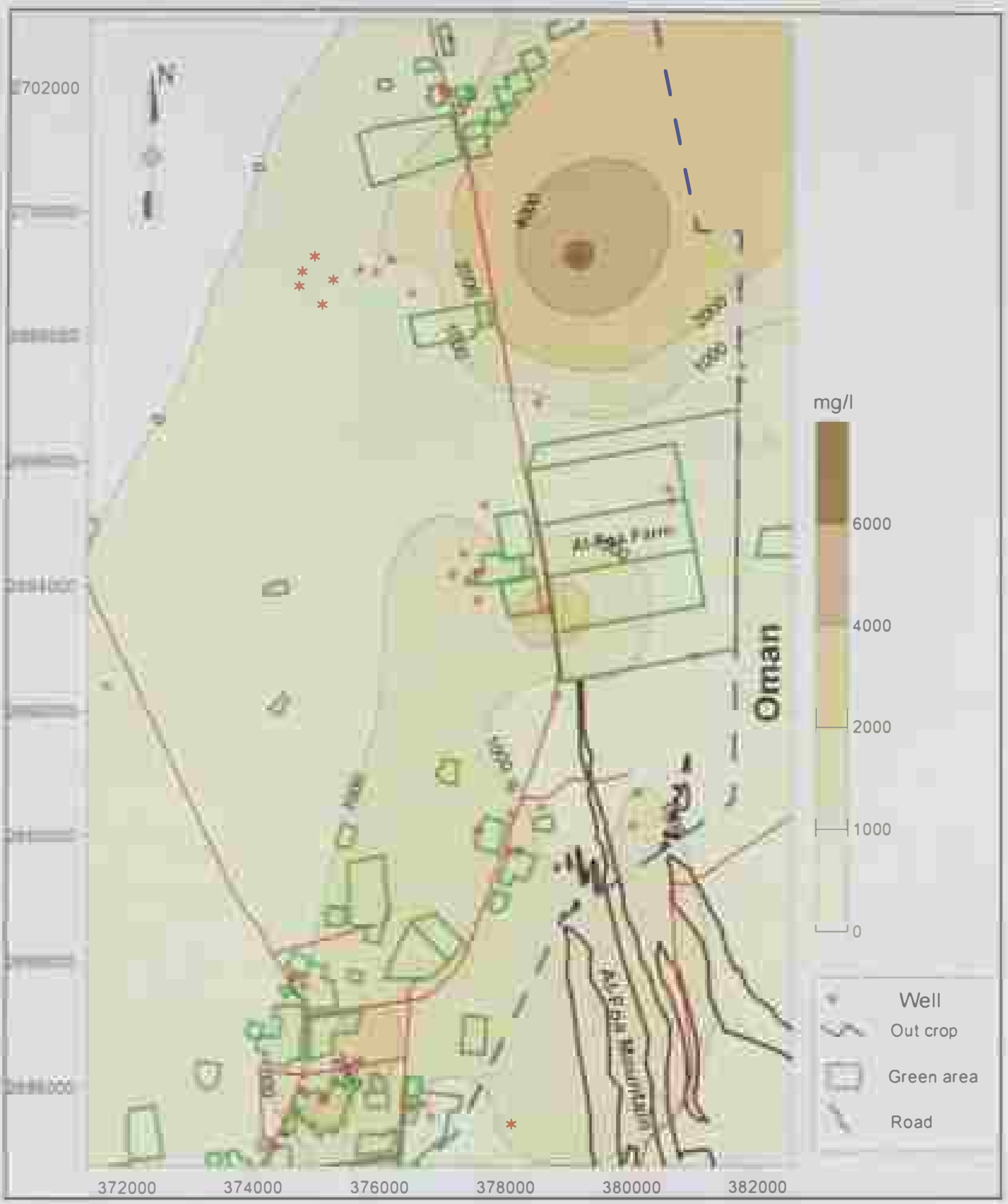

Figure (4.6) Map showing the distribution of the chloride anion (mg/l) in Al-Foah area.

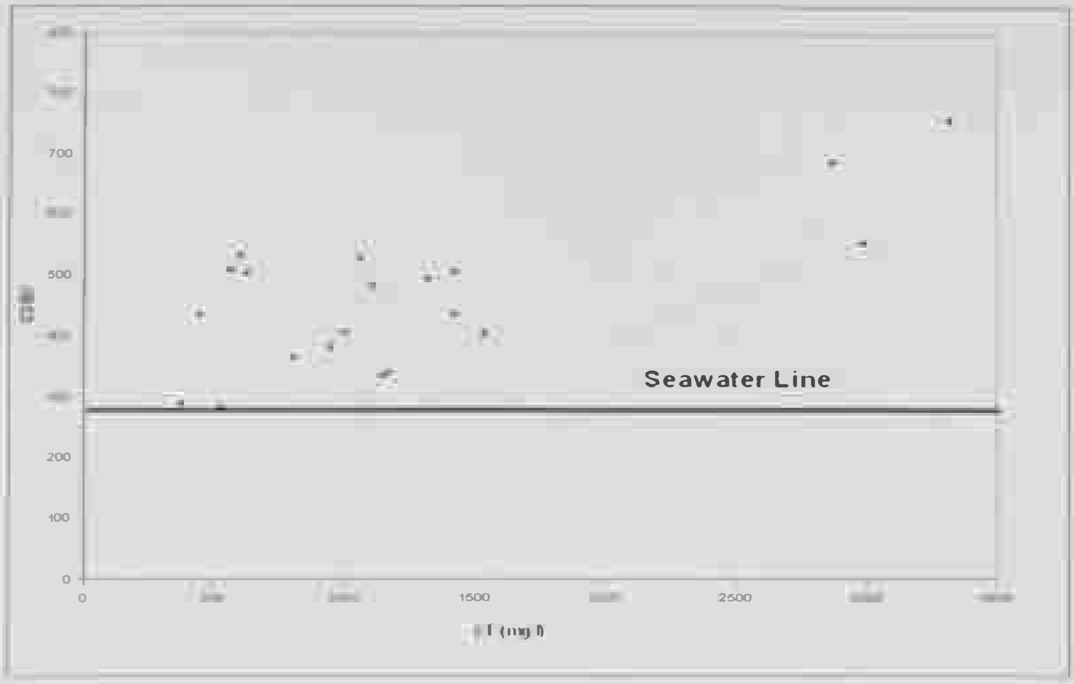

Figure (4.7) Plot showing Cl/Br Ratio vs. Cl for groundwater samples in the Al-Foah area.

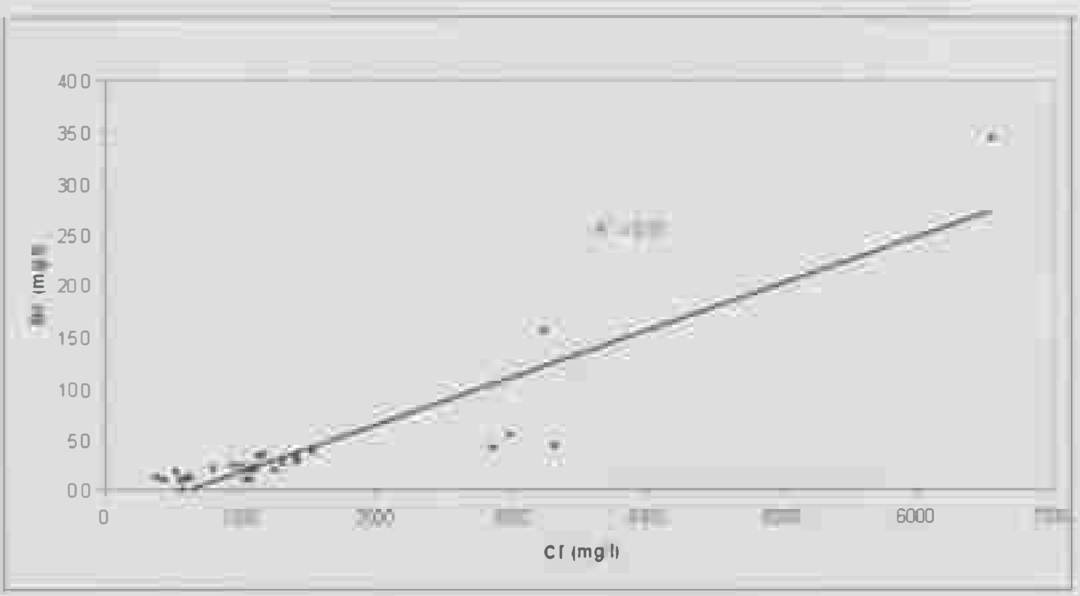

Figure (4.8) The relationship between chloride and bromine for the groundwater in the Al-Foah area.

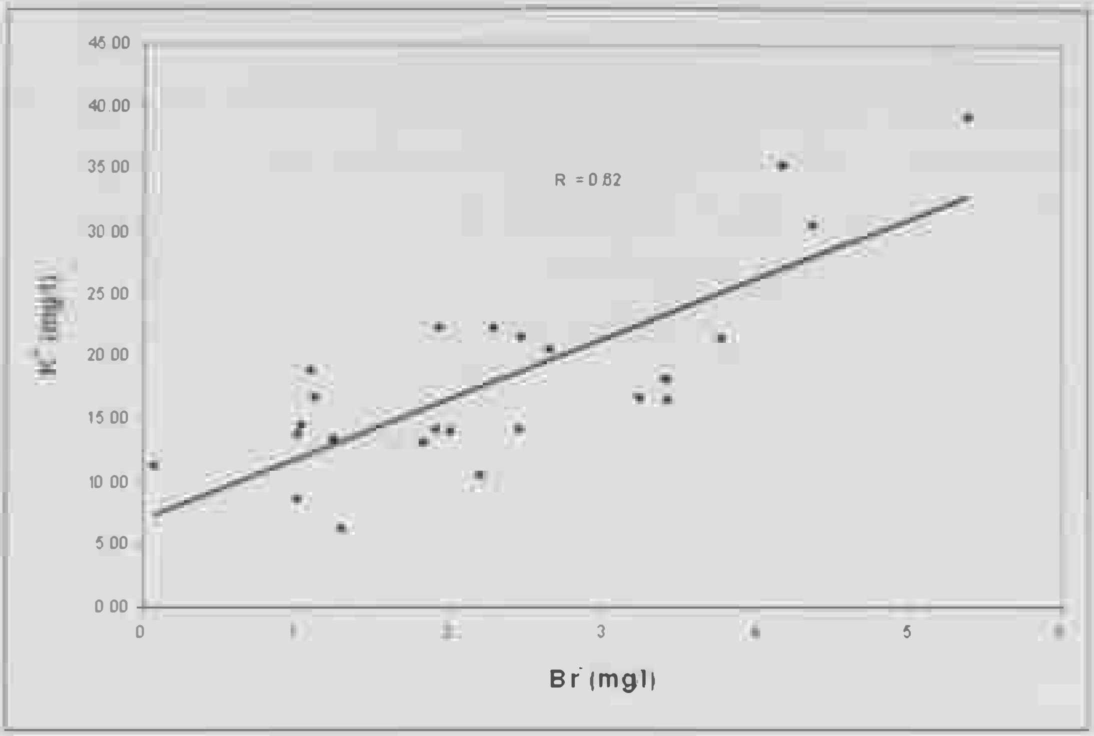

Figure (4.9) The relationship between bromine and potassium for the groundwater in the Al-Foah area.

4.5.2 Sulfate (SO_4^{2-})

Despite a relatively large amount of sulfur, mostly in the form of sulfates (SO_4^{2-}) in water and in sedimentary rocks, sulfur is only a minor constituent of igneous rocks. All atmospheric precipitation contains sulfate, which although common in absolute concentrations of less than 2 ppm, is one of the major dissolved constituents of rain and snow. The sulfate in the atmosphere is derived from dust particles containing sulfate minerals from the oxidation of sulfur dioxide gas and from the oxidation of hydrogen sulfide gas (Davis and DeWeist, 1966).

The values of the sulfate in the Al-Foah area ranged between 40 and 3090 ppm. The high values are in the southern area of Al-Foah (Figure 4.10). The most extensive occurrences of sulfate ions in water are sedimentary rocks as gypsum ($CaSO_4.2H_2O$) and anhydrite ($CaSO_4$). These two minerals are present in the study area as thick beds or streaks in limestone strata and are sufficiently soluble to cause water in contact with them to be high in sulfate. Further additions of sulfate to groundwater arise from the breakdown of organic substances in soil from the addition of leachable sulfate in fertilizers and from other human influences (Matthess, 1982).

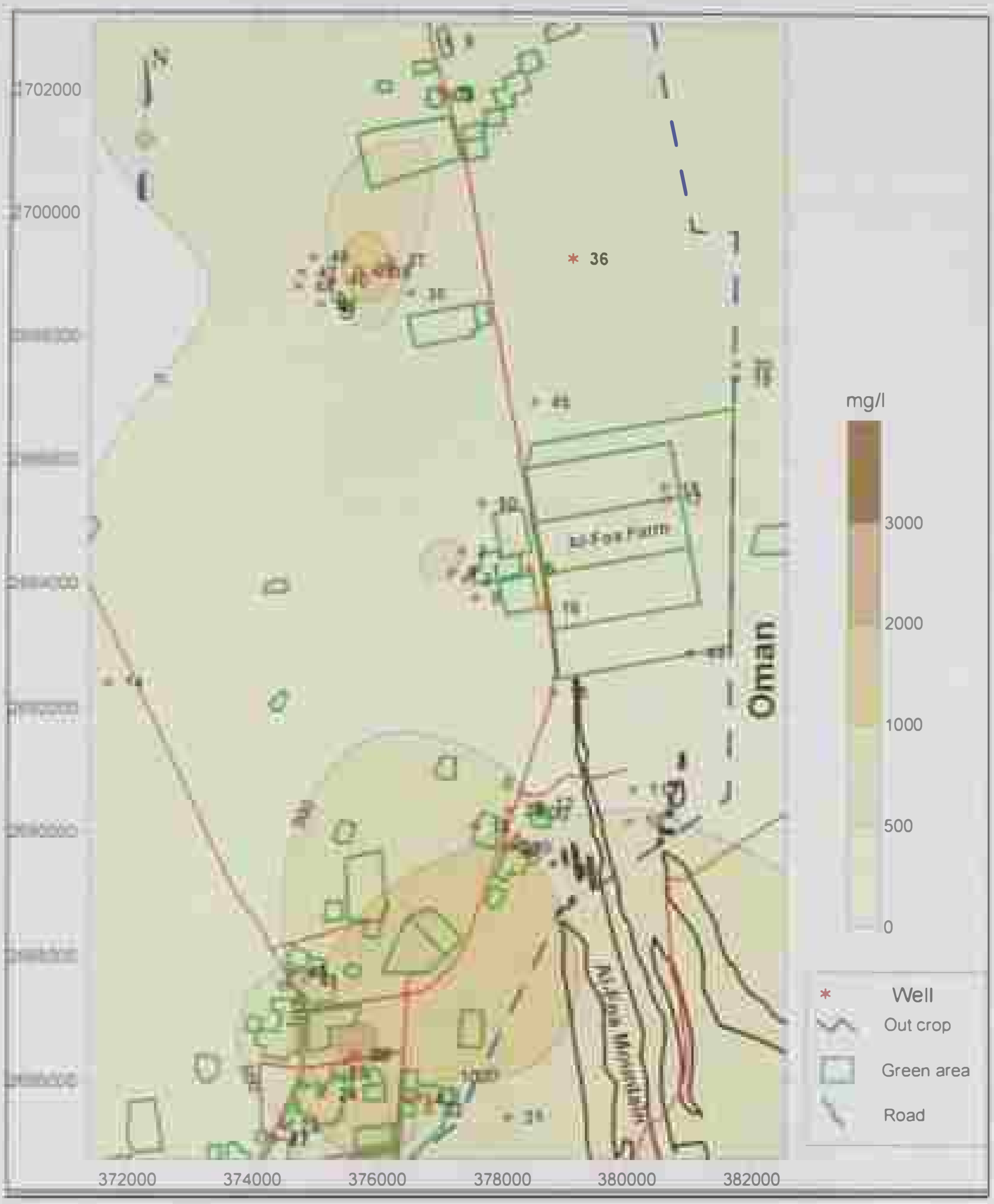

Figure (4.10) Map showing the distribution of the sulfate anion (mg/l) in Al-Foah area.

4.5.3 Bicarbonate (HCO_3^-)

The presence of bicarbonate ions (HCO_3^-) in groundwater is derived from carbon dioxide in the atmosphere, soils and dissolution of carbonate rocks (Davis and DeWeist, 1966). In the absence of calcareous sediments and carbonate rocks, most HCO^- in groundwater results from the dissolution of carbon dioxide within the soil zone by organic decay.

Bicarbonate ion concentration in groundwater of the Quaternary aquifer in the Al-Foah area ranged from 85 ppm in the north to 515 ppm in the south of Al-Foah. The iso-concentration contour map (Figure 4.11) shows a steady increase in HCO_3^- concentration from north to south, because of presence of limestone from Simsima Formation.

4.5.4 Carbonate (CO_3^{2-})

Because the dominant carbon form in natural water is HCO_3^- (Freeze and Cherry, 1979), the concentration of the CO_3^{2-} in groundwater within the study area is generally low, within a pH range of 6 to 8. Therefore the CO_3^{-2} is not significant. In water with a pH greater than 8, carbonate ions (CO_3^{2-}) exist.

In the Al-Foah area, CO_3^{2-} concentration generally increased from east to west (southern side) (Figure 4.12), and the concentration of carbonate in groundwater ranged from 4 to 23 mg/l with an average of 8 mg/l.

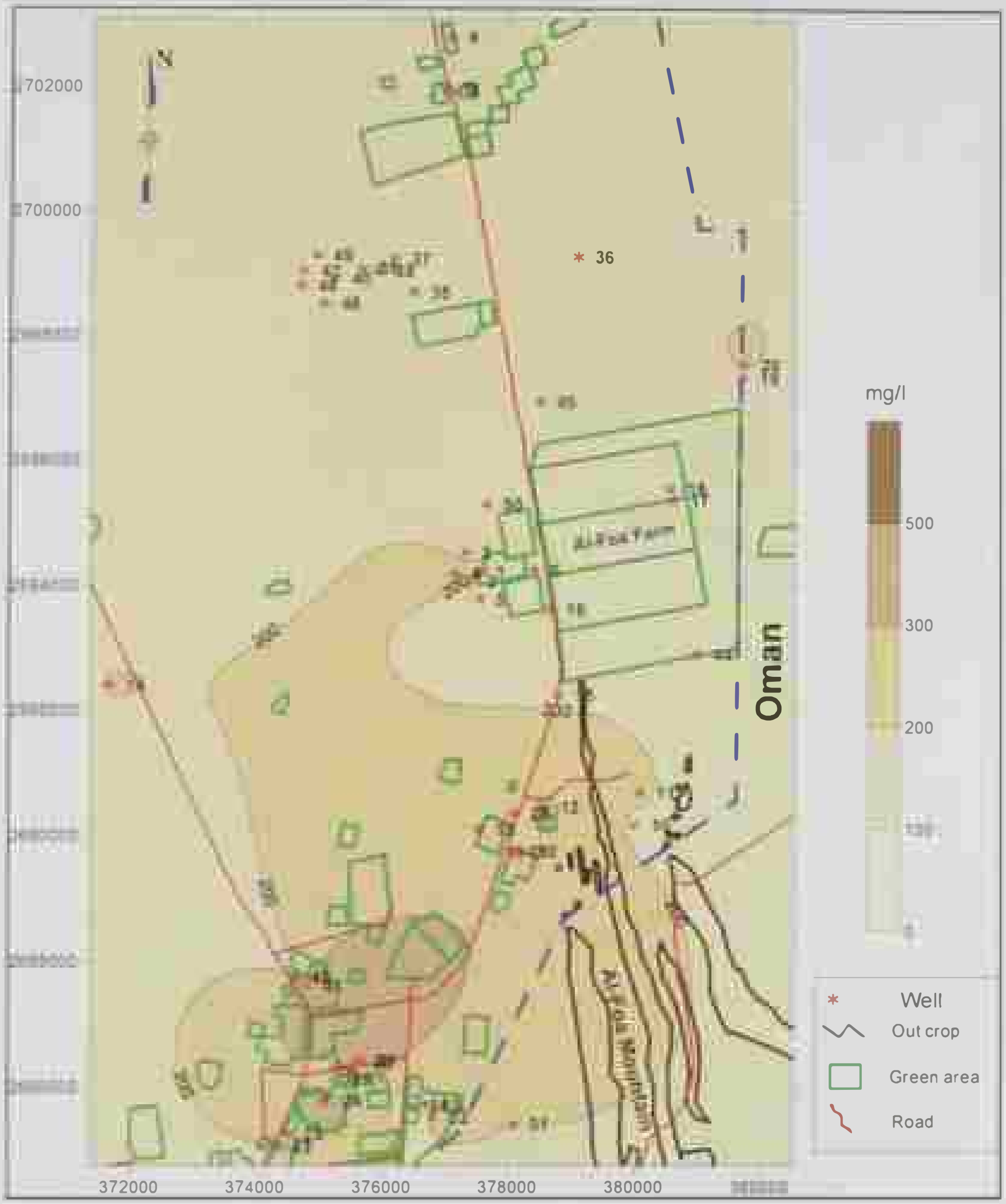

Figure (4.11) Map showing the distribution of the bicarbonate anion (mg/l) in Al-Foah area.

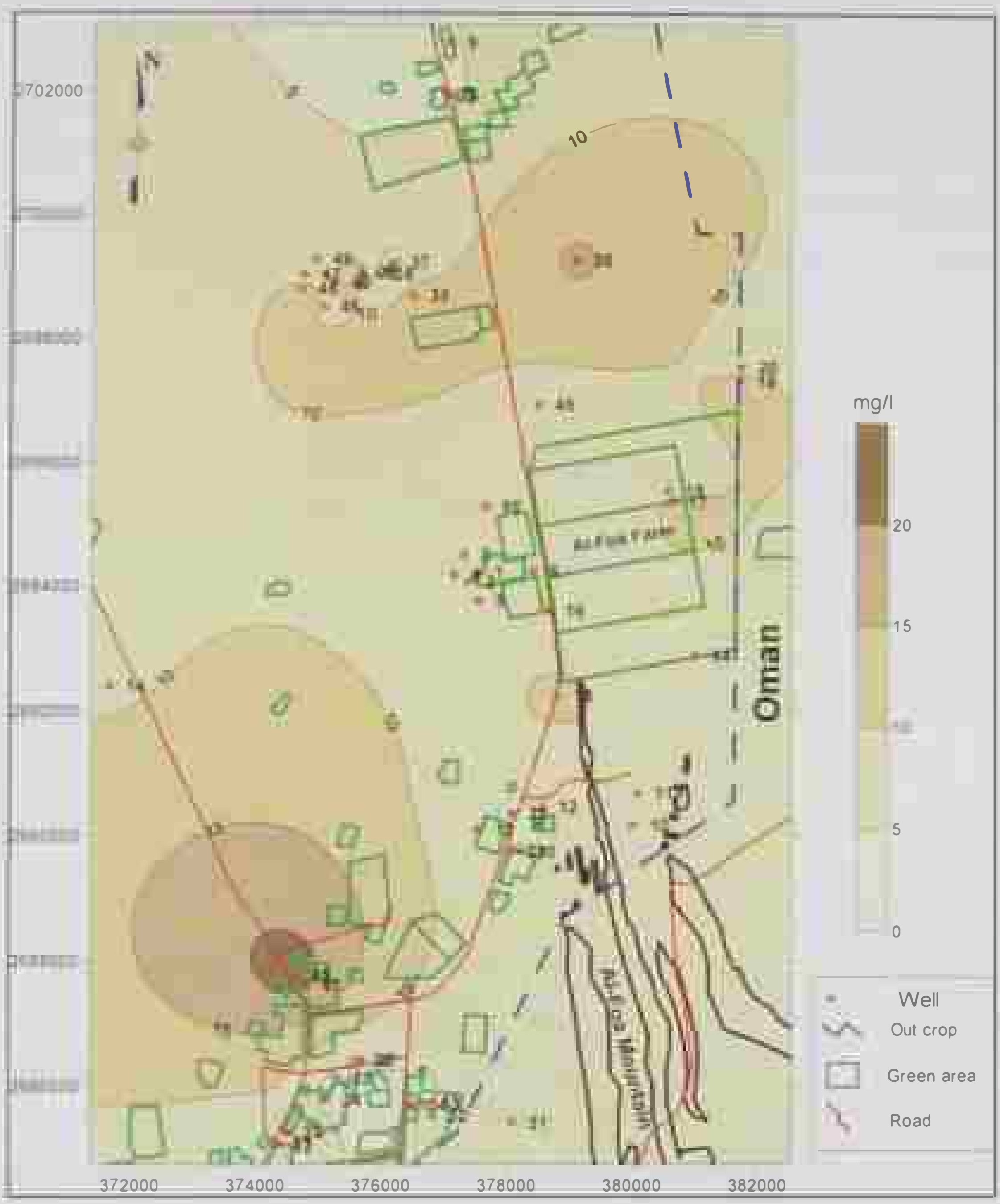

Figure (4.12) Map showing the distribution of carbonate anion (mg/l) in Al-Foah area.

4.5.5 Nitrate (NO_3^-)

Nitrates are nitrogen-oxygen chemical units that combine with various organic and inorganic compounds. They are essential nutrients for plants, which absorb them from soil. The excess of nitrates not used by plants is carried through the soil to groundwater in a process called "leaching". Once in water, they remain there until used by plants or another organism, or removed by water treatment techniques (Freeze and Cherry, 1979).

Because the concentration of nitrate in groundwater is not limited by solubility constraints, dissolved nitrogen in the form of nitrates (NO_3^-) is the most common contaminant identified in groundwater (Freeze and Cherry, 1979).

The greatest source of nitrates is agricultural activities, which mainly depend on the application of pesticides and fertilizers. Animal and human wastes also contain nitrogen in the form of ammonia. Decomposing plants and animal materials also generate nitrates. According to the World Health Organization (WHO) the maximum contaminant level for nitrates is 50 ppm. High levels of nitrates can cause health problems, including methemoglobinemia, commonly known as "blue baby syndrome". Nitrate concentrations of groundwater samples collected from the Quaternary aquifer in Al-Foah area ranged from 2 ppm in the middle and north to 230 ppm in the south (Figure 4.13). All the nitrate concentrations of the groundwater in the study area were less than 50 mg/l except wells no. 7, 8, 9, 29, 31, 32, 33 and 34, which are located in the cultivated area. Figure 4.14 shows that there is a trend of increasing nitrate with potassium, which mainly supports the hypothesis that the agricultural activities are one of the main sources affecting groundwater quality.

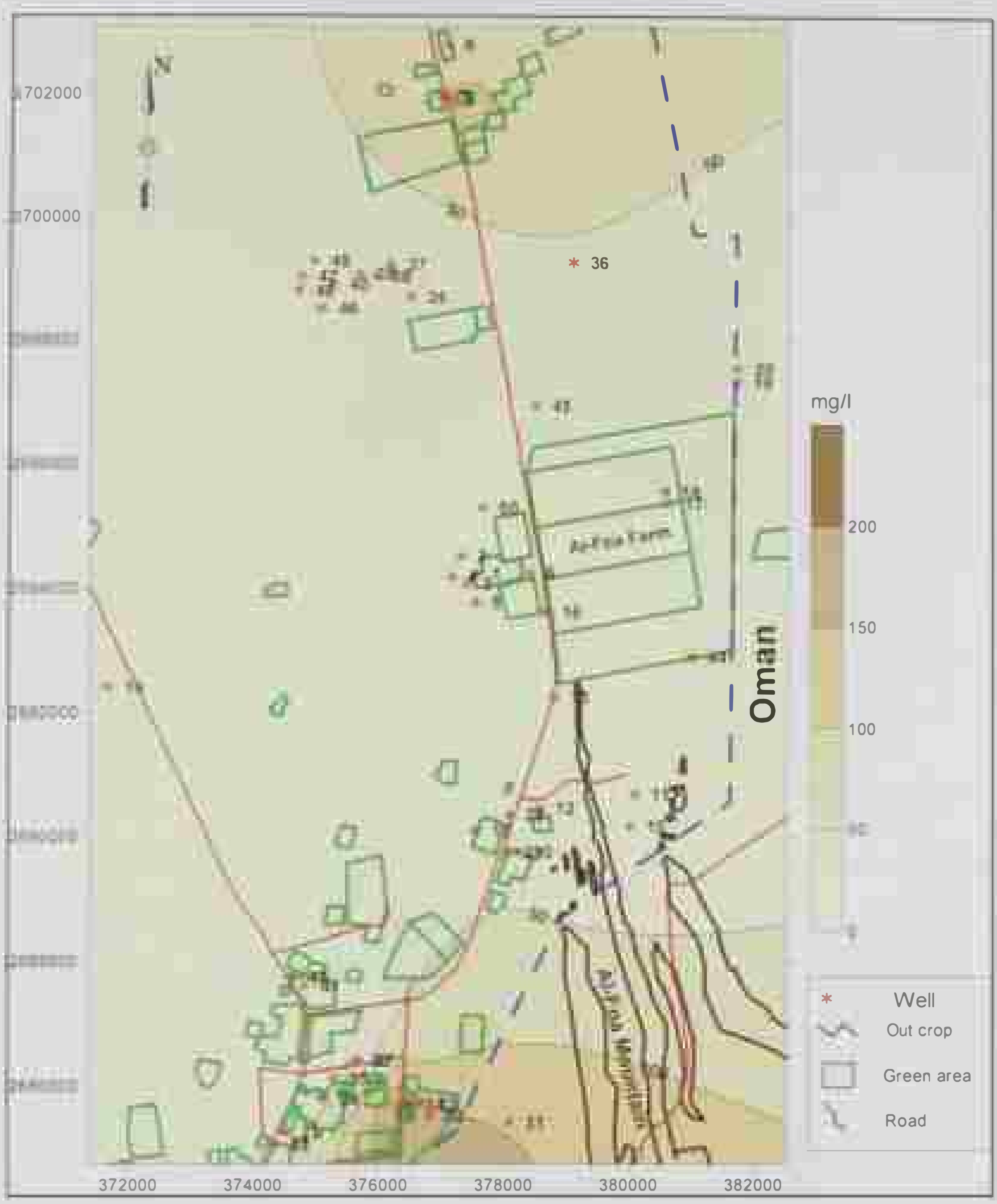

Figure (4.13) Map showing the distribution of the nitrate anion (mg/l) in Al-Foah area.

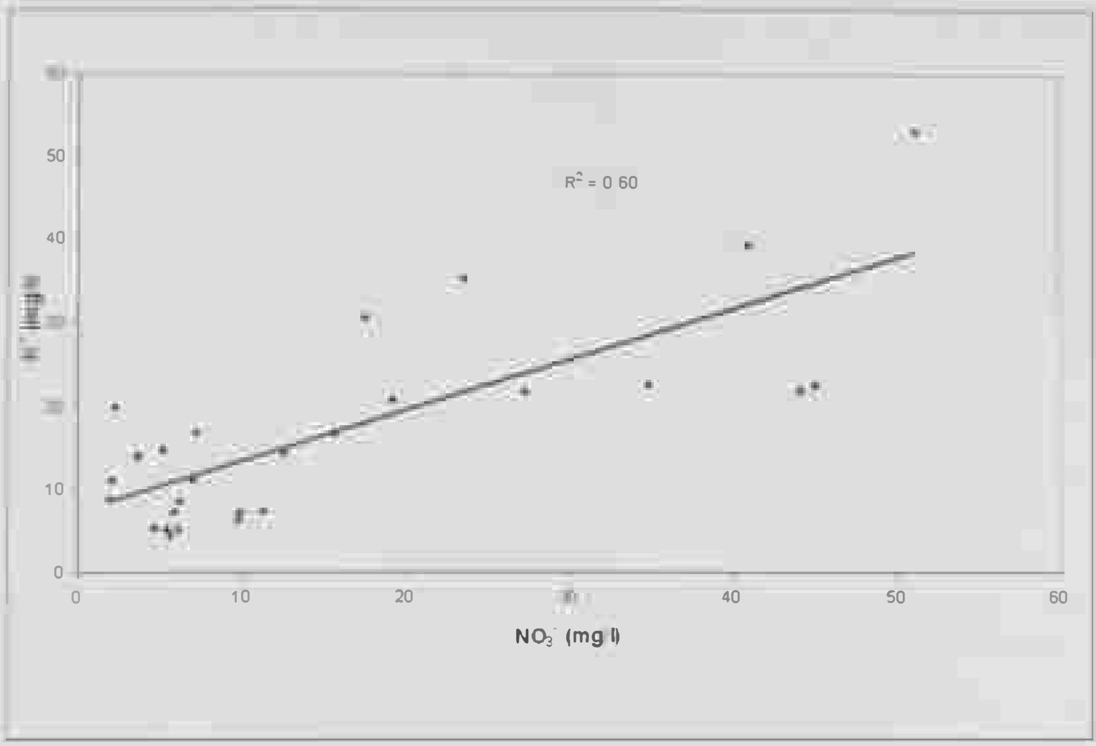

Figure (4.14) The relationship between nitrate and potassium for the groundwater in the Al-Foah area.

4.6 Major Cation

The sequence of cations dominance in groundwater of the Quaternary aquifer in Al-Foah area is in the order of: $Na^{+} > Mg^{+2} > Ca^{+2} > K^{+}$. The following is brief discussions of these cations.

4.6.1 Sodium (Na^{+})

Sodium unlike calcium, magnesium and silica is not found as an essential constituent of many of the common rock forming minerals. The primary source of most sodium in natural water is from the release of soluble products during the weathering of plagioclase feldspars. In areas of evaporite deposits, the solution of halite is also important. Clay minerals under certain conditions release large quantities of exchangeable sodium (Davis and DeWiest, 1966).

Sodium concentration in groundwater of Quaternary aquifer in Al-Foah area ranged from 103 ppm in the north to 1634 ppm in the middle and south of Al-Foah. The iso-concentration contour map shows the distribution of sodium in the study area (Figure 4.15). The high concentration values were observed within the cultivated areas which support the theory that irrigation water is one of the causes of increasing sodium in groundwater. The positive relation between sodium and chloride (r^2=0.9) (Figure 4.16) indicates that the salinity is present which might come from the high evaporation rate in region, agricultural activities and urbanization.

4.6.2 Magnesium (Mg^{+2})

The common sources of magnesium in the hydrosphere are dolomite in sedimentary rocks, olivine, biotite, hornblende, and augite in igneous rocks, and serpentine, talc, diopside, and tremolite in metamorphic rocks. In addition, most calcite contains some magnesium, so a solution of limestone commonly yields abundant magnesium as well as calcium (Davis and DeWeist, 1966).

In Al-Foah area, the highest concentration of magnesium is in the south (Figure 4.17) and decreased towards the north. The concentration of magnesium in groundwater samples ranged from 12 ppm to 637 ppm with an average of 177 ppm. The high concentration of Mg^{+2} in groundwater in the study area may be related to the leaching through the interaction between the groundwater and dolomite which located in the east of the study area and weathering of ophiolite rocks.

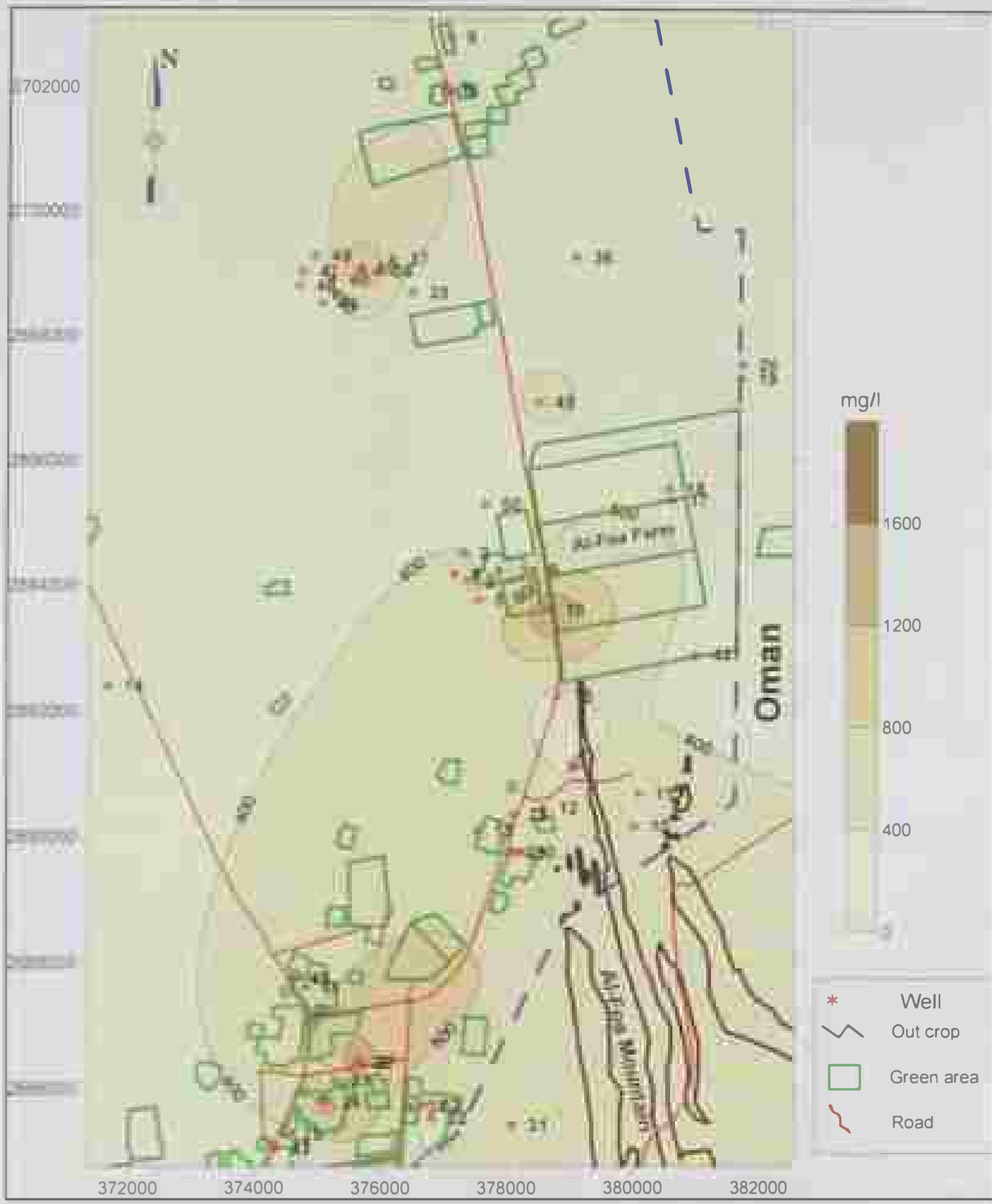

Figure (4.15) Map showing the distribution of the sodium cation (mg/l) in Al-Foah area.

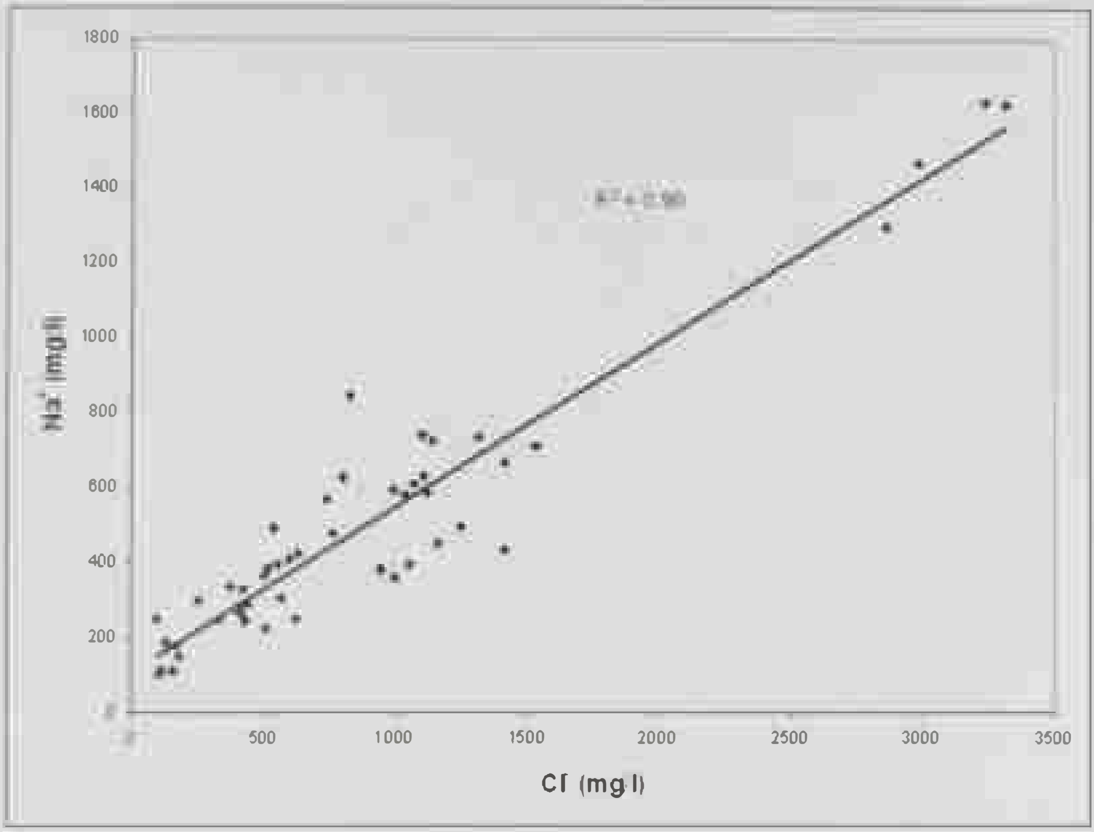

Figure (4.16) The relationship between sodium and chloride for the groundwater in the Al-Foah area.

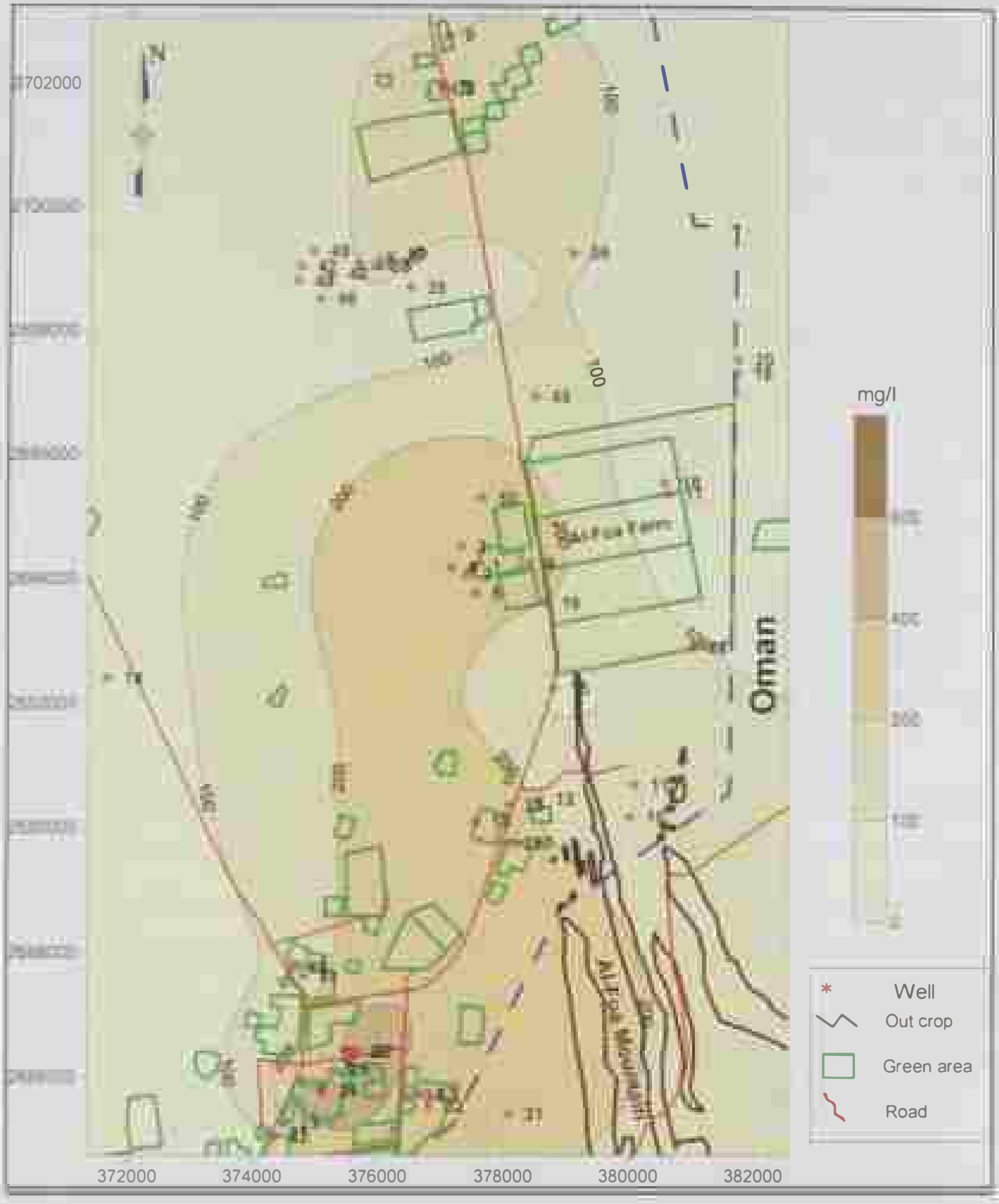

Figure (4.17) Map showing the distribution of the magnesium cation (mg/l) in Al-Foah area.

4.6.3 Calcium (Ca^{2+})

Groundwater in contact with sedimentary rocks obtains the majority of their calcium from the dissolution of calcite, dolomite, anhydrite, gypsum and aragonite. The more carbon dioxide, sodium and potassium present, the more solubility of calcium carbonate in groundwater (Davis and DeWiest, 1966).

The range of calcium concentration in Al-Foah area is 9 ppm in the north of the study area and 383 ppm in the south (Figure 4.18). The presence of limestone from the Simsima Formation could elevate the concentrations of calcium in the aquifer.

4.6.4 Potassium (K^+)

Products formed by the weathering of orthoclase, microline, biotite, leucite and nepheline in igneous and metamorphic rocks are the common sources of potassium. Water percolating through evaporite deposits may contain very large quantities derived from the dissolution of sylvite and niter (Walton, 1970).

The iso-concentration contour map shows an increase in potassium concentration from the north to the south (Figure 4.19). The concentration of potassium ranged from 4 ppm to 53 ppm with an average of 15 ppm. Figure 4.13 shows a slight relationship (r^2=0.63) between potassium (K^+) and nitrate (NO_3^-), which mainly supports the fact that the agricultural activities are significant in the study area. In addition, return flow (water irrigation) and interactions between ophiolite rocks are other sources for releasing K^+ in the study area.

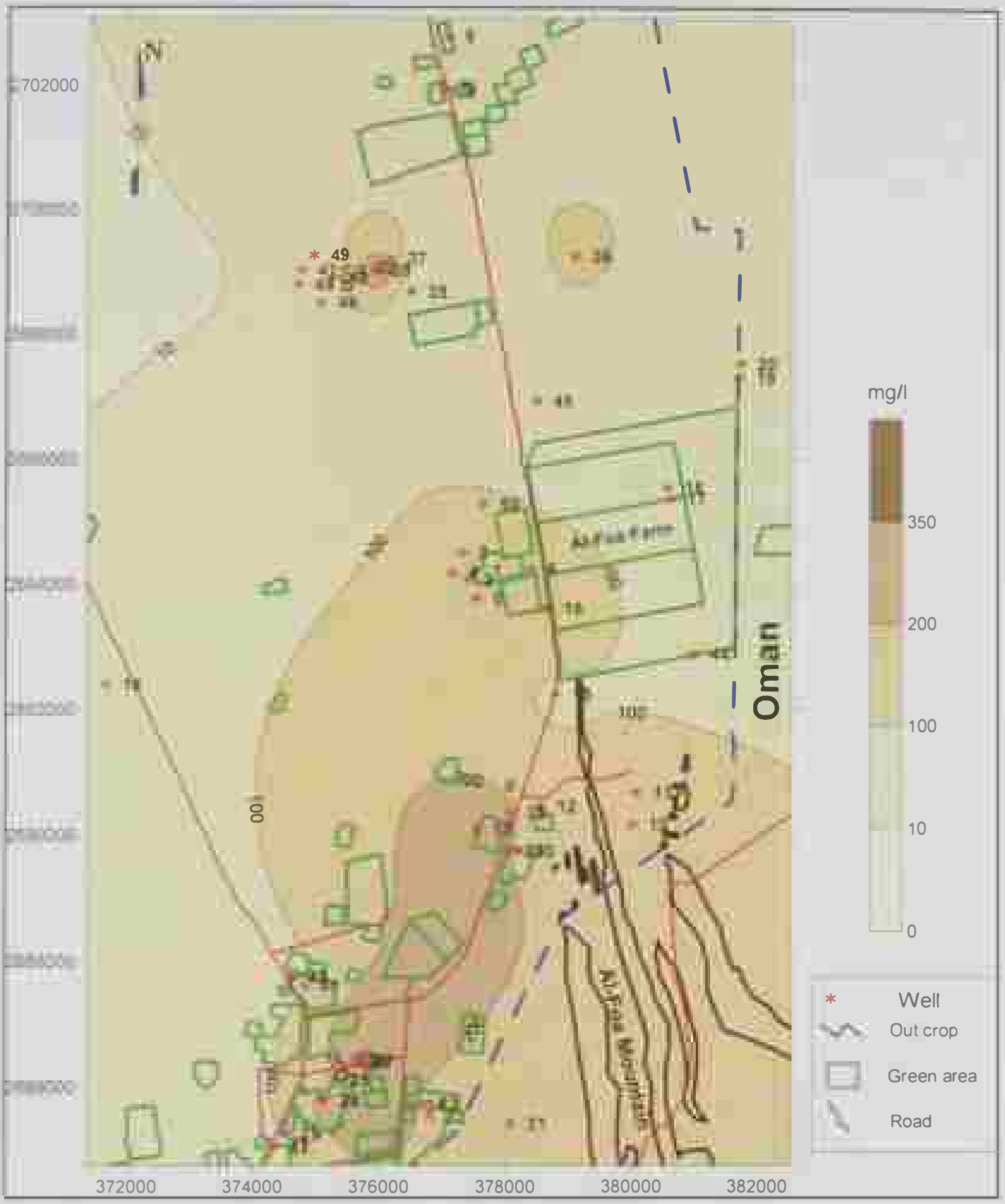

Figure (4.18) Map showing the distribution of the calcium cation (mg/l) in Al-Foah area.

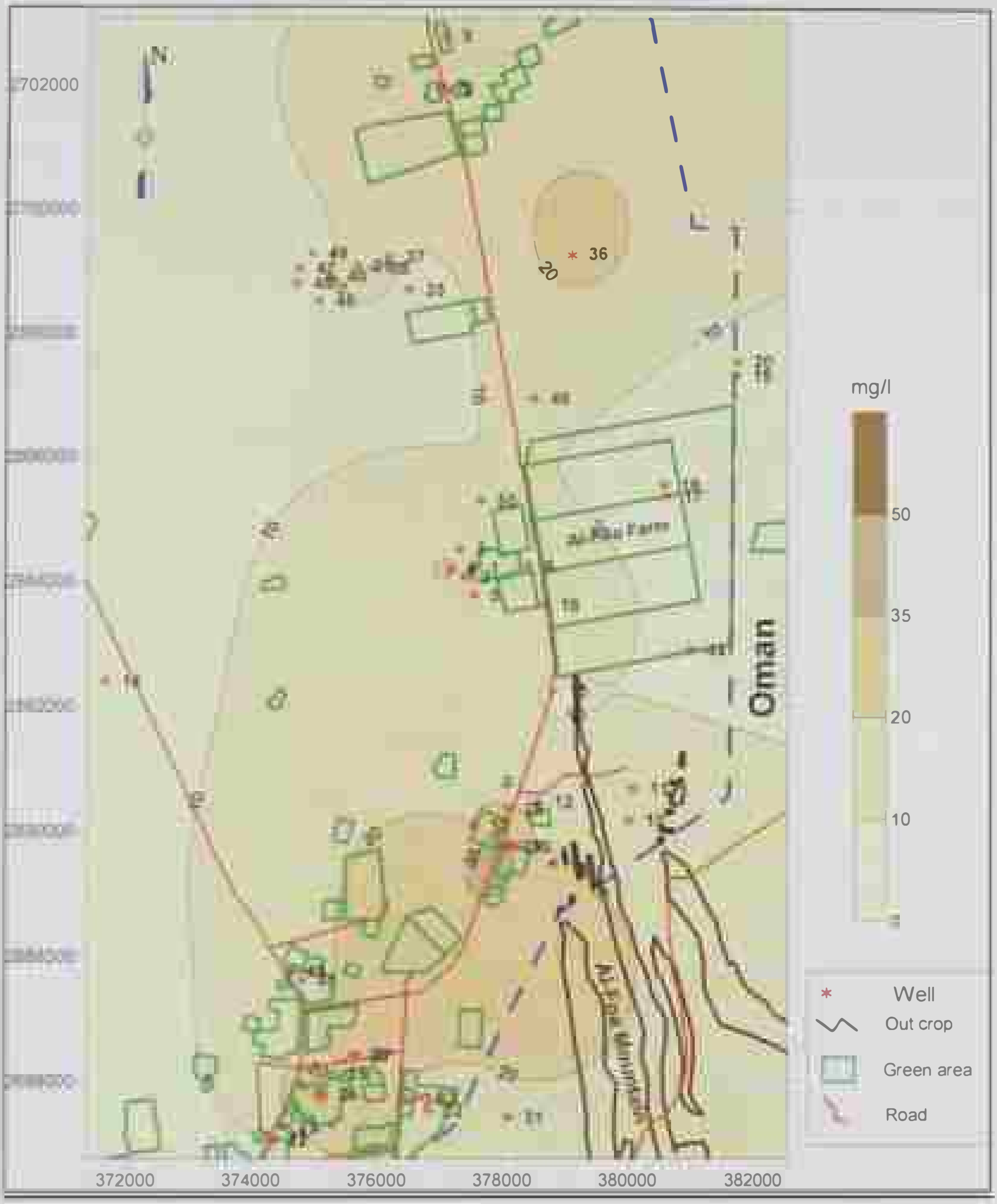

Figure (4.19) Map showing the distribution of the potassium cation (mg/l) in Al-Foah area.

4.7 Trace metals

Serious hazards affect human health if high concentrations of trace metals are present in groundwater. Groundwater samples collected from Al-Foah area were analyzed for several trace metals (Mn. Cu. Fe. F. Pb. B. Ba. Sr. Al. Cr and Zn). but there were no significant values observed that could affect human health and the groundwater.

4.8 Trilinear diagram

Trilinear diagrams are often used in water chemistry studies to classify natural waters (Figure 4.20). These diagrams are useful in determining the similarities and/or differences in the composition of water from specific hydrogeologic units and are convenient for displaying a large number of analyses. The diagrams may help to show whether particular units are hydraulically separated or connected and whether groundwater has been affected by dissolution or precipitation of a salt (Sara and Gibbons. 1991).

The data of the chemical analysis of the groundwater samples in the study area is plotted on a Piper diagram (Figure 4.21). The samples fall in the upper triangle of the diamond shape field which means that the dominant groundwater type is (Na-Cl). Analyzing the position of the samples shows that the groundwater in the southern part of the study area is enriched in magnesium.

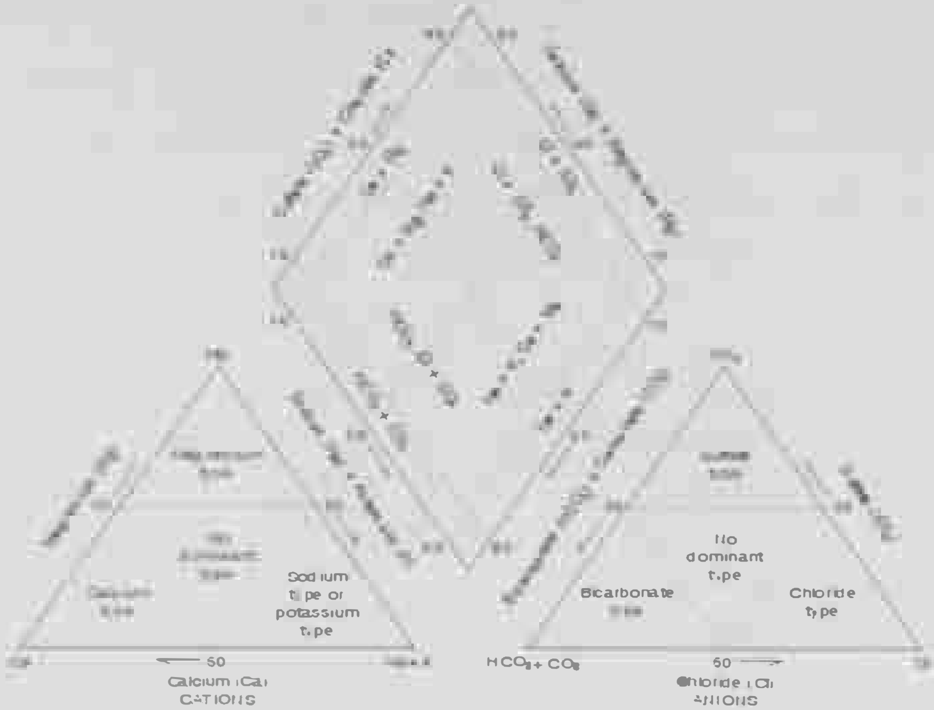

Figure (4.20) Water type of hydrochemical facies (modified after Back, 1966)

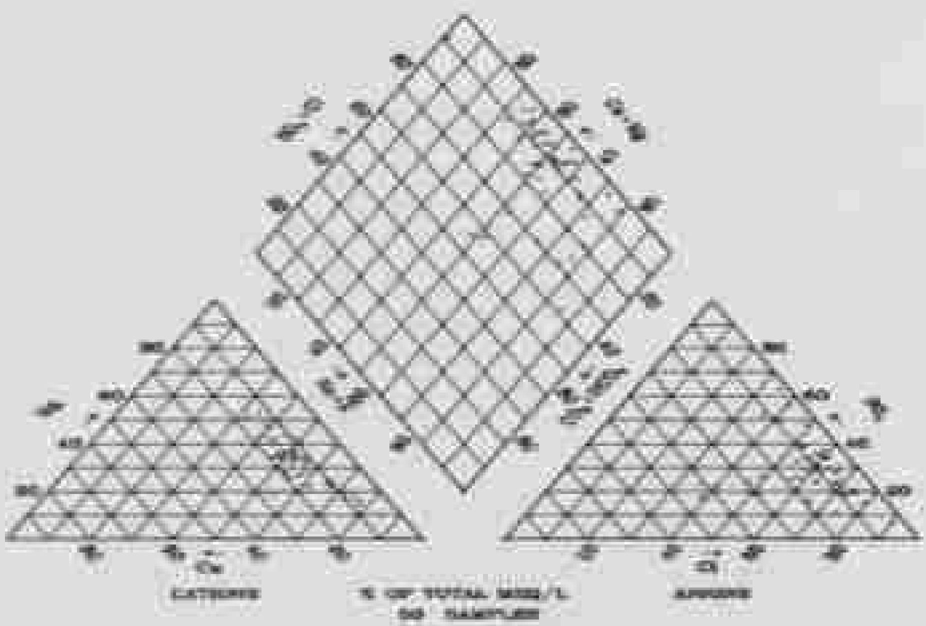

Figure (4.21) Piper's trilinear diagram for classification of the groundwater samples in Al-Foah area.

4.9 Sodium Adsorption Ratio (SAR)

Sodium Adsorption Ratio (SAR), which is a ratio of specific available cations in the soil solution, indicates if the accumulation of sodium in the soil exchange complex will lead to a degradation of soil structure, and thus a sharp reduction in infiltration and permeability rates (U. S. Salinity Staff, 1954). The formula for calculating the SAR is:

$$S.A.R = \frac{Na^{+}}{\sqrt{\frac{Ca^{++} + Mg^{++}}{2}}}$$

where the concentrations are in milli-equivalents per liter (meq/l).

Although high concentrations of sodium are toxic to some plants (especially tree fruits and berries) which could reduce the soil permeability due to the detrimental effect of sodium on soil structure (Richards, 1969).

On the positive side, sodium is beneficial for the growth of some plants such as the beet family, spinach, cabbage, oats, and potatoes. The benefit is greatest when potassium nutrition is poorest.

According to the S.A.R. values (Figure 4.22 and Table 4.2), the groundwater in the study area has a low harmful effect on vegetation when used for irrigation. The SAR values ranged between 2.3 and 20 with an average of 7.23. About 88% of the study area represents low sodium hazard water, about 10% represents medium sodium hazard water and about 2% represents high sodium hazard water which lies near the cultivated area.

Table 4.2 Classification of sodium hazard (Richards, 1969)

Sodium hazard	**Value**
Low sodium hazard water	Less than 10
Medium sodium hazard water	Between 10 and 18
High sodium hazard water	Between 18 and 26
Very high sodium hazard water	More than 26

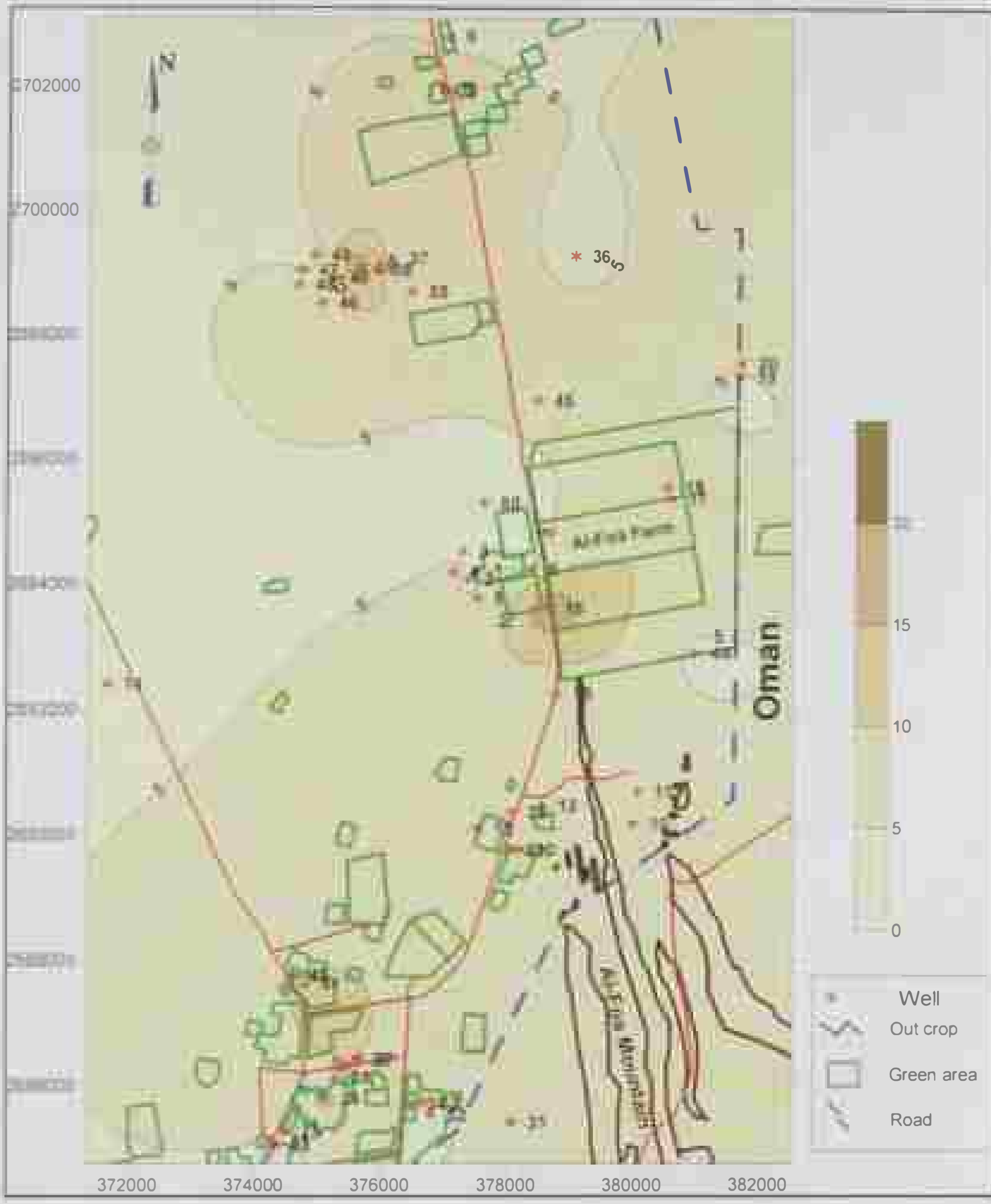

Figure (4.22) Map showing the distribution of the sodium adsorption ratio (SAR) in Al-Foah area.

Chapter V

GEOPHYSICAL STUDIES

Part A

THEORY OF THE USED GEOPHYSICAL METHOD

CHAPTER V

PART A

THEORY OF THE USED GEOPHYSICAL METHOD

5.1 Introduction

Geophysical methods are commonly used in solving many geological and environmental problems such as hydrogeology, engineering, archaeology, and geoenvironmental investigations. This achievement is related to the expanding interpretative skills of the geophysicists and the increasing acquaintance of engineers and geologists with basic geophysical principles.

Surface-geophysics methods offer quick and inexpensive means to help characterize subsurface hydrogeology (Elwood et al., 1994 and Powers, et al. 1999). They provide information on subsurface properties, such as thickness of layers and saturation zones, depth to bedrock, location and orientation of bedrock fractures, fracture zones and faults. Surface and borehole geophysical methods may form a part of preliminary site evaluation for groundwater investigation. The data from the geophysical surveying can guide the selection of the sites of test borings and provide data to correlate between them.

In the present study the Direct Current (DC) resistivity method is implemented and a privous study of Time Domain Electromagnetic is correlated with DC resistivity measurements. The following provides a brief description of these geoelectrical methods:

5.2 Electrical Resistivity Survey

Electrical methods include different techniques and instruments depending on the nature of the method used in prospecting. Some of these methods make use of natural currents and others depend on injection of artificial currents into the earth. For more details about these different techniques refer to Renyolds; 1997, Telford; et al., 1990, Parasnis; 1986, Dobrin; 1976 and Robinson and Courth; 1988.

The resistivity measurements are normally made by injecting current into the ground through two current electrodes (A and B, Figure 5.1), and measuring the resulting voltage difference at two potential electrodes (M and N, Figure 5.1). From the current (I) and voltage (V) values, an apparent resistivity (p_a) value is calculated.

$$p_a = k\, V / I$$

Where k is the geometric factor which depends on the arrangement of the four electrodes.

Figure 5.2 shows the most common electrode arrays used in resistivity surveys together with their geometric factors. Resistivity meters normally give a resistance value, R = V/I, so in practice the apparent resistivity value is calculated by

$$p_a = k\, R$$

The calculated resistivity value is not the true resistivity of the subsurface, but an "apparent" value which is the resistivity of a homogeneous ground which will give the same resistance value for the same electrode arrangement. The relationship between the "apparent" resistivity and the "true" resistivity is a complex one. To determine the true subsurface resistivity, an inversion of the measured apparent resistivity values using a computer program must be carried out. The larger the electrode spacing, the deeper the ground disturbance which can be detected.

The classical resistivity survey techniques are the Vertical Electrical Soundings (VES) and profiling. In VES, the center point of the electrode array remains fixed, but the spacing between the electrodes is increased to obtain more information about the deeper sections of the subsurface (Figure 5.3,a).

In profiling, the spacing between the electrodes remains fixed, but the entire array is moved along a straight line (Figure 5.3.b). This gives some information about lateral changes in the subsurface resistivity, but it cannot detect vertical changes in the resistivity. Interpretation of data from profiling surveys is mainly qualitative.

The most severe limitation of the resistivity sounding method is that horizontal (lateral) changes in the subsurface resistivity are commonly found. Lateral changes in the subsurface resistivity will cause changes in the apparent resistivity values that might be, and frequently are, misinterpreted as changes with depth in the subsurface resistivity. In many engineering and environmental studies, the subsurface geology is very complex where the resistivity can change rapidly over short distances. The resistivity sounding method might not be sufficiently accurate for such situations.

However, one of the new developments in recent years is the use of 2-D electrical imaging/tomography surveys to map areas with moderately complex geology (Griffiths and Barker 1993).

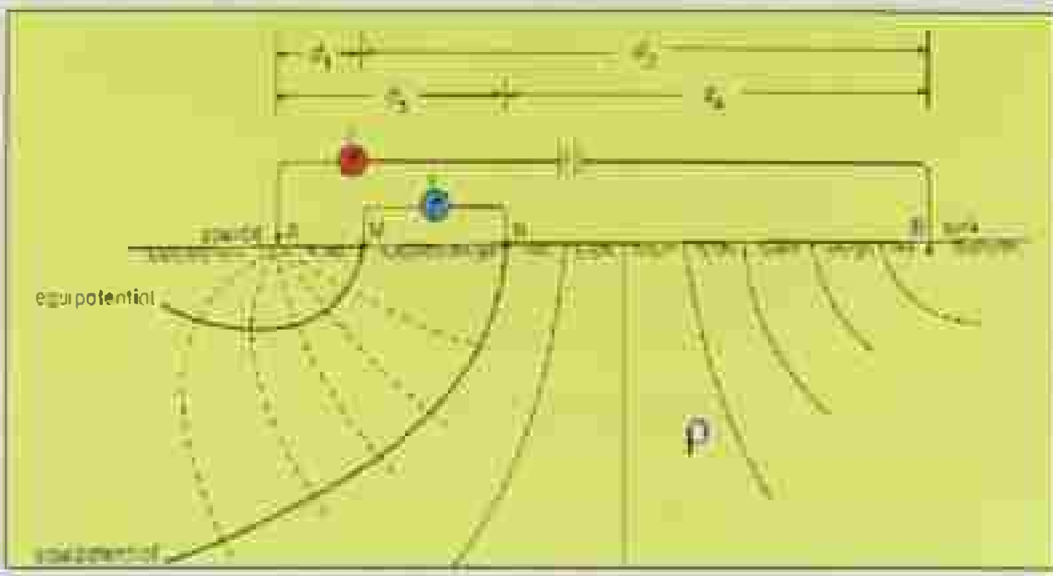

Figure (5.1) Current electrodes A and B and potential electrodes M and N are used to measure potential difference V, which depends on the zone resistivity.

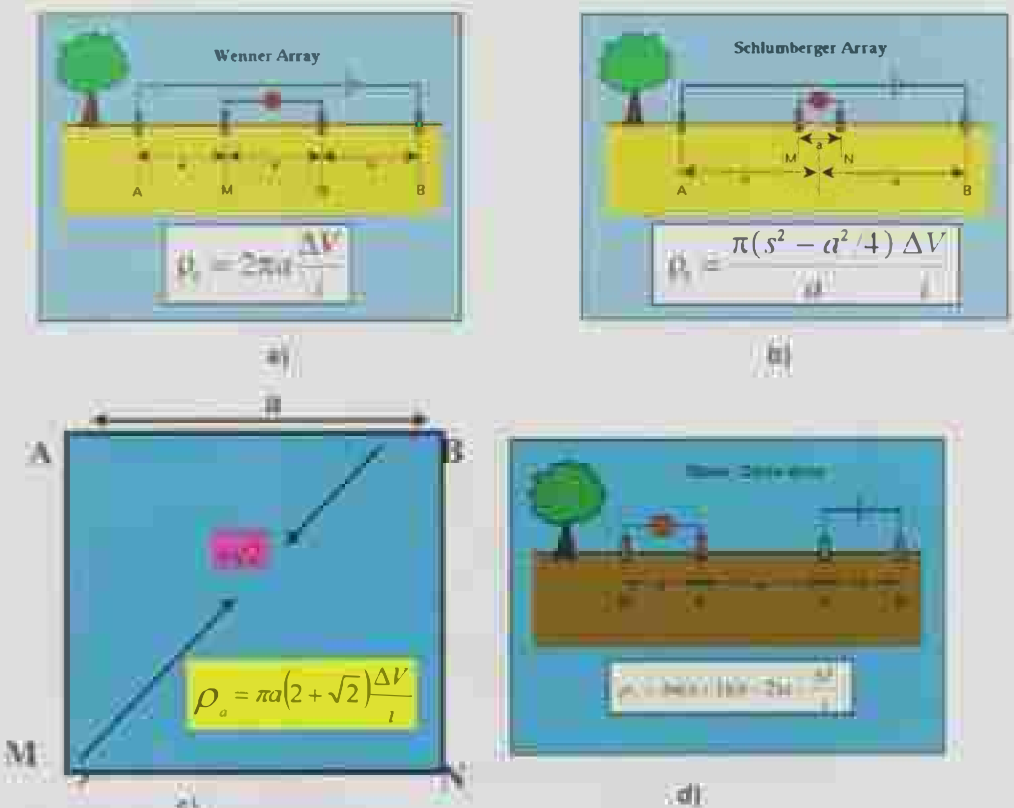

Figure (5.2) Common electrode arrays (configurations) used in DC resistivity and their corresponding geometrical factor.

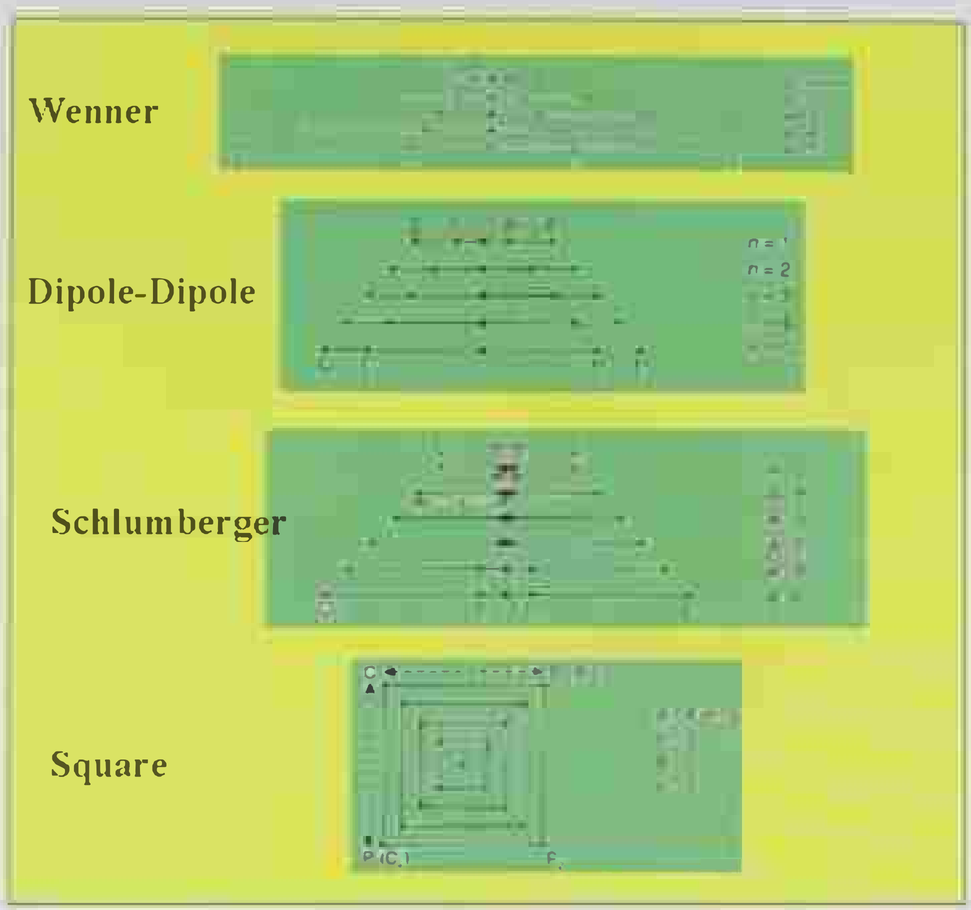

Figure (5.3,a) VES expanded electrodes with different arrays.

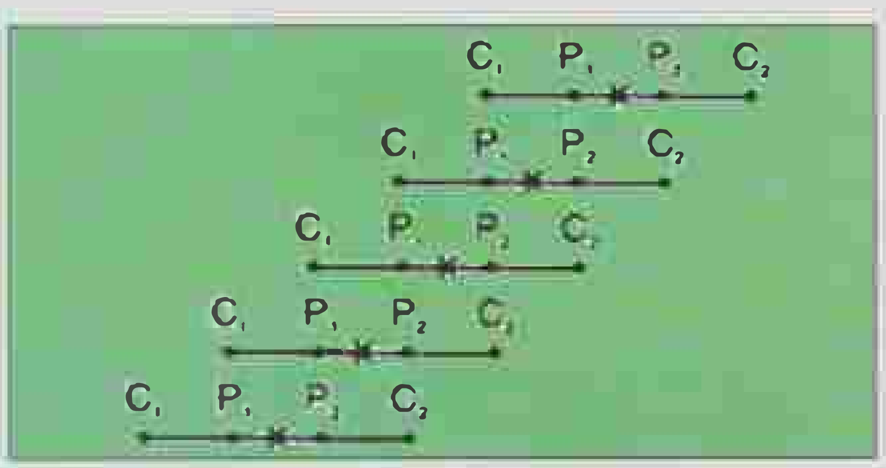

Figure (5.3,b) Constant separation profiling in which the electrode separation is kept fixed.

5.3 The relationship between geology and resistivity

Before dealing with the 2-D resistivity surveys, a brief look at the resistivity values of some common rocks, soils and other materials. Resistivity surveys give a picture of the subsurface resistivity distribution. To convert the resistivity picture into a geological picture, some knowledge of typical resistivity values for different types of subsurface materials and the geology of the area surveyed is important.

Table 5.1 gives the resistivity values of common rocks, soil materials and chemicals (Keller and Frischknecht 1966, Daniels and Alberty 1966). Igneous and metamorphic rocks typically have high resistivity values. The resistivity of these rocks is greatly dependent on the degree of fracturing, and the percentage of the fractures filled with groundwater. Sedimentary rocks which usually are more porous and have higher water content normally have lower resistivity values. Wet soils and fresh groundwater have even lower resistivity values. Clay soil normally has a lower resistivity value than sandy soil. However, an overlap exists in the resistivity values of the different classes of rocks and soils. This is because the resistivity of a particular rock or soil sample depends on a number of factors such as the porosity, the degree of water saturation and the concentration of dissolved salts.

The resistivity of groundwater varies from 10 to 100 ohm.m. depending on the concentration of dissolved salts. The low resistivity (about 0.2 ohm.m) of the seawater is due to the relatively high salt content. This makes the resistivity method an ideal technique for mapping the saline and fresh water interface in coastal areas.

The resistivity values of several industrial contaminants are also given in Table 5.1. Metals, such as iron, have extremely low resistivity values. Chemicals which are strong electrolytes, such as potassium chloride and sodium chloride, can greatly reduce the resistivity of groundwater to less than 1 ohm.m even at fairly low concentrations. The effect of weak electrolytes, such as acetic acid, is comparatively smaller. Hydrocarbons, such as xylene, typically have very high resistivity values.

Resistivity values have a much larger range compared to other physical quantities mapped by other geophysical methods. The resistivity of rocks and soils in a survey area can vary by several orders of magnitude. In comparison, density values used by gravity surveys usually change by less than a factor of 2, and seismic velocities usually do not change by more than a factor of 10. This makes the resistivity and other electrical or electromagnetic based methods very versatile geophysical techniques.

Table 5.1. Resistivities of some common rocks, minerals and chemicals (Keller and Frischknecht 1966).

Material	Resistivity (Ω.m)	Conductivity (Siemens/m)
Igneous and Metamorphic Rocks		
Granite	$5x10^3$ - 10^6	10^{-6} - $2x10^{-4}$
Basalt	10^3 - 10^6	10^{-6} - 10^{-3}
Slate	$6x10^2$ - $4x10^7$	$2.5x10^{-8}$ - $1.7x10^{-3}$
Marble	10^2 - $2.5x10^8$	$4x10^{-9}$ - 10^{-2}
Quartzite	10^2 - $2x10^8$	$5x10^{-9}$ - 10^{-2}
Sedimentary Rocks		
Sandstone	8 - $4x10^3$	$2.5x10^{-4}$ - 0.125
Shale	20 - $2x10^3$	$5x10^{-4}$ - 0.05
Limestone	50 - $4x10^2$	$2.5x10^{-3}$ - 0.02
Soils and waters		
Clay	1 - 100	0.01 - 1
Alluvium	10 - 800	$1.25 x10^{-3}$ - 0.1
Groundwater (fresh)	10 - 100	0.01 - 0.1
Sea water	0.2	5
Chemicals		
Iron	$9.074x10^{-8}$	$1.102x10^7$
0.01 M Potassium chloride	0.708	1.413
0.01 M Sodium chloride	0.843	1.185
0 01 M acetic acid	6.13	0.163
Xylene	$6.998x10^{16}$	$1.429x10^{-17}$

5.4 Two Dimensional resistivity imaging surveys

A more accurate mode of the subsurface invetsigation is a two-dimensional (2-D) model where the resistivity changes in the vertical direction, as well as in the horizontal direction along the survey line. The 2-D electrical imaging tomography surveys are implemented in this study and more detail about this technique is elaborated below.

The 2D DC-resistivity profiling method uses the same techniques and the same principles as the direct current resistivity method but is conducted by making many measurements at different locations along the profile at different offsets. The 2-D DC-resistivity profiling data is inverted to create a tomograph-like model of resistivity along a section of the subsurface that can be used to detect and define individual fracture zones.

5.5 Field survey method and measurement procedure

The 2-D electrical imaging surveys are usually carried out using a large number of electrodes, connected to a multi-core cable. A laptop microcomputer together with an electronic switching unit is used to automatically select the relevant four electrodes for each measurement (Figure 5.4). Figure 5.4 shows the typical setup for a 2-D survey with a number of electrodes along a straight line attached to a multi-core cable. Normally a constant spacing between adjacent electrodes is used. The multi-core cable is attached to an electronic switching unit which is connected to a laptop computer. The sequence of measurements to take, the type of array to use and other survey parameters (such as the current to use) is normally entered into a text file which can be read by a computer program in a laptop computer. Different resistivity meters use different formats for the control file. After reading the control file, the computer program then automatically selects the appropriate electrodes for each measurement. In a typical survey, most of the fieldwork is in laying out the cable and electrodes. After that, the measurements are taken automatically and stored in the computer. Most of the survey time is spent waiting for the resistivity meter to complete the set of measurements.

To obtain a good 2-D picture of the subsurface, the coverage of the measurements must be 2-D as well. As an example, Figure 5.4 shows a possible sequence of measurements for the Wenner electrode array for a system with 20 electrodes. In this example, the spacing between adjacent electrodes is "a". The first step is to make all the possible measurements with the Wenner array with electrode spacing of "1a". For the first measurement, electrodes number 1, 2, 3 and 4 are used. In this procedure, electrode 1 is used as the first current electrode C1, electrode 2 as the first potential electrode P1, electrode 3 as the second potential electrode P2 and electrode 4 as the second current electrode C2. For the second measurement, electrodes number 2, 3, 4 and 5 are used for C1, P1, P2 and C2 respectively. This is repeated down the line of electrodes until electrodes 17, 18, 19 and 20 are used for the last measurement with "1a" spacing. For a system with 20 electrodes, there are 17 (20 - 3) possible measurements with "1a" spacing for the Wenner array.

After completing the sequence of measurements with "1a" spacing, the next sequence of measurements with "2a" electrode spacing is made. First electrodes 1, 3, 5 and 7 are used for the first measurement. The electrodes are chosen so that the spacing between adjacent electrodes is "2a". For the second measurement, electrodes 2, 4, 6 and 8 are used. This process is repeated down the line until electrodes 14, 16, 18 and 20 are used for the last measurement with spacing "2a". For a system with 20 electrodes, there are 14 (20 - 2x3) possible measurements with "2a" spacing.

The same process is repeated for measurements with "3a", "4a", "5a" and "6a" spacing. To get the best results, the measurements in a field survey should be carried out in a systematic manner so that, as far as possible, all the possible measurements are made. This will affect the quality of the interpretation model obtained from the inversion of the apparent resistivity measurements (Dahlin and Loke 1998).

As the electrode spacing increases, the number of measurements decreases. The number of measurements that can be obtained for each electrode spacing for a given number of electrodes along the survey line depends on the type of array used. The Wenner array gives the smallest number of possible measurements compared to the other common arrays that are used in 2-D surveys.

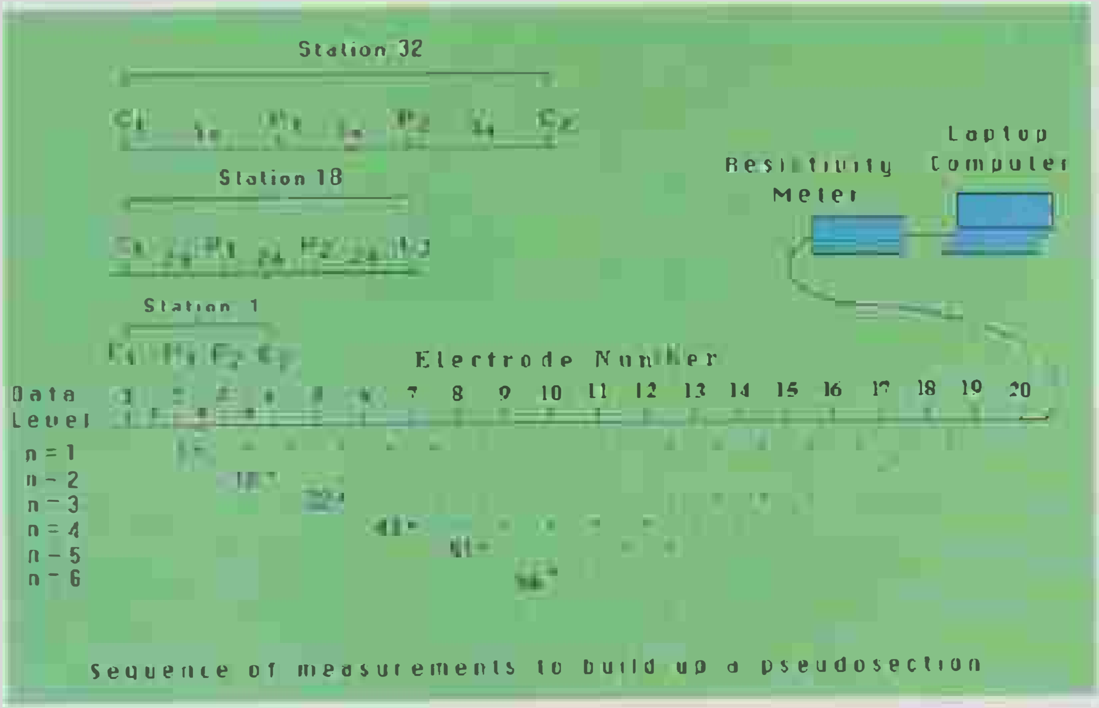

Figure (5.4) The arrangement of electrodes for a 2-D electrical survey and the sequence of measurements used to build up a pseudosection.

Part B

GEOPHYSICAL INVESTIGATIONS

CHAPTER V

PART B

GEOPHYSICAL INVESTIGATIONS

5.6 Site Characterization

The Al-Foah area is dominated by rocks ranging in age from Upper Cretaceous to Holocene. Most of the Al-Foah area is covered by Quaternary deposits. Exposures of the fractured rocks can be seen at Jabal Al Oha; a 16-Kilometer long by 30-meter high outcrop of the Simsima Formation of Late Cretaceous.

The 2-D resistivity data was collected from the low land between Jabal Al Oha (Fig. 5.5.a) and the western part of Jabal Huwayyah on the Oman side of the Al-Foah area, quite near to the border with Oman at this site. The surface of this area is covered with sand alluvium and boulders of limestone. Locals are constructing cotes for camels and sheep in the study area (Fig. 5.5.b). The area contains Al-Foah cemetery and the biggest farm, Al-Foah wheat farm located to the north of the area covered by the geophysical investigations. The limestone is mainly overlying sands (Figure 5.6. a) but in some locations, is underlain by clay formation (Figure 5.6. b). The limestone in Jabal Al Oha is highly fractured (Figure 5.7.a and b). Many cavities characterize the outcropping limestone of the study area (Figure 5.8).

Figure (5.5,a) Al Oha Limestone mountain to the west border of the study area.

Figure (5.5,b) Cotes for camels and sheep in the study area.

Figure (5.6,a) Jabal Al Oha Limestone exposure overlying the eolian sand.

Figure (5.6,b) Limestone overlying the clay layer of Al Oha Limestone mountain.

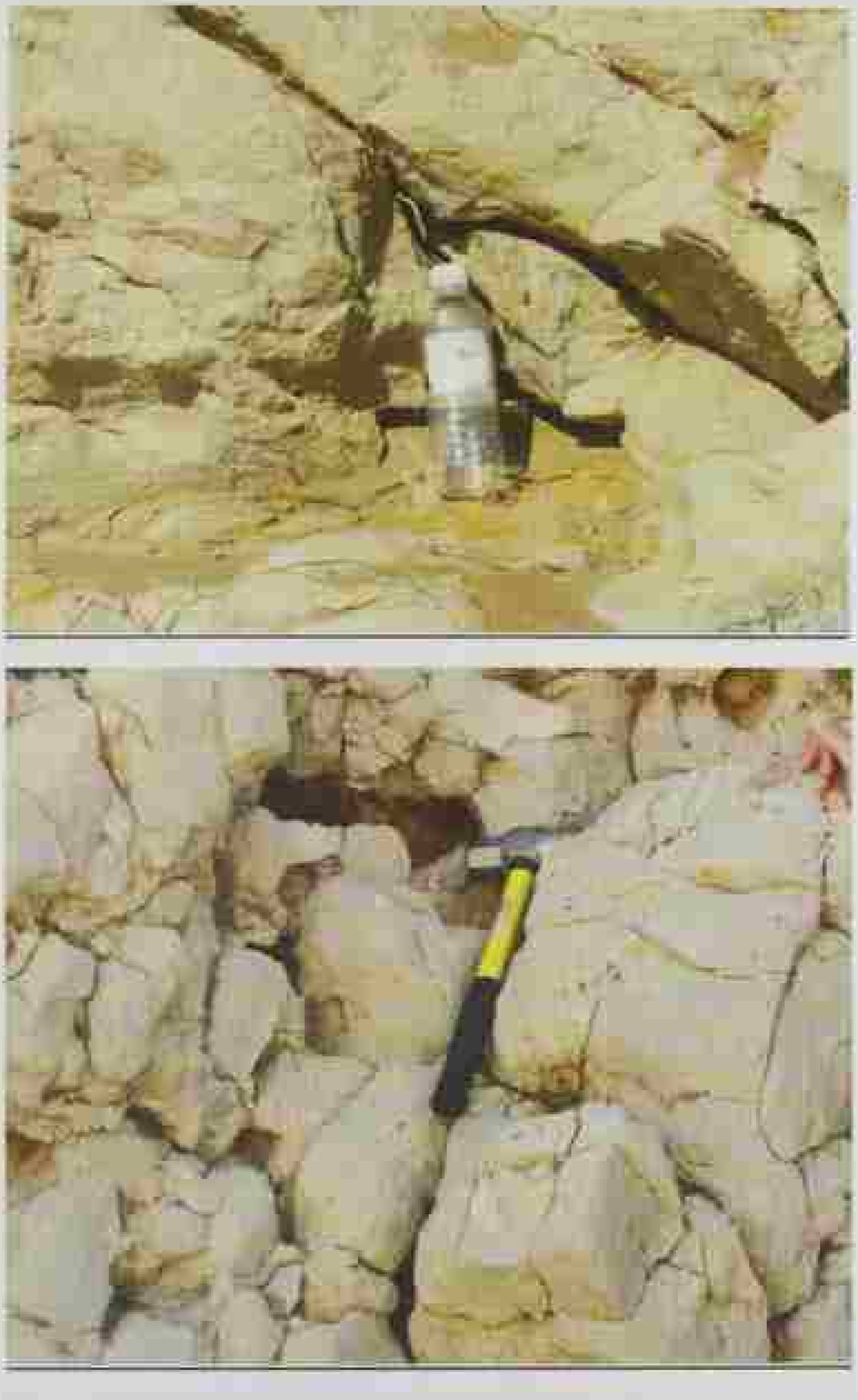

Figure (5.7) Highly fractured limestone of Al Oha mountain.

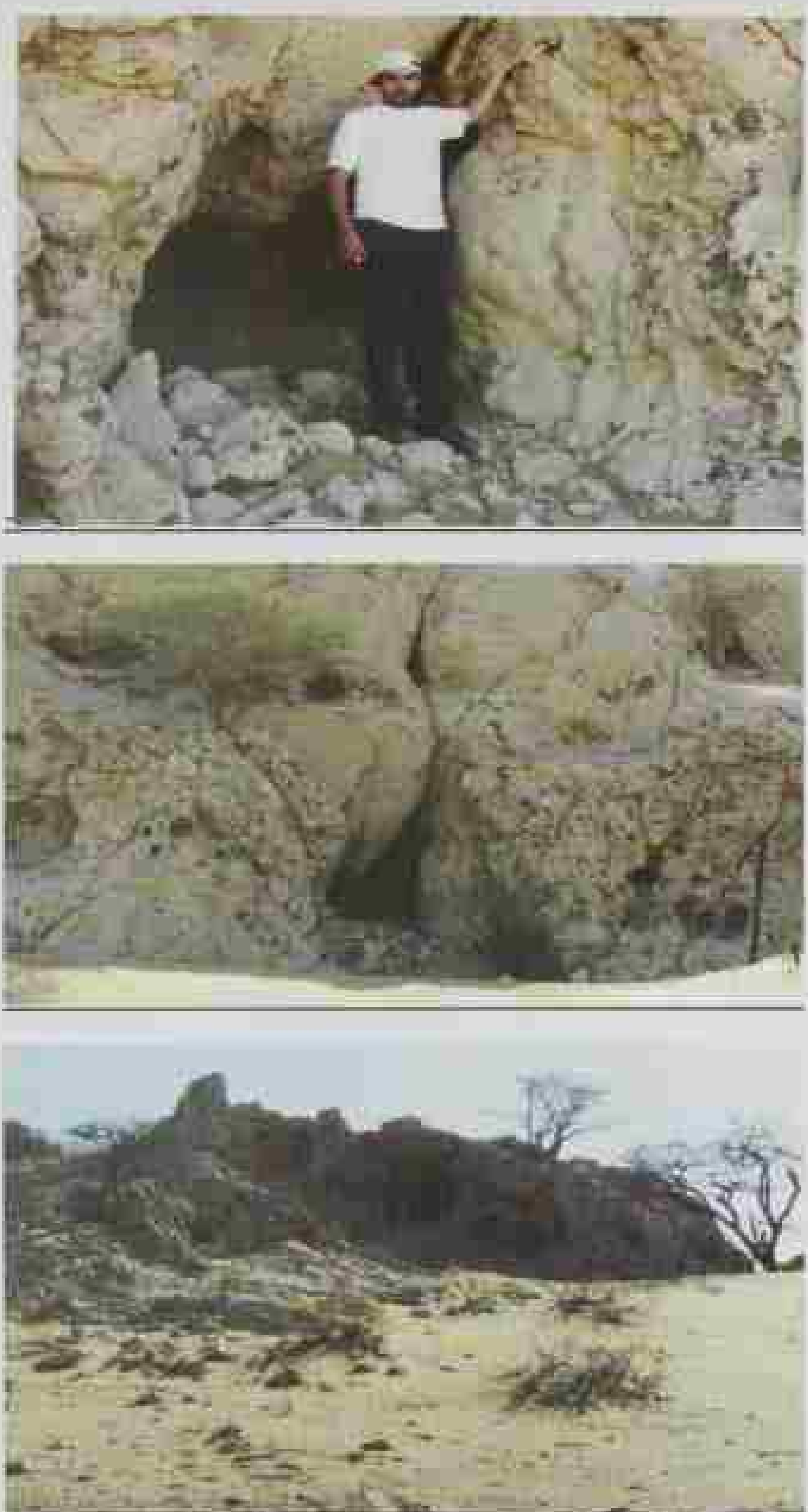

Figure (5.8) Photos showing the karst and cavities that characterize the lime stone of Jabal Al Oha.

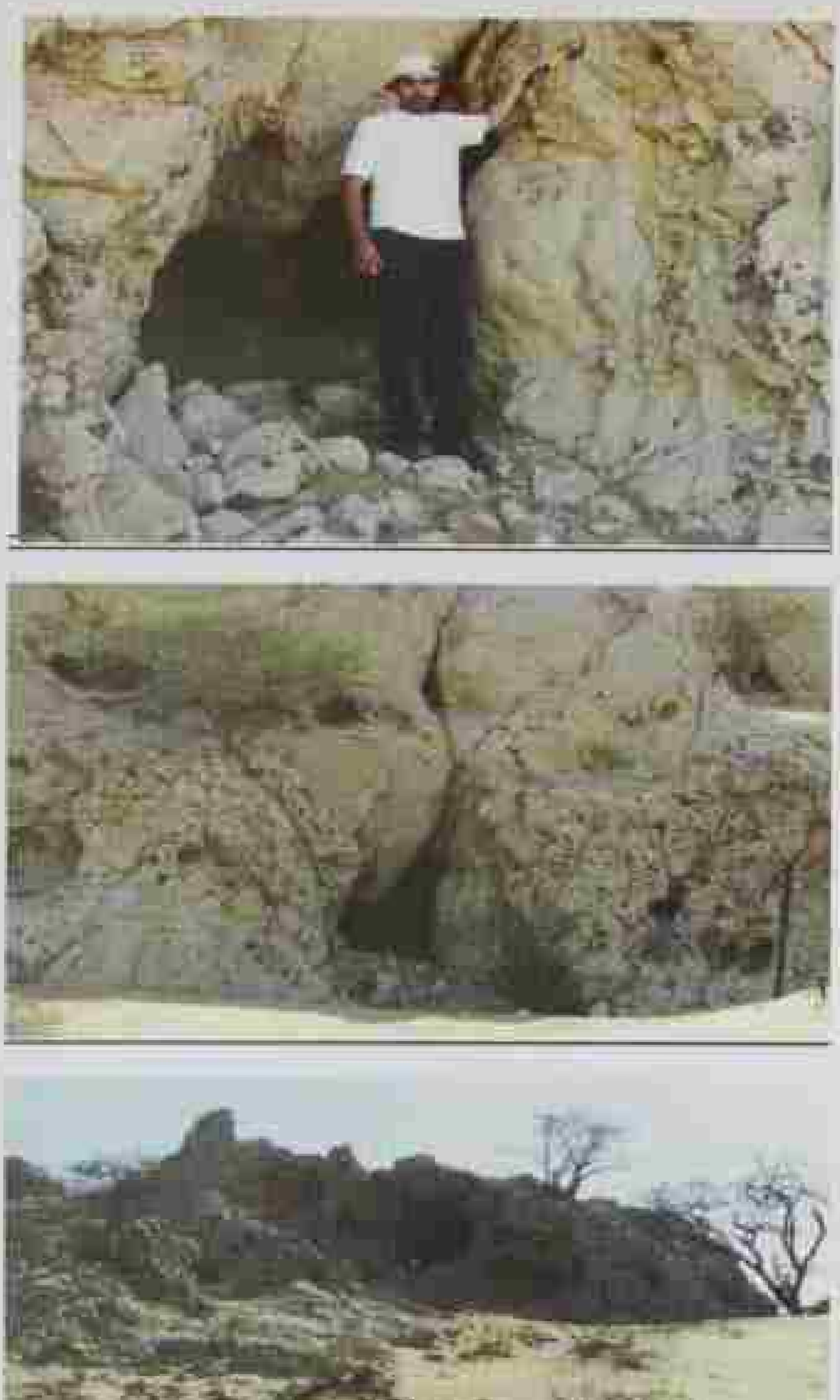

Figure (5.8) Photos showing the karst and cavities that characterize the limestone of Jabal Al Oha.

5.7 Two-Dimensional Resistivity Data acquisition and processing

Nine (2-D) electrical tomography profiles were made using Wenner electrode configuration along some selected profiles parallel to the strike of the limestone exposures at Al-Foah area (Figure 5.9). Due to the unavailability of a 2D DC-resistivity profiling system, a single channel Memory Earth Resistivity and IP Meter instrument (Figure 5.10) manufactured by Advanced Geosciences, Inc. and available at the Geology Department, United Arab Emirates University was used with four wheels of electric wires as a substitute for the multicore cable and a manual reading instead of the control unit. The distances were controlled manually by marching along the profile forward and backward. Figure 5.11a shows photos of the 2-D data acquisition in Al-Foah area (February-March, 2006).

The nine profiles extend to a length of 600 m, with a 20 m electrode spacing. For each profile, Wenner array (Figure 5.11, b) was used in resistivity data acquisition. The nine 2-D resistivity profiles were conducted and oriented along the strike direction to intersect the maximum possible number of geologic features.

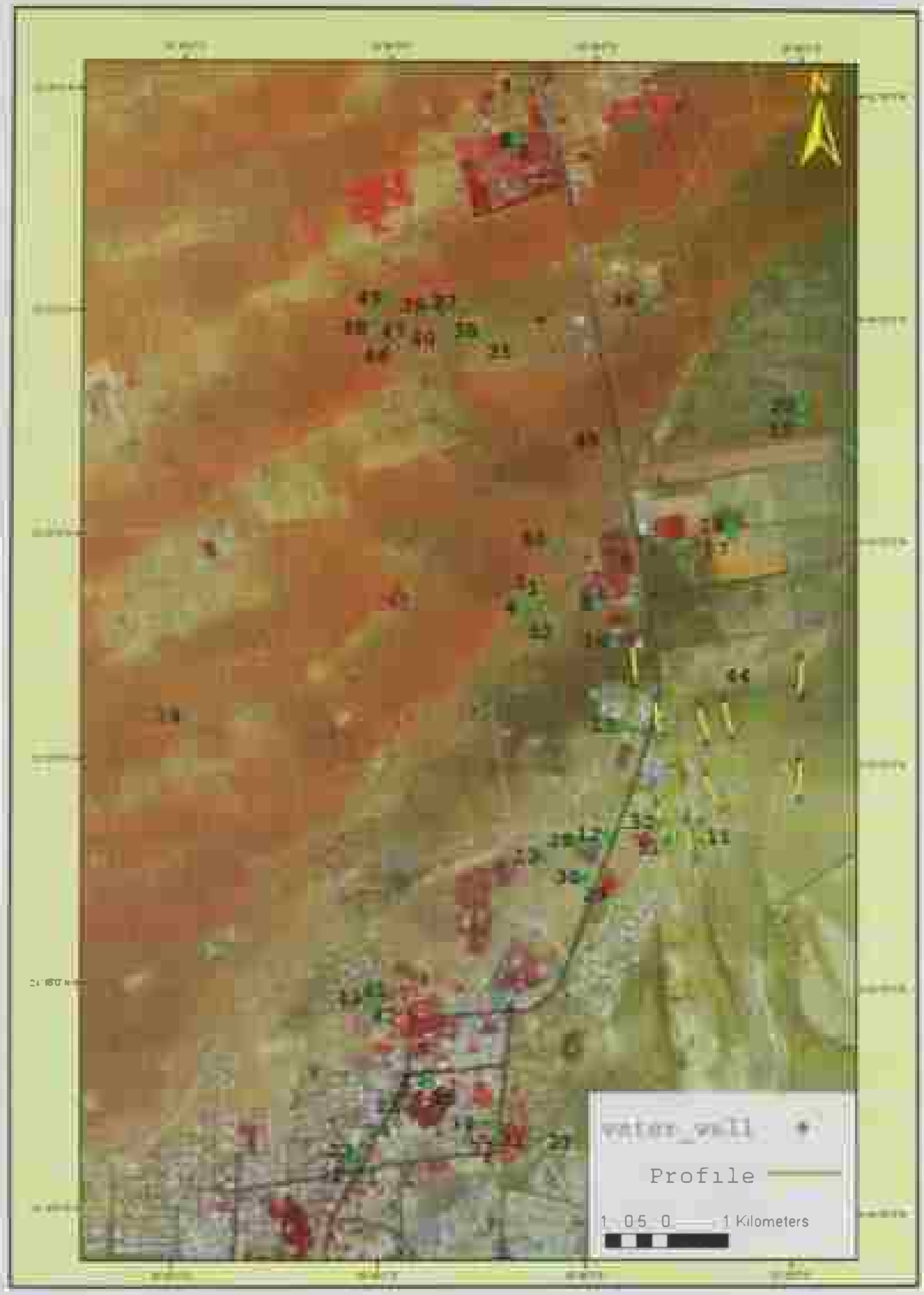

Figure (5.9) Base map showing the locations of 2-D profiles and the locations of the water wells at Al Foah area, Al Ain area.

Figure (5.10) Super Sting R1 IP earth resistivity and IP meter and its accessories.

Figure (5.11,a) The arrangement of electrodes for a 2-D electrical survey at Al Foah area.

Figure (5.11,b) The 2-D data acquisition at Al Foah area.

5.8 Two-Dimensional Resistivity Data processing and presentation

The apparent resistivity data was inverted to create a model of the resistivity of the subsurface using Res2dinv, ver. 3.54. Res2dinv uses an iterative smoothness-constrained least-squares method (DeGroot-Hedlin and Constable, 1990; Loke and Barker 1996).

Apparent resistivity data collected by the 2D DC-resistivity system is inverted to create a model of subsurface resistivity that approximates the true subsurface resistivity distribution (Loke, 1997). The resistivity models were used to generate synthetic apparent resistivity data. The resistivity models were adjusted and simplified to qualitatively match the field-data inversions. Generating resistivity models helped to constrain interpretation of the field-data inversions to identify locations and orientations of anomalies.

The 2D DC-resistivity field-data inversion, resistivity model and synthetic-data inversion for the profile one is shown in Figure 5.12 as example. The depth of penetration in all of these profiles is about 120 m. The discussions of these nine tomographs will be discussed hereafter.

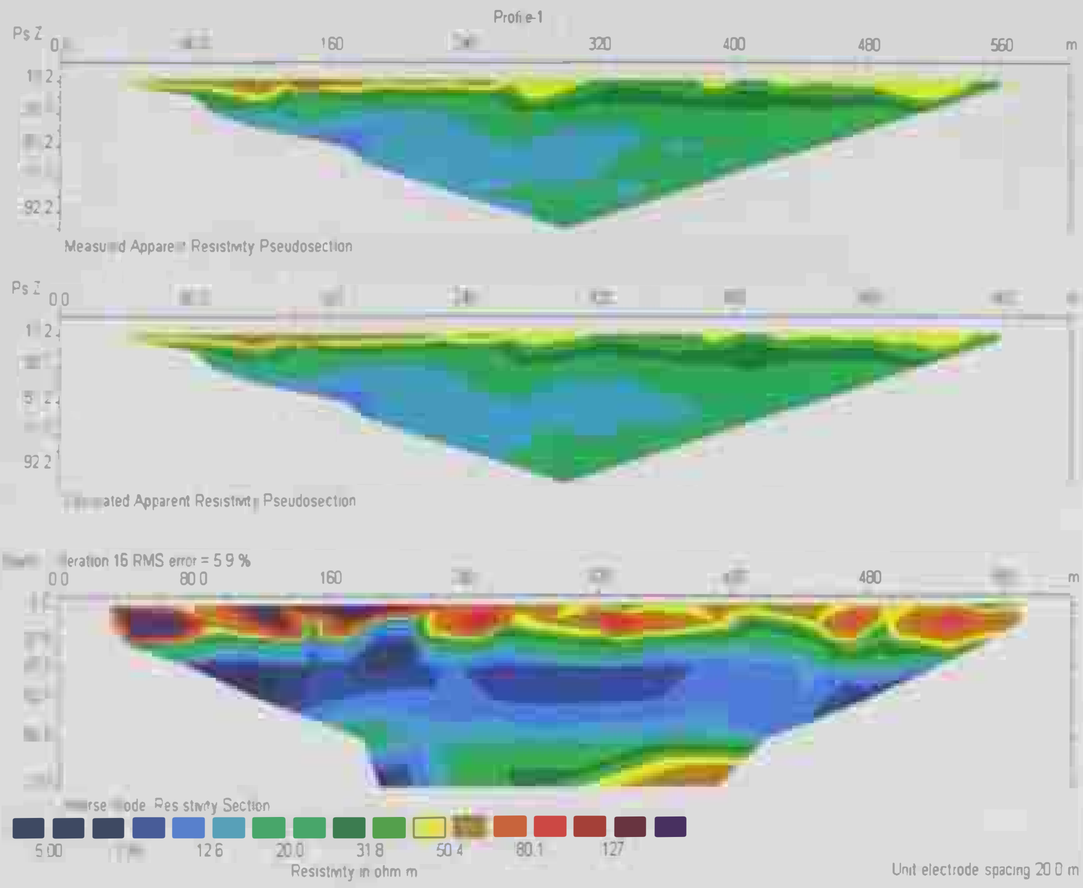

Figure (5.12) 2-D Resistivity profile along line 1-1`

5.9 Resistivity model at the study area

To relate the inverted 2-D resistivity tomograms with lithology and hydrogeological conditions, previous work done by US Geological Survey, (1993) has been correlated with the 2-D tomograms and the lithology information available borehole in considered. The base map of the electromagnetic profiles done by the US Geological Survey, (1993) in the northern part of Al-Ain is shown in Figure (5.13). Figure (5.14) shows a summary of the resistivities ranges with the main lithological and hydrogeological units at Al Qura'a area to the north of the study area (US Geological Survey, 1993). Also the information about the lithology and the total dissolved solids of the water wells which are located nearby the conducted geophysical profiles which are Well Numbers 10, 11, 12, 15, 16 , 44, 51 & 52 which constitutes what is known of Jabal Al Oha well field (see Fig. 5.9 for the locations of these wells). Figures (5.15 and 5.16) are geoelectric resistivity columns along Jabal Al Oha using TEM Soundings (Jama et. al., 1997). From these two resistivity columns, it could be notice that four and five–layer profile models of subsurface resistivity were developed from Time Domain electromagnetic in the Jabal Al Oha area.

The main four identified geoelectric-lithologic units along these geoelectric resistivity columns (Figures 5.15 and 5.16) are:-

Layer-1 is a surficial zone of eolian sand and/or hard limestone at some locations. This zone corresponds to the upper part of the very resistive layer. The resistive nature of this layer is indicative of dry conditions in the upper part of the alluvium and/or existing of hard dry limestone.

Layer-2 is a thick zone of gravel and sand comprising the bulk of the alluvium. The moderate to relatively small resistivity in this middle interval suggests partial saturation and/or the presence of a clay-rich matrix.

Layer-3 which is characterizing by its high-resistivity at different depth intervals and is interpreted as carbonate (limestone). According to data of the drilled boreholes the depth to top of this limestone layer ranges from 18 to 34

5.9 Resistivity model at the study area

To relate the inverted 2-D resistivity tomograms with lithology and hydrogeological conditions, previous work done by US Geological Survey, (1993) has been correlated with the 2-D tomograms and the lithology information available borehole is considered. The base map of the electromagnetic profiles done by the US Geological Survey, (1993) in the northern part of Al-Ain is shown in Figure (5.13). Figure (5.14) shows a summary of the resistivities ranges with the main lithological and hydrogeological units at Al Qura`a area to the north of the study area (US Geological Survey, 1993). Also the information about the lithology and the total dissolved solids of the water wells which are located nearby the conducted geophysical profiles which are Well Numbers 10, 11, 12, 15, 16 , 44, 51 & 52 which constitutes what is known of Jabal Al Oha well field (see Fig. 5.9 for the locations of these wells). Figures (5.15 and 5.16) are geoelectric resistivity columns along Jabal Al Oha using TEM Soundings (Jama et. al., 1997). From these two resistivity columns, it could be notice that four and five–layer profile models of subsurface resistivity were developed from Time Domain electromagnetic in the Jabal Al Oha area.

The main four identified geoelectric-lithologic units along these geoelectric resistivity columns (Figures 5.15 and 5.16) are:-

Layer-1 is a surficial zone of eolian sand and/or hard limestone at some locations. This zone corresponds to the upper part of the very resistive layer. The resistive nature of this layer is indicative of dry conditions in the upper part of the alluvium and/or existing of hard dry limestone.

Layer-2 is a thick zone of gravel and sand comprising the bulk of the alluvium. The moderate to relatively small resistivity in this middle interval suggests partial saturation and/or the presence of a clay-rich matrix.

Layer-3 which is characterizing by its high-resistivity at different depth intervals and is interpreted as carbonate (limestone). According to data of the drilled boreholes the depth to top of this limestone layer ranges from 18 to 34 meter, while the depth to the bottom of this limestone layer ranges from 30 to greater than 183 m (Jama et. al., 1997). The massive limestone that characterizes the Simsima Formation generally has low permeability, contains little water except in solution cavities and fractures, and it should have high resistivity.

Layer-4 has a resistivity range of less than 10 Ohm-m. This low resistivity layer is composed of bedrock consisting of marl, clay, mudstone, or siltstone. In some places in the deeper depth this zone would have resistivities of less than 5 Ohm-m probably due to the increase of salinity with depth.

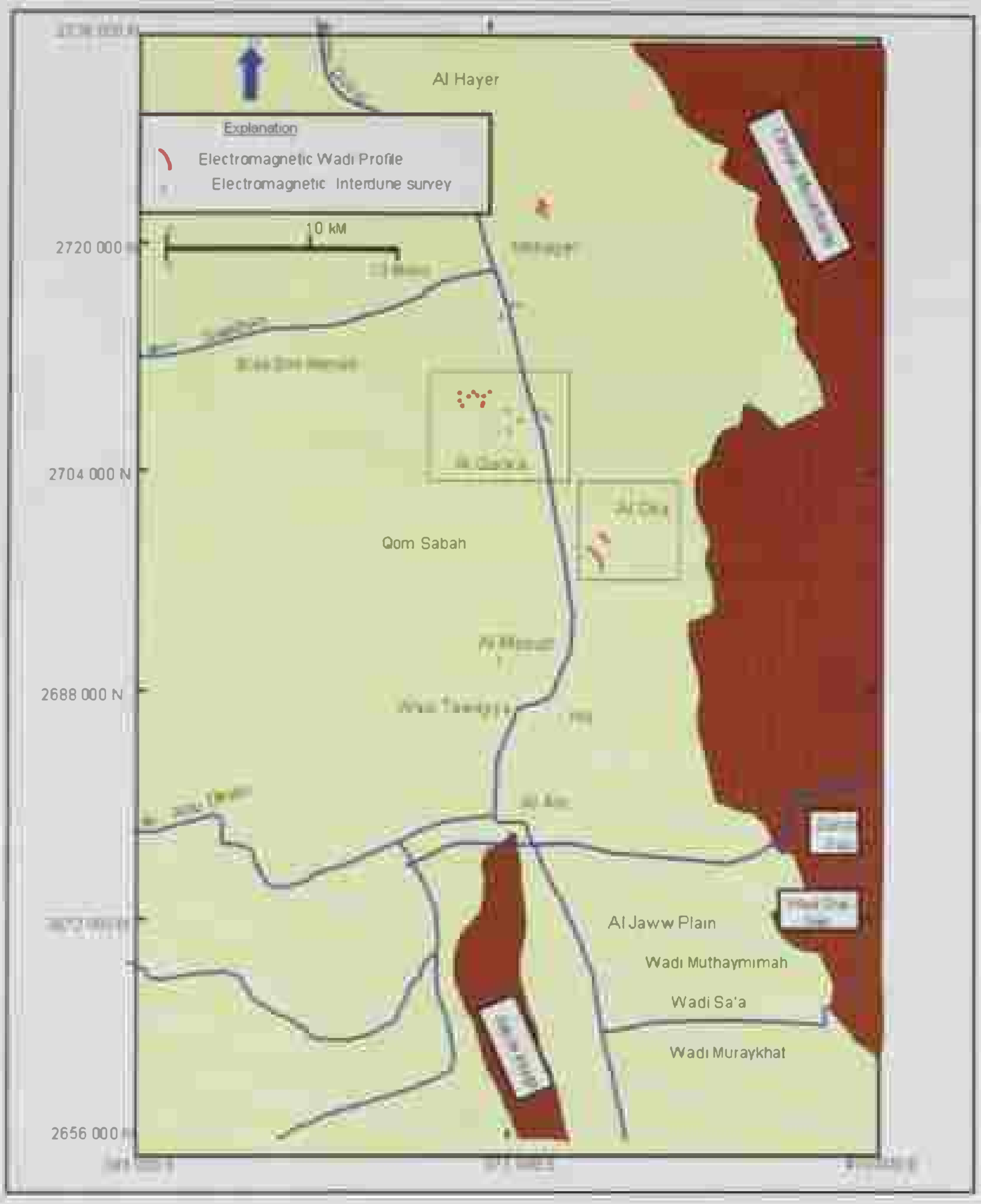

Figure (5.13) Base map showing the Electromagnetic survey at Al Qura'a and Al Foah areas (after US Geological Survey, 1993).

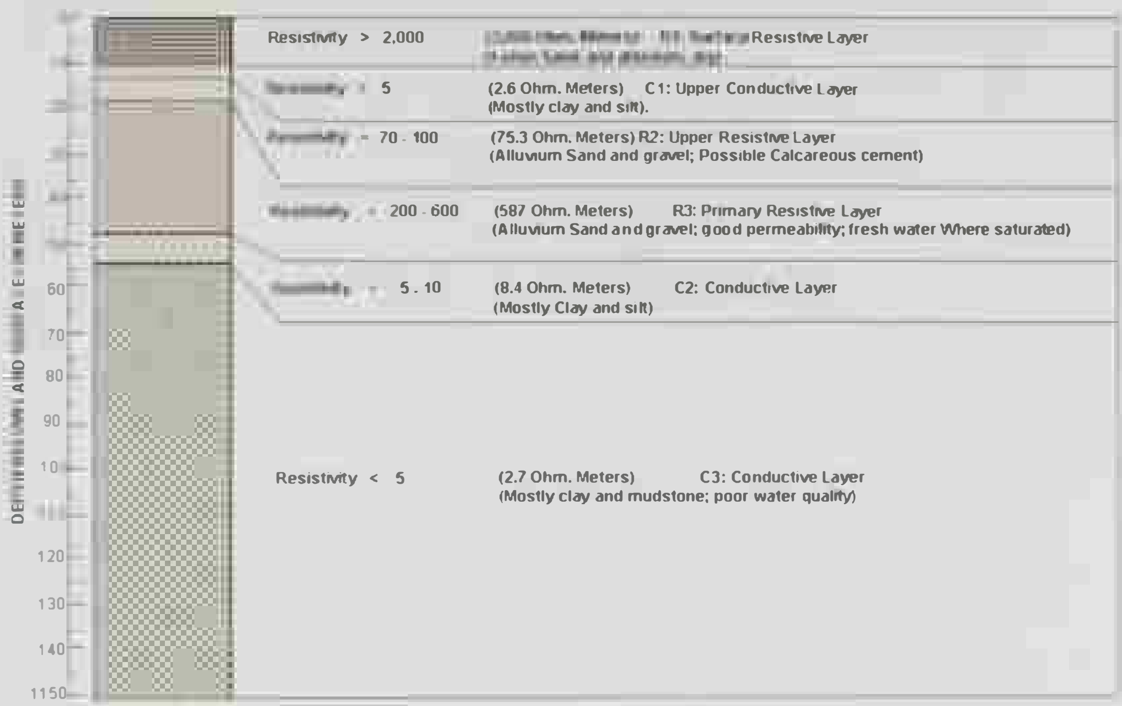

Figure (5.14) Resistivity model of typical resistivities for interdune soundings at Al Qura'a, north of Al Ain (after US Geological survey, 1993).

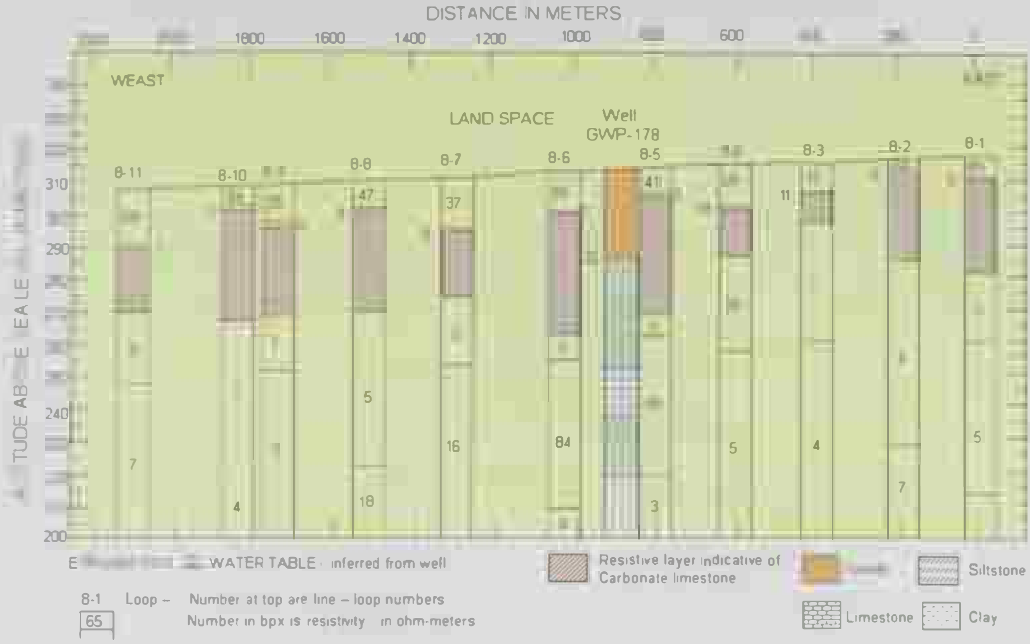

Figure (5.15) Geoelectric Columns along Jabal Al Oha using TEM Soundings (after Jama et. al., 1997). , see Fig. 21 (for location).

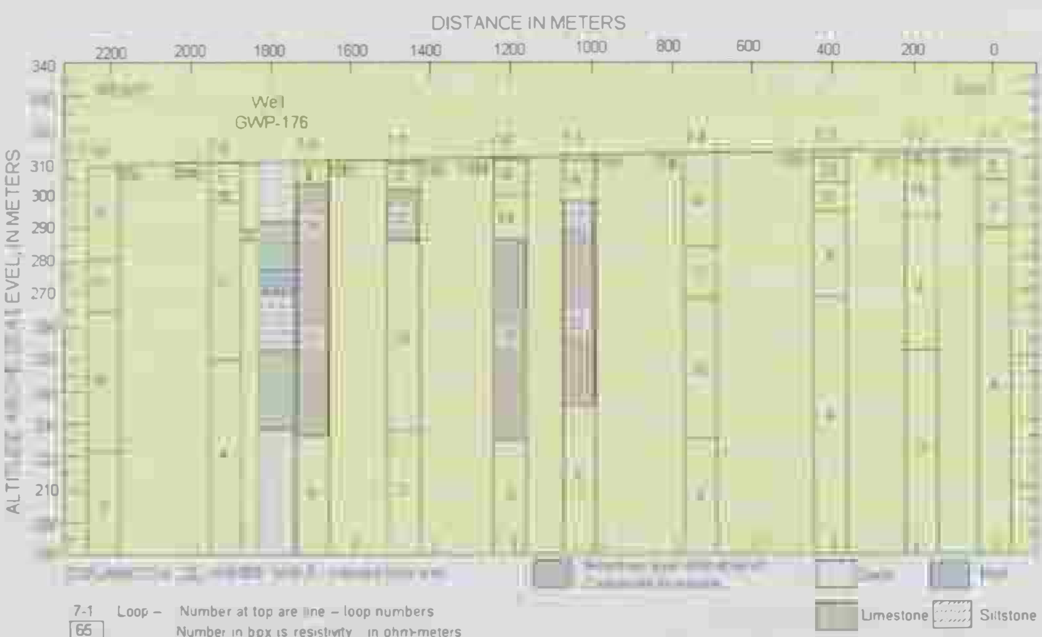

Figure (5.16) Geoelectric Columns along Jabal Al Oha using TEM Soundings (after Jama et. al., 1997). , see Figure 13 (for location).

5.10 Discussions and Interpretation of the Inverted Resistivity tomograms

The nine (2-D) resistivity tomograms were analyzed taking into account available borehole information (see Fig. 5.9, for location) and guided with the geoelectric model given by US Geological Survey, (1993), presented in Figure (5.22) and the work done by Jama et. al., (1997). Figures 5.22 to 5.24 identify the main hydrostratigraphic units of the aquifer system in northern part of Al Ain area. However, the geoelectric models in the Al Qura`a area and the interdune area are different. The interdune area in the Al Qura`a area does not contain any high resistivity with depth while the investigated area at Al-Foah is characterized by high resistive zones, attributed to the existing of carbonate (limestone) at different depths. This is shown on the inverted interpreted tomograms below. While, thick resistive accumulations of variably-cemented dune sand overlies conductive bedrock in the interdune area (see Fig. 5.14).

The inverted data which are displayed as a cross section of resistivity data approximated the true subsurface resistivity distribution. The obtained information about the subsurface, along the resistivity profiles, is interpreted from the distribution of areas of high and low resistivities.

Investigations of the inverted resistivity tomograms (Figs 5.17 to 5.25), reveals the following features:-

1) There is excellent match between the inverted resistivity tomograms (Figs 5.25 to 5.33) with the geoelectric TEM resistivity model of Jama et. al., (1997) shown in Figures 5.15 and 5.16.
2) In general, all resistivity tomograms are characterized by a surficial layer of high resistivity which is attributed to the dry eolian sand and the existence of dry and massive limestone at some profiles carried out near to Jabal Al Oha, for example see resistivity tomograms of profiles 1-1` and 9-9`, (Figures 5.17 and 5.25).

3) The underlying alluvial and mudstone deposits, seen as outcrops at some sites in Jabal Oha (see photo of Figure 5.6, b) are characterized by low to medium resistivities depending upon the percentage of clay.

4) The massive limestone that characterizes the Simsima Formation of Late Cretaceous generally has high resistivity and low permeability, except areas where caverns and fractured limestone are existing (See Figures 5.7 and 5.8). According to Jama, (1997), the high-capacity wells could be completed in shallow karstic limestone.

5) Fractured and karstic limestone are recognized at some profiles see for examples the interpreted tomograms of profiles 3-3`, 5-5`, 6-6` and 9-9` of figures 5.19, 5.21, 5.22 and 5.25 respectively.

6) The basal claystone and siltstone formations exhibit lower resistivity, as shown in Figures (5.18 and 5.20) along the interpreted 2D resistivity profiles 2-2` and 4-4` respectively. In some places in the deeper depth this zone would have resistivities of less than 5 Ohm-m probably due to the increase of salinity with depth.

7) Also there is a good agreement between the interpreted lithology along the resistivity tomograms and the lithology of the available borehole information, for example see the lithology information of Well No. (176) of Figure (5.16) which is corresponding to well no. 10 according to this study codes (see Figure 5.9 and appendix A) and cross section of profile 2-2'. The limestone according to this well is exist at 34 m and extends to a depth of 82 m and it is clear that along the tomogram of profile 2-2` (Figure 5.18) the limestone is displayed with a good match of depth of well (176) of figure (5.16).

8) Lateral variation of lithological units is recognized along all nine of these resistivity tomograms. This reflects how complex the area is from the stratgraphic and hydrogeologic point of view.

9) Very high resistive zones of more than 80 Ohm-m which attributed to the existing of massive limestone are displayed along profiles 3-3` and

8-8` of Figures (5.19 and 5.24) respectively. High resistivity layers indicate favorably with the presence of limestone formations, which suggest that 2-D resistivity surveys can be useful in selecting sites for test drilling in such interesting areas.

10) Aquifers at the area covered by profiles 1-1`, 2-2` and 3-3` are characterized by a relatively high salinity of more than 2000 mg/l. While the profiles 4-4`, 5-5`, 6-6`, 7-7` and 9-9` are located of relatively low salinity below 2000 mg/l (see Figure 4.3 and appendix A).

11) With comparison of the bicarbonate (HCO_3^-) and calcium (Ca^{2+}) distribution in the groundwater of study area, it is worthy to mention that there is a general increase in both HCO_3^- and Ca^{2+} concentration in the area covered by the 2-D resistivity profiles .This support the existing of limestone aquifer of Simsima Formation of Late Cretaceous at this area.

Test drilling, conducted at selected limestone exposures north of Al-Ain at Jabal Mohayyer (National Drilling Company, 1992), Qarn Saba (Budebes, 1994), Qarn Bida Bint Saud (Omer and Nasr, 1994) and at Jabal Al Oha (Jama et. al., 1997) (See Figure 5.13 for locations), indicated that the subsurface extensions of the limestone outcrops had potential for yielding as much as 1,000 gallons per minute (Imes and others, 1993).

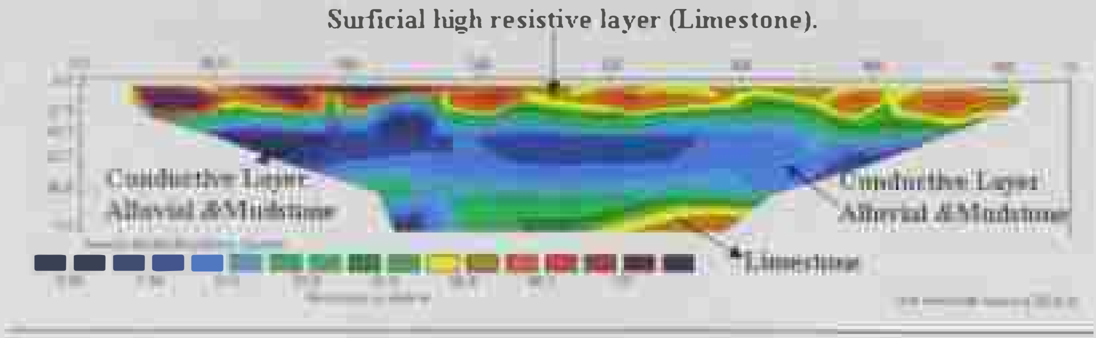

Figure (5.17) Interpreted 2-D Resistivity profile along line 1-1`

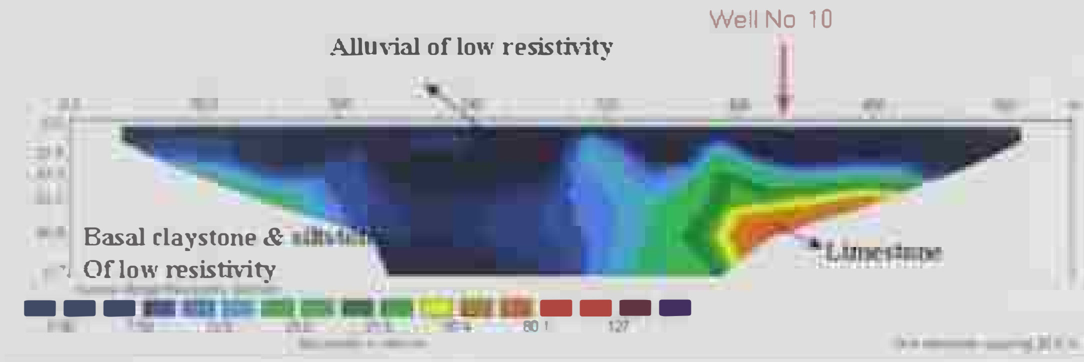

Figure (5.18) Interpreted 2-D Resistivity profile along line2-2`

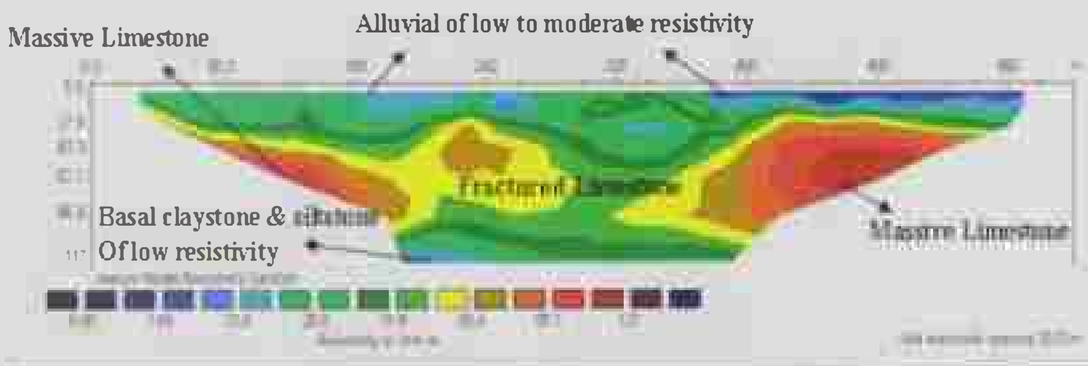

Figure (5.19) Interpreted 2-D Resistivity profile along line3-3`

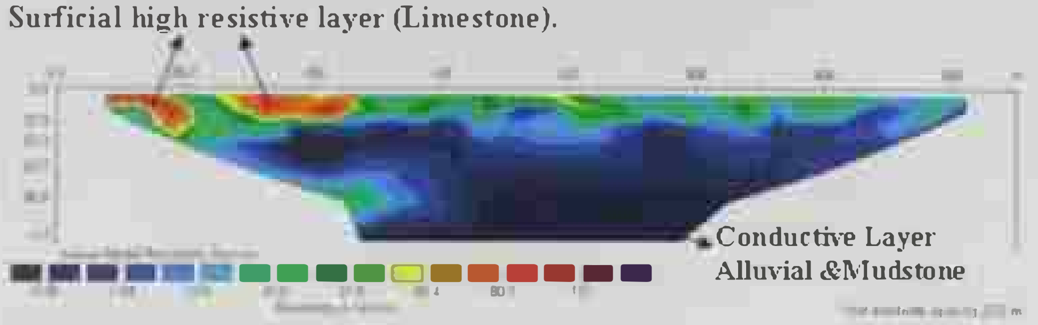

Figure (5.20) Interpreted 2-D Resistivity profile along line4-4`

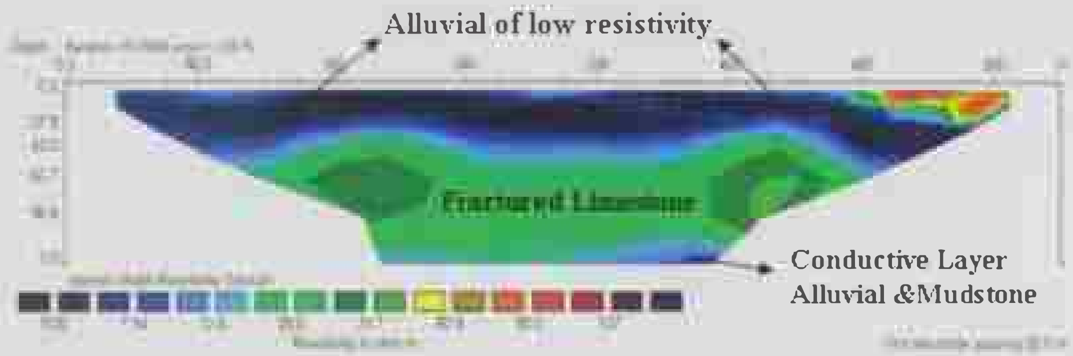

Figure (5.21) Interpreted 2-D Resistivity profile along line5-5`

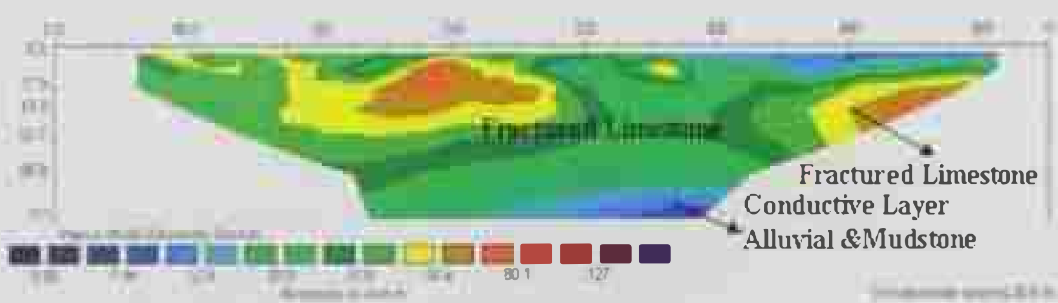

Figure (5.22) Interpreted 2-D Resistivity profile along line 6-6`

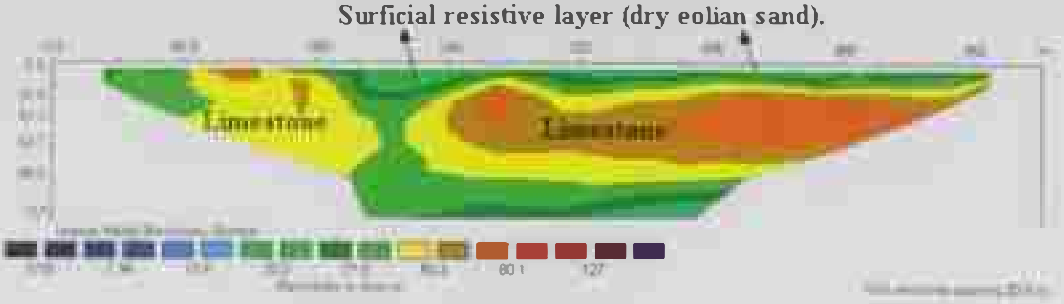

Figure (5.23) Interpreted 2-D Resistivity profile along line 7-7`

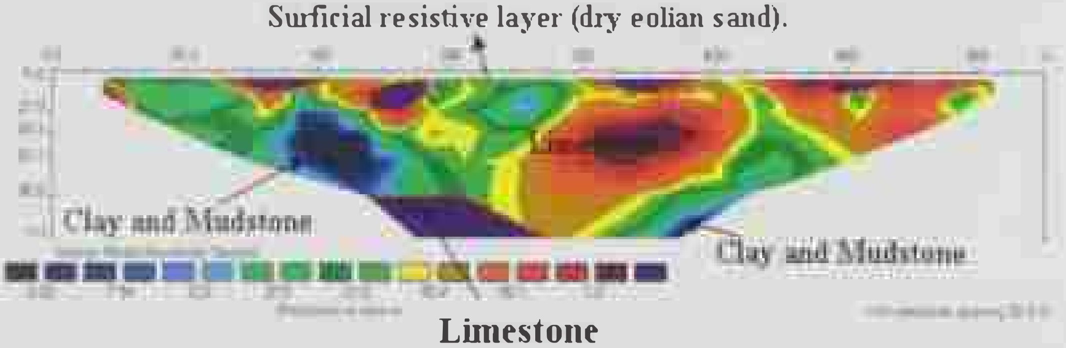

Figure (5.24) Interpreted 2-D Resistivity profile along line 8-8`

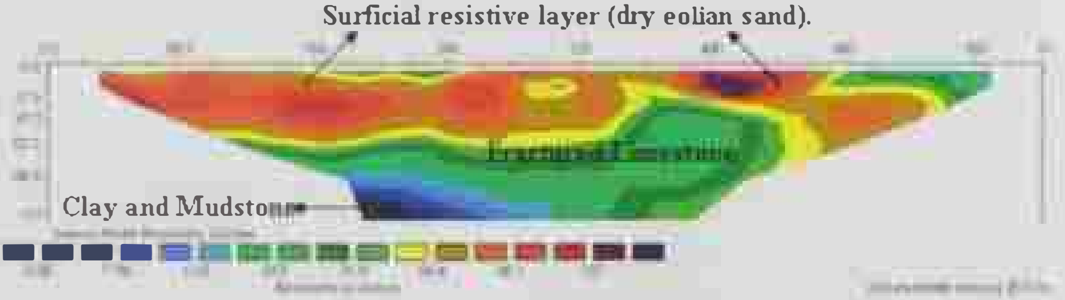

Figure (5.25) Interpreted 2-D Resistivity profile along line 9-9`

Chapter VI

CONCLUSION

CHAPTER VI

CONCLUSION

Results of the present study can be summarized in the following points:

- The depth to groundwater in the study area is about 30 m.
- According to the TDS content, about 82% of the groundwater analyzed in this study is unsuitable for drinking because of the high concentration of TDS in the north and the south of the study area (cultivated area) which exceeds the WHO recommended limit.
- Agricultural activities, return flow, fertilizers and pesticides are playing a vital role in increasing the concentrations of the anions and cations in the study area.
- The sequence of anions dominance in groundwater of the Quaternary aquifer in Al-Foah area is in the order of: $Cl^- > SO_4^{-2} > HCO_3^{-2} > CO_3^{-2}$. While the sequence of cations dominance in groundwater of the Quaternary aquifer in Al-Foah area is in the order of: $Na^+ > Mg^{+2} > Ca^{+2} > K^+$.
- According to WHO, standards all the nitrate concentrations of the groundwater in the study area were less than 50 mg/l except wells no. 7, 8, 9, 29, 31, 32, 33 and 34 which are located in cultivated area.
- There were no significant values of analyzed trace metals observed that could affect human health and groundwater in the study area.
- According to the Piper's diagram, the samples fall in the upper triangle of the diamond shape field which means that the dominant groundwater type is sodium-chloride. Analyzing the position of the samples shows that the groundwater in the southern part of the study area is enriched in magnesium.

- Based on S.A.R. classification. the groundwater in the study area has a low harmful effect on vegetation when used for irrigation. The SAR values ranged between 2.7 and 20 with an average of 7.23. About 88% of the study area represents low sodium hazard water. about 10% represents medium sodium hazard water and about 2% represents high sodium hazard water which lies near to the cultivated area.
- Resistivity tomograms of the nine profiles indicate remarkably the different hydrostratigraphic units of the aquifer system in Al-Foah area. Information about aquifer geometry and about the two main aquifers in the Al-Foah area in particular has been obtained through this study. Such information is essential for groundwater assessment. High resolution of 2-D resistivity is useful in acquiring hydrogeologic data in Jabal Al Oha area.
- Two main aquifers exist at Al-Foah. which are the Quaternary Alluvium aquifer and Limestone aquifer of Simsima Formation. A veneer of eolian sand covers the limestone aquifer. The Cretaceous limestone of Jabal Al Oha north of Al-Ain represents a good aquifer with high specific capacity wells. Recharge of Al-Foah occurs through surface flow of wadis. originating primarily as runoff from the northern Oman Mountains. Recharge can also occur by direct infiltration. In addition. it has been suggested that recharge occurs as flow through fractures in surrounding limestone ridges.

REFERENCES

REFERENCES

Al-Nuaimi, H.S., (2003). Hydrogeological and geophysical studies on Al-Jaww plain. Al-Ain area. U.A.E.. M.Sc. Thesis. United Arab Emirates University. 64-88p.

Al-Shamsei, M.H., (1993). Drainage basins and flash flood hazards in Al-Ain area. United Arab Emirates. M.Sc. Thesis. United Arab Emirates University. 151p.

Bin Braik, W.N., (1997). Evaluation of groundwater quality in shallow aquifers under cultivated lands at al Oha area. United Arab Emirates. M.Sc. thesis. United Arab Emirates University. 10p.

Budebes, Osama, (1994). Geohydrologic conditions at Qarn Saba. Abu Dhabi Emirate: National Drilling Company Technical Report 94-01.58 p.

Boonstra, J., and de Ridder N.A., (1981). Numerical modeling of groundwater basins – A user oriented manual: ILDRI. Wageningen. Netherlands. 227 p.

Dahlin, T. and Loke, M.H., (1997). Quasi-3D resistivity imaging-mapping of three dimensional structures using two dimensional DC resistivity techniques. Proceedings of the 3rd Meeting of the Environmental and Engineering Geophysical Society. 143-146.

Daniels F. and Alberty R.A., (1966). Physical Chemistry. John Wiley and Sons. Inc. deGroot-Hedlin. C. and Constable. S.. 1990. Occam's inversion to generate smooth. twodimensional models form magnetotelluric data. Geophysics. 55. 1613-1624.

Davis, S. N. and De Weist, R. J. (1966). Hydrogeology. John Wiley and Sons. New York. 108p.

DeGroot-Hedlin, C., and Constable, S., (1990). Occam's inversion to generate smooth. two-dimensional models from magneto telluric data. Geophysics. v. 55. 1613-1624.

Dobrin, M.B., (1976). Introduction to geophysical prospecting. Third ed.. Mc Graw-Hill Co.. New York.

Domenico, P.A., and Schwartz, F.W., (1990). Physical and chemical hydrology: John Wiley and Sons. New York. 824 p.

El-Shami, F., (1990). The hydrochemistry of the spring at Ain bu Sukhnah. UAE. Arab J. Scient. Res.. V8 no 1.p 34-46

Elwood, B. B., Harrold, F.B. and Marks, A. E. (1994). Site Identification and Correlation Using Geoarchaeological Methods at the Cabe o do Porto Marinho (CPM) Locality. Rio Maior. Portugal. Journal of Archaeological Science 21. PP.779 – 784.

Embabi, N.S., (1991). Dune types and patterns in the United Arab Emirates using Landsat TM-data. 24th Intern. Symp. On Remote Sensing of Environment. Rio dejaneiro. Brazil. p 27-31.

Freeze, R.A., and Cherry, J.A., (1979). Groundwater. Prentice-Hall. Englwood Cliffs. N.J.. 604p.

Garamoon, H.K., (1996). Hydrogeological and geomorphological studies on the Abu Dhabi-Dubai-Al Ain triangle. UAE. Unpublished Ph.D. thesis. Geol. Dep.. Fac. Sci.. Ain Shames University. Egypt. 277p.

Ghoneim, A., (1991). Physical geology of UAE: Reading for all bubl.. Dubai. 242p.

George, T., and Edward, D.S., (1987). Water Quality: Addison-Wesley. California. U.S.A. 91 p.

Griffiths D.H. and Barker R.D., (1993). Two-dimensional resistivity imaging and modelling in areas of complex geology. Journal of Applied Geophysics. vol.29. pp 121. 129.

Griffiths D.H., Turnbull J. and Olayinka A.I. (1990), Two-dimensional resistivity mapping with a computer- controlled array. First Break 8. 121-129.

Gymer, R.G., (1973). Chemistry: An Ecological Approach. Harper and Row. New York.

Hamdan, A.A., and Anan, H.S. (1993). Cretaceous/Tertiary boundary in the United Arab Emirates. M.E.R.C.. Ain Shams Univ.. Earth Sci. Ser.. (7). p 223-231.

Hamdan, A.A., and El-Deeb, W.Z., (1990). Stratigraphy of the Paleogene succession of Jabel Malaqet. West of the Northern Oman Mountains.. Fac. Sci.. UAE University. (2). p30-39.

Hamdan, A.R.A., and Bahr, S.A., (1992). Lithostratigraphy of the Paleocene succession of northern Jabel Hafit. Al-Ain. UAE. MERC. Ain Shams University. Earth science. v.6. p 201-204.

Hunting Geology and Geophysics Ltd. (1979). Report on a mineral survey of UAE., Al Ain Area. Ministry of Petroleum and Mineral Resources., Abu Dhabi., (9). 1-22p.

Hyde, L.W., (1992). Interregional advisory mission of water resources management. Abu Dhabi Emirate: United Nations Department of Technical Cooperation for Development. 86p.

Imes, J. L, Signor, D.C., and Woodward, D.G., (1993). Hydrology and water quality: in Maddy, D.V., ed., 1993. Groundwater resources of Al Ain area, Abu Dhabi Emirate: U.S. Geological Survey Administrative Report 93-001, p.168-283.

Jama, F.E., Kattampilly, M. M. and Murad A. O. (1997). Transient electromagnetic techniques for ground-water exploration near limestone exposures in Jabal Oha area, Abu Dhabi Emirate. National Drilling Company, Technical Report 97-02. 76 p.

Keller G.V. and Frischknecht F.C., (1966). Electrical methods in geophysical prospecting. Pergamon Press Inc., Oxford.

Koefoed O., (1979). Geosounding Principles 1 : Resistivity sounding measurements. Elsevier Science Publishing Company, Amsterdam.

Loke, M. H. and Barker, R.D., (1996). Rapid least-squares inversion of apparent resistivity pseudosections by a quasi-Newton method. Geophysical Prospecting, 44 131-152.

Loke, M.H., (1997). Electrical imaging surveys for environmental and engineering studies. A practical guide to 2D and 3D survey. Penang, Malaysia, Sains Malaysia University, short training course lecture note.

Matthess, G. (1982). The properties of groundwater. New York, John Wiley and Sons. 215-255 p.

Menges and Woodward, US Geological Survey and United Arab Emirates National Drilling Company, (1993). Ground Water Resources of Al-Ain area, Abu Dhabi Emirate. Unpublished administrative report 93-001, National Drilling Company, Abu Dhabi, UAE. 315 p.

Mussett, A.E. and Khan, M.A., (2000). Looking into the Earth: An Introduction to Geological Geophysics. Cambridge University Press. 492pp.

National Drilling Company, (1992). Geohydrologic conditions near Jabal Mohayer. Abu Dhabi Emirate: National Drilling Company Adinistrative Report 92-001. 53 p.

Noweir, M.A. and Alsharhan, A.S., (2000). Structural Style and Stratigraphy of the Huwayyah Anticline: an example of an Al-Ain Tertiary Fold Northern Oman Mountains. GeoArabia: Middle East Petroleum Geosciences. v. 5, no. 3. p. 387-400.

Omer, Hassan, and Nasr, Mustafa Al Amin, (1994). Geohydrologic conditions at Qarn Bida Bint Saud. Abu Dhabi Emirate: National Drilling Company Technical Report 94-02.65p.65 p.

Parasnis, D. (1997). Principles of Applied Geophysics. London: Chapman & Hall.

Powers, C.J., Wilson. J. Haeni, F.P. and Johnson, C.D., (1999). Surface-geophysical investigation of the University of Connecticut. landfill. Storrs. Connecticut: U.S. Geological Survey Water-Resources Investigations Report 99.

Reynolds, J.M., (1997). An Introduction to Applied and Environmental Geophysics. John Wiley & Sons. pp 796.

Richards, L. A., (1969). Diagnosis and improvement of saline and alkali soils. United States Salinity Laboratory Staff, Agriculture Handbook No.60. U.S. Government Printing Office. Washington. D.C., USA.

Rizk, Z.S., (1999). A review article on water resources in the United Arab Emirates. Unpublished Article. Department of Geology. Faculty of Science-Menoufia University. Shebin El Kom. Egypt. 11p

Robinson, E.S., and Courth, C. (1988). Basic Exploration Geophysics. Cambridge University Press.

Sara, M. N. and R. Gibbons. (1991). Organization and Analysis of Water Quality Data. In: D.M.Nielsen (editor). Practical Handbook of Ground Water Quality. Lewis Publishers. Inc. Chelsea. Michigan. pp. 541-588.

Sayed, S.M.G. and Mersal, M.A. (1998). Surface geology of Jebel Rawdah. Oman Mountains. GeoArabia: Middle East Petroleum Geosciences. v. 3, no. 3. p. 401-414.

Teleford, W.M., Geldart, L.P., Sheeriff, R.E and Keys, D.A. (1990). Applied Geophysics. 2nd edn. Cambrigde: Cambridge University Press.

Todd, D.K., (1980). Groundwater hydrology: John Wiley and Sons. Icn.. New York. U.S.A.. 535 p.

US Geological Survey and United Arab Emirates National Drilling Company, (1993). Ground Water Resources of Al Ain area. Abu Dhabi Emirate. Unpublished administrative report 93-001. National Drilling Company. Abu Dhabi. UAE. 315 p.

U. S. Salinity Laboratory Staff, (1954). Diagenesis and improvement of saline and alkali soils: U. S. Dept. Adri.. Agricultural Handbook no. 60. pp. 60-160.

Walton, W.C., (1970). Groundwater resources evaluation. McGraw-Hill Book Company. New York. 445p.

Warrak, M. (1987). Synchronous deformation of neoautochthonous sediments of the Northern Oman Mountains. 5th Conf. S.P.E.. Bahrain.. p129-136.

APPENDIX

CHEMICAL ANALYSES RESULTS

Well ID	Well Destination	GPS (UMT Unit)		Conductivity (mS)	Salinity (%l)	TDS (mg/l)	Tem. °C	Result (mg/l)									
		North	East					pH	Cl^-	NO_3	SO_4	CO_3	HCO_3	Ca	K^+	Mg^{++}	Na^+
1	Private Department	2694211	377535	3 86	2 0	1950	29.7	7 4	946 7	44 1	336 6	ND	221 4	81 1	21 7	199	380
2	Nihayan Farm	2694064	377399	4 17	2 2	2120	29 6	7 4	1000 0	34 9	363 0	ND	184 5	105	14 2	253	358
3	Nihayan Farm	2694508	377318	5 47	2 9	2840	32 0	7 4	1416 0	42 9	534 0	ND	181 0	140	16 8	354	431
4	Hamad Al Badi Farm	2694177	377163	5 15	2 8	2690	30.2	7 5	1250 0	45 0	535 4	ND	230 6	106	22 3	302	496
5	UAE Farm	2693768	377548	4 72	2 5	2440	33 8	7 5	1165 0	15 6	302 0	ND	147 6	129	16 7	237	448
6	Ministry of agricultural farm	2694240	378415	4 45	2 3	2250	33 3	7 5	1056 0	22 0	363 6	ND	145 3	124	14 1	257	394
7	Ministry of agricultural	2701968	376978	3 18	1 6	1590	33 1	7 9	556 5	84 9	434 7	4 5	145 3	73 6	18 9	135	391
8	Ministry of agricultural	2701911	377078	3 20	1 7	1600	31 4	7 9	504 0	119 0	511 0	4 5	143 0	81 0	17 2	145	365
9	Ministry of agricultural	2702797	377069	2 16	1 1	1050	33 3	7 8	335 0	70 0	274 0	ND	143 0	60 9	11 0	97 2	250
10	Al Ain Distribution (well 176)	2690166	380020	4 77	2 5	2480	31 3	6 92	1074	5 23	518	5 67	183	185	14 6	150	607
11	Al Ain Distribution (well 175)	2690682	380092	4.62	2 5	2380	31 5	7 09	1036	3.7	483	6 80	212	182	13 8	164	580
12	Sief bin Zayed farm	2690455	378568	3 34	1 7	1660	31 5	7 08	597	7 18	362	5.67	319	121	16 7	153	406
13	Sief bin Zayed farm	2690095	377550	6 22	3 4	3270	32.1	6 90	1312	19 2	832	6 80	242	257	20 6	287	732
14	Bedea Bin Masood	2692399	371668	0 95	0 5	454	30 6	7.53	112	6 19	66.7	9 07	201	34.5	5.02	42.6	108
15	Near to the (fuel station)	2692243	378803	2.23	1 1	1080	32.0	7 65	440	1 93	150	11 6	187	74 3	8 67	73 7	288
16	On road to dubai	2693610	378663	9 94	5.6	5420	35 8	6 92	3240	ND	328	5 67	174	206	18 2	200	1634
17	Al Foa Farm (well 73)	2695365	380622	2.01	1.0	968	31 0	7 82	374	9 77	119	11 3	166	29 0	6 19	34 5	336
18	Al Foa Farm (well 71)	2695550	380573	1 41	0.7	677	34.6	7 42	96.7	4 69	42 3	6 80	155	25 9	5 18	27 5	250
19	Al Foa Farm (well 110)	2697313	381721	0.91	0 4	432	33 3	7 69	100	12 3	87.1	11 6	178	22 0	4 60	38.3	103
20	Al Foa Farm (well 95)	2697534	381740	1.64	0 8	807	27.4	7 05	253	6 0	184	7 94	206	24 9	7 11	32 0	294
21	Haza'a farm	2685105	374329	2.86	1 5	1410	31.1	6 62	569	30 9	374	4 00	207	79 4	11 3	122	306
22	Haza'a farm	2685050	374340	2 31	1 2	1130	30 2	6 69	427	25.1	258	4 00	199	59 0	9 49	84	246
23	Salem al tajer Farm	2685266	374502	2 94	1 5	1460	30 1	6 84	625	31 5	326	11 34	192	98 5	13 4	150	249

Well ID	Well Destination	GPS (UMT Unit)		Conductivity	Salinity	TDS	Tem.	Result (mg/l)									
		North	East	(mS)	(%l)	(mg/l)	°C	pH	Cl^-	NO_3	SO_4	CO_3	HCO_3	Ca	K^+	Mg^{++}	Na^+
24	Khalifa Al mansory Farm	2685779	375122	11.16	6.3	6180	28.8	6.31	2985	40.9	1730	3.78	423	237	39.3	637	1470
25	**SURFACE WATER**	2686121	375285	3.27	1.7	1630	32.3	6.95	631	3.64	528	3.78	127	97.2	13.9	82.2	422
26	Al Mansory Farm	2686409	375617	11.62	6.6	6430	30.2	6.08	3320	17.5	3090	ND	515	338	30.6	533	1625
27	Al Mansory Farm	2686410	375680	10.62	6.0	5870	29.4	6.08	2865	23.6	2175	ND	400	383	35.3	613	1299
28	Aisha Farm	2690350	378090	6.13	3.3	3230	33.4	6.56	1530	27.3	882	3.78	242	223	21.5	280	710
29	Hameed Farm	2689744	378065	6.02	3.3	3210	29.3	6.30	1418	51.1	1194	ND	300	202	53.0	285	664
30	Hameed Farm	2689748	378217	5.43	2.9	2870	28.3	6.39	1104	34.8	1108	ND	300	191	22.4	250	741
31	Ali Ahmad Farm	2685409	378090	5.15	2.7	2660	33.3	6.44	1140	145	918	ND	200	131	18.3	223	721
32	Ali Ahmad Farm	2685521	376812	3.18	1.6	1580	33.1	6.57	413	175	805	7.56	211	120	11.7	228	268
33	Bakeet Al Nuaymy Farm	2685727	376694	3.50	1.8	1750	32.4	6.80	520	115	844	3.78	177	127	13.2	198	383
34	Bakeet Al Nuaymy Farm	2685701	376481	5.94	3.2	3110	32.6	6.50	1120	230	1498	ND	131	324	18.2	341	584
35	Tahnon Farm	2698693	376490	1.01	0.5	481	32.3	7.41	133	5.67	101	12.0	195	8.73	4.32	11.8	184
36	Tahnon Farm	2699258	379100	12.63	7.2	6990	33.3	6.89	6550	ND	39.5	16.0	171	114	23.8	105	243
37	Evaluation GW Project well#180	2699223	376168	4.09	2.2	2090	34.2	6.96	992	7.03	862	4.00	122	130	11.1	152	591
38	Evaluation GW Project well #181	2699035	375921	5.82	3.2	3040	33.2	7.03	824	2.23	2002	4.00	85.4	357	19.8	160	844
39	Evaluation GW Project well #182	2699070	375661	6.33	3.4	3330	38.4	7.00	978	ND	1850	12.0	122	152	12.3	89.4	1282
40	Evaluation GW Project well #183	2698907	375234	6.83	3.7	3610	34.6	6.96	536	2.14	446	10.0	153	69.9	10.9	87.3	491
41	Mohammed Al Kheli Farm	2687606	374811	5.80	3.1	3030	29.6	6.35	1110	12.6	948	ND	415	85.9	14.2	119	628
42	Mohammed Al Kheli Farm	2687746	374614	4.21	2.2	2140	25.7	6.55	800	26.7	564	ND	215	90.9	14.1	121	626
43	**Basin Water**	2687755	374630	3.82	2.0	1940	22.7	7.38	736	33.8	476	22.7	173	73.4	15.3	109	565
44	Beside the graveyard	2692893	380995	2.26	1.1	1100	32.2	7.06	510	6.28	99.2	7.56	158	40.9	8.46	105	224
45	Municepility	2696938	378496	3.75	2.0	1890	32.4	6.8	766	32.4	465	7.56	196	92.1	11.6	147	477
46	Municepility	2698507	375061	1.19	0.6	569	33.2	7.08	172	5.46	118	9.45	163	15.5	5.09	22.1	177

Well ID	Well Destination	GPS (UMT Unit)		Conductivity	Salinity	TDS	Tem.	Result (mg/l)									
		North	East	(mS)	(%l)	(mg/l)	°C	pH	Cl^-	NO_3	SO_4	CO_3	HCO_3	Ca	K^+	Mg^{++}	Na^+
47	Municepility	2699029	374742	1 66	0 8	807	31 5	6 99	184	11 3	88 2	7 56	165	21 2	7 35	30 9	148
48	Municepility	2698797	374696	2.61	1.3	1290	32 4	7 22	422	ND	212	11 3	127	34 1	8 39	47 5	329
49	Municepility	2699277	374941	1.10	0.5	528	32.5	6 94	159	9 93	80 0	7 56	150	25 4	7 13	39 2	109
50	Municepility	2695288	377652	3 50	1 8	1750	37 1	6 73	802	29.3	275	ND	161	104	10 6	275	197

Well ID	Well Destination	Result (mg/l)																				
		*F	*Br	*PO_4^{4}	NO_2^-	Sr	Al	As	Ba	Cd	Co	Cr	Cu	Fe	Mn	Mo	Ni	P	Pb	V	Zn	B
1	Private Department	< 1 0	2.5	ND	ND	ND	0 01	ND	0 05	ND	ND	0 02	ND	0 01	ND	ND	ND	ND	ND	ND	0 00	0 00
2	Nihayan Farm	< 1 0	2.5	ND	ND	ND	0 02	ND	0 10	ND	ND	0 02	ND	0 03	ND	ND	ND	ND	ND	ND	0 11	0 00
3	Nihayan Farm	< 1 0	3 2	ND	ND	ND	0 02	ND	0 07	ND	ND	0 04	ND	ND	ND	ND	ND	ND	ND	ND	0 01	0 00
4	Hamad Al Badi Farm	< 1 0	1 9	ND	ND	ND	0 02	ND	0 06	ND	ND	0 02	ND	0 08	ND	ND	ND	ND	ND	ND	0 00	0 00
5	UAE Farm	1 1	3.4	ND	ND	ND	0 02	ND	0 12	ND	ND	0 01	ND	0 14	ND	ND	ND	ND	ND	ND	0 07	0 00
6	Ministry of agricultural farm	< 1.0	2 0	ND	ND	ND	0 02	ND	0 11	ND	ND	0 02	ND	0 04	ND	ND	ND	ND	ND	ND	0.03	0 00
7	Ministry of agricultural	< 1 0	1 1	ND	ND	ND	0 02	ND	0 06	ND	ND	0 07	ND	0 51	ND	ND	ND	ND	ND	ND	0 11	0 00
8	Ministry of agricultural	< 1 0	< 1 0	ND	ND	ND	0 01	ND	0 05	ND	ND	0 07	ND	ND	ND	ND	ND	ND	ND	ND	0 21	0 00
9	Ministry of agricultural	< 1.0	ND	ND	ND	ND	0 01	ND	0 06	ND	ND	0.05	ND	0 35	ND	ND	ND	ND	ND	ND	0 11	0 00
10	Al Ain Distribution (well 176)	1 18	1 03	ND	ND	ND	ND	ND	0 04	ND	ND	0 02	ND	0.20	ND	ND	ND	ND	ND	ND	0 01	0 00
11	Al Ain Distribution (well 175)	0 93	1 01	ND	ND	ND	0 02	ND	0.04	ND	ND	0.08	ND	1 05	ND	ND	ND	ND	ND	ND	0 00	0 00
12	Sief bin Zayed farm	0 59	1 12	ND	ND	ND	ND	ND	0 06	ND	ND	0 01	ND	ND	ND	ND	ND	ND	ND	ND	0 03	0 00
13	Sief bin Zayed farm	1 48	2.65	ND	ND	ND	0.02	ND	0 05	ND	ND	0 01	ND	ND	ND	ND	ND	ND	ND	ND	0.01	0 00
14	Bedea Bin Masood	ND	ND	ND	ND	ND	0 05	ND	0 06	ND	ND	0 01	ND	0 22	0 02	ND	ND	ND	ND	ND	0 08	0 00
15	Near to the (fuel station)	ND	1 01	ND	ND	ND	ND	ND	0 13	ND	ND	ND	ND	1.24	ND	ND	ND	ND	ND	ND	0.13	0 00
16	On road to dubai	0.75	15.6	ND	ND	ND	0.04	ND	0.35	ND	ND	ND	ND	ND	0 08	ND	ND	ND	ND	ND	0 01	0 00
17	Al Foa Farm (well 73)	ND	1 29	ND	ND	ND	ND	ND	0 06	ND	ND	0 01	ND	ND	ND	ND	ND	ND	ND	ND	0 01	0 00
18	Al Foa Farm (well 71)	ND	ND	ND	ND	ND	0 08	ND	0 04	ND	ND	0 02	ND	0.39	0 04	ND	ND	ND	ND	ND	0 18	0 00
19	Al Foa Farm (well 110)	ND	ND	ND	ND	ND	ND	ND	0 04	ND	ND	0.02	ND	ND	ND	ND	ND	ND	ND	ND	0.16	0.00
20	Al Foa Farm (well 95)	ND	ND	ND	ND	ND	ND	ND	0 05	ND	ND	0 02	ND	ND	ND	ND	ND	ND	ND	ND	0 16	0 00

Well ID	Well Destination	Result (mg/l)																				
		*F	*Br	*PO_4^{-4}	NO_2^-	Sr	Al	As	Ba	Cd	Co	Cr	Cu	Fe	Mn	Mo	Ni	P	Pb	V	Zn	B
21	Haza'a farm	ND	0.07	ND	ND	ND	0.02	ND	0.07	ND	ND	0.03	ND	0.05	ND	ND	ND	ND	ND	ND	0.17	0.00
22	Haza'a farm	ND	ND	ND	ND	ND	0.02	ND	0.06	ND	ND	0.02	ND	0.04	ND	ND	ND	ND	ND	0.01	0.13	0.00
23	Salem al tajer Farm	ND	1.24	ND	ND	ND	0.01	ND	0.09	ND	ND	0.02	ND	0.05	ND	ND	ND	ND	ND	0.00	0.20	0.00
24	Khalifa Al mansory Farm	ND	5.38	ND	ND	ND	0.02	ND	0.05	ND	ND	0.02	ND	0.01	ND	ND	0.01	ND	ND	0.00	0.16	0.00
25	**SURFACE WATER**	ND	ND	ND	ND	ND	0.02	ND	0.01	ND	ND	0.02	ND	0.03	ND	ND	0.01	ND	ND	0.00	0.01	0.00
26	Al Mansory Farm	ND	4.37	ND	ND	ND	0.01	ND	0.00	ND	ND	ND	ND	ND	ND	ND	ND	ND	ND	ND	0.08	0.00
27	Al Mansory Farm	ND	4.17	ND	ND	ND	0.03	ND	0.04	ND	ND	0.01	ND	ND	ND	ND	0.01	ND	ND	ND	0.00	0.00
28	Aisha Farm	ND	3.77	ND	ND	ND	0.02	ND	0.07	ND	ND	0.01	ND	ND	ND	ND	0.01	ND	ND	ND	0.04	0.00
29	Hameed Farm	ND	2.80	ND	ND	ND	0.02	ND	0.02	ND	ND	0.01	ND	ND	ND	ND	0.01	ND	ND	0.00	0.02	0.00
30	Hameed Farm	ND	2.28	ND	ND	ND	0.02	ND	0.02	ND	ND	0.01	ND	ND	ND	ND	0.01	ND	ND	ND	0.09	0.00
31	Ali Ahmad Farm	0.6	3.41	2.77	2.21	ND	0.02	ND	0.06	ND	ND	0.02	ND	ND	ND	ND	0.01	ND	ND	ND	0.06	0.00
32	Ali Ahmad Farm	ND	ND	7.38	ND	ND	0.02	ND	0.07	ND	ND	0.03	ND	ND	ND	ND	0.01	ND	ND	ND	0.07	0.00
33	Bakeet Al Nuaymy Farm	ND	1.83	ND	ND	ND	0.06	ND	0.04	ND	ND	0.02	ND	0.08	ND	ND	0.01	ND	ND	ND	0.11	0.00
34	Bakeet Al Nuaymy Farm	ND	ND	ND	ND	ND	0.03	ND	0.05	ND	ND	0.01	ND	0.02	ND	ND	0.01	ND	ND	ND	0.17	0.00
35	Tahnon Farm	ND	ND	ND	ND	ND	0.00	ND	0.01	ND	ND	0.05	ND	ND	ND	ND	ND	ND	ND	0.01	0.26	0.00
36	Tahnon Farm	1.62	34.5	ND	ND	ND	0.04	ND	0.70	ND	ND	ND	ND	0.07	0.05	ND	ND	ND	ND	ND	1.30	0.02
37	Evaluation Project well#180	ND	ND	ND	ND	ND	0.01	ND	0.03	ND	ND	0.11	ND	0.11	ND	ND	ND	ND	ND	0.01	0.09	0.00
38	Evaluation Project well #181	ND	ND	7.02	ND	ND	0.02	ND	0.01	ND	ND	0.01	ND	ND	0.01	ND	ND	ND	ND	ND	2.25	0.00
39	Evaluation Project well #182	ND	ND	ND	ND	ND	0.01	ND	0.01	ND	ND	0.12	ND	0.28	0.01	ND	ND	ND	ND	0.00	0.18	0.00
40	Evaluation Project well #183	ND	ND	ND	ND	ND	0.03	ND	0.01	ND	ND	0.06	ND	0.20	0.01	ND	ND	ND	ND	ND	0.38	0.00

Well ID	Well Destination	Result (mg/l)																					
		*F	*Br	*PO_4^{4}	NO_2^-	Sr	Al	As	Ba	Cd	Co	Cr	Cu	Fe	Mn	Mo	Ni	P	Pb	V	Zn	B
41	Mohammed Al Kheli Farm	ND	1 91	ND	ND	ND	0 02	ND	0 02	ND	ND	0 06	ND	0 05	ND	ND	ND	ND	ND	0 01	0 14	0 00
42	Mohammed Al Kheli Farm	ND	ND	ND	ND	ND	0 01	ND	0 02	ND	ND	0 06	ND	0 03	ND	ND	ND	ND	ND	0 01	0 16	0 00
43	**Basin Water**	ND	ND	ND	ND	ND	0 01	ND	0 04	ND	ND	0 06	ND	0 03	ND	ND	ND	ND	ND	0 01	0 07	0 00
44	Beside the graveyard	ND	ND	ND	ND	ND	0 01	ND	0 19	ND	ND	0 02	ND	0 02	ND	ND	ND	ND	ND	ND	ND	0 00
45	Municepility	0 64	ND	ND	ND	ND	0 02	ND	0 06	ND	ND	ND	ND	0 04	ND	ND	0 02	ND	ND	ND	0 02	0 00
46	Municepility	ND	ND	ND	ND	ND	ND	ND	0 01	ND	ND	0 07	ND	ND	ND	ND	ND	ND	ND	0 01	0 05	0 00
47	Municepility	ND	ND	ND	ND	ND	0 01	ND	0 05	ND	ND	0 05	ND	ND	ND	ND	ND	ND	ND	0 01	0 08	0 00
48	Municepility	ND	ND	ND	ND	ND	0 01	ND	0 02	ND	ND	0 20	ND	0 04	ND	ND	ND	ND	ND	0 01	0 07	0 00
49	Municepility	ND	ND	ND	ND	ND	0 01	ND	0 08	ND	ND	0 05	ND	0 28	ND	ND	ND	ND	ND	ND	0 25	0 00
50	Municepility	ND	2 20	ND	ND	ND	0 01	ND	0 13	ND	ND	0 03	ND	0 70	ND	ND	ND	ND	ND	ND	0 06	0 00

ملخص الرسالة

نتيجة للتطور السريع الذي شهدته دولة الإمارات العربية المتحدة في العقود الأخيرة التي شملت جميع نواحي الحياة: المدنية والصناعية و الزراعية وغيرها، أصبحت مصادر المياه التقليدية تنخفض بصورة حرجة. إن ندرة المياه الطبيعية ونمو الفجوة بين الطلب و الكمية المتوفرة من المياه الصالحة للشرب في معظم مناطق الدولة، أجبرت الحكومة على مواجهة التحديات المتعلقة بسياساتها وقراراتها المتعلقة بالمياه.

تعتبر المصادر التقليدية وغير التقليدية من أهم مصادر المياه التي تعتمد عليها دولة الإمارات العربية المتحدة لسد حاجاتها من المياه، وتعتبر المياه الجوفية من أهم المصادر التقليدية بالدولة.

وهذا البحث يركز على منطقة الفوعة (الفوعة سابقاً) والتي تقع شمال مدينة العين، وتعد واحدة من أهم المناطق الزراعية في إمارة أبوظبي، ويوفر المياه الجوفية في تلك المنطقة معظم متطلبات المياه على المستويين الزراعي و المنزلي. ويهدف هذا البحث إلى تقييم المياه الجوفية وتحديد أماكن تواجدها في منطقة الفوعة.

بناءاً على الدراسات الحقلية و المعملية و المكتبية على المنطقة يمكن تلخيص نتائج الدراسة الحالية في النقاط التالية:

- تتكون الظواهر الأساسية في منطقة العين من الجبال و السهول و الكثبان الرملية.
- تمثل الصخور في منطقة الفوعة العصور الممتدة من العصر الطباشيري إلى العصر الحديث، معظم منطقة الفوعة مغطاة برسوبيات العصر الرباعي حيث أن تكشفات الصخور الجيرية المتكسرة يمكن رؤيتها في تركيب جبل الفوعة.
- وجود نوعين من الخزانات المائية في المنطقة أحدهما مكون من ترسبات العصر الرباعي و الآخر مكون من الصخور الجيرية المتكسرة من العصر الطباشيري حيث أنه يمثل خزان جيد للمياه الجوفية في تلك المنطقة.
- حوالي 88% من المياه الجوفية الموجودة في المنطقة غير صالحة للشرب وذلك لارتفاع ملوحتها ووجود الترسبات العالقة و تركيز العناصر الكيميائية فيها، وذلك نتيجة للإفراط بضخ المياه من الآبار واستخدام الكثير للأسمدة ونتيجة أيضاً لعوامل التبخر.
- أوضحت النتائج الجيوفيزيائية الوضع الطبقي للمنطقة، والتي لها انعكاسات مباشرة على الوضع الهيدرولوجي لخزانات منطقة الفوعة، كما أوضحت أماكن الربط بين الخزانين الموجودين في تلك المنطقة.

جـــامعة الامارات العربية المـــتحدة
عمـــادة الدراســـات العليـــــا
برنامج ماجستير علوم موارد المياه

عنوان الرسالة

دراسات هيدروجيولوجية وجيوفيزيائية على منطقة القوعة، شمال مدينة العين - دولة الإمارات العربية المتحدة

اسم الباحث

سامح يحيى علي سليمان

المشرفون

م	الاسم	الوظيفة
1	د. أحمد مراد	رئيس قسم الجيولوجيا - أستاذ مساعد في جيولوجيا المياه - قسم الجيولوجيا - كلية العلوم - جامعة الإمارات العربية المتحدة
2	د. أحمد المحمودي	أستاذ مساعد في الجيوفيزياء - قسم الجيولوجيا - كلية العلوم - جامعة الملك فيصل - المملكة العربية السعودية.
3	د. حيدر بكر	أستاذ تطبيقات الجيوفيزياء - قسم الجيولوجيا - كلية العلوم - جامعة الإمارات العربية المتحدة

جامعة الامارات العربية المتحدة
عمادة الدراسات العليا
برنامج ماجستير علوم موارد المياه

دراسات هيدروجيولوجية وجيوفيزيائية على منطقة الفوعة، شمال مدينة العين – دولة الإمارات العربية المتحدة

إعداد

سامح يحيى علي سليمان

رسالة مقدمة إلى

عمادة الدراسات العليا
جامعة الإمارات العربية المتحدة

لاستكمال متطلبات الحصول على درجة الماجستير في
علوم موارد المياه

عمادة الدراسات العليا
جامعة الإمارات العربية المتحدة
يونيو 2007